

MODELING STREAM-AQUIFER INTERACTIONS DURING FLOODS AND  
BASEFLOW: UPPER SAN PEDRO RIVER, SOUTHEASTERN ARIZONA.

by

Scott Carlyle Simpson

---

Copyright © Scott Carlyle Simpson 2007

A Thesis Submitted to the Faculty of the

DEPARTMENT OF HYDROLOGY AND WATER RESOURCES

In Partial Fulfillment of the Requirements

For the Degree of

MASTER OF SCIENCE  
WITH A MAJOR IN HYDROLOGY

In the Graduate College

THE UNIVERSITY OF ARIZONA

2007



## ACKNOWLEDGEMENTS

I would like to thank the following people (in no particular order) for their help at various points during the duration of this research project:

Thomas Meixner (UA-HWR): Thank you for all the mental time and effort exerted during this project: both in getting it started and in guiding it in the proper directions between then and completion.

James Leenhouts (USGS-Tucson): Thank you for your initial input and expertise regarding the study area and for allowing the use of so much of your data in this model. It is safe to say that this project would not have been possible to the extent that it was without your data.

Bill Childress (BLM): Thank you for allowing access to the study sites in SPRNCA and for dealing personally with the myriad accessibility issues early on.

Kate Baird (UA-HWR): Thank you for allowing the use of the ET curves you developed with Drs. Maddock and Stromberg. They proved to be a truly integral component of this model.

James Hogan (UA-HWR, SAHRA): Thank you for providing such helpful and constructive criticisms regarding this thesis and for steering this manuscript in the proper direction for the subsequent journal submission.

Carlos Soto, Jeff Gawad and Caitlin Zlatos (UA-HWR): Thank your all for your help in the field and/or lab.

## TABLE OF CONTENTS

ABSTRACT.....	7
1. INTRODUCTION.....	9
2. STUDY AREA / BACKGROUND.....	12
3. FIELD SAMPLING & ANALYTICAL METHODS.....	14
4. MODEL STRUCTURE: WATER BALANCE .....	16
4.1    Background.....	16
4.2    Model Domain Partitioning.....	17
4.3    Basin/Riparian Groundwater Exchange and Evapotranspiration.....	18
4.3.1        Gaining River Reach ET and Groundwater Estimates.....	19
4.3.2        Losing River Reach ET and Groundwater Estimates .....	21
4.4    River/Aquifer Exchange .....	24
4.4.1        Diffusivity Estimation.....	26
4.5    Transfer of Water Downstream.....	27
5. MODEL STRUCTURE: CONSERVATIVE TRACERS.....	30
5.1    Summary: Tracking Water Movement Through The Model.....	30
5.2    Basin/Riparian Groundwater Exchange.....	31
5.3    Evapotranspiration.....	32
5.4    River/Aquifer Exchange.....	33
5.5    Transfer of Water Downstream.....	34

TABLE OF CONTENTS – *Continued*

6. MODEL INPUTS.....	35
6.1 Streamflow Volume.....	35
6.2 Surface Flow Chemistry.....	36
6.3 Groundwater Flux and Chemistry.....	37
7. MODEL OUTPUTS.....	39
8. RESULTS: BASE-CASE MODEL SIMULATION.....	40
8.1 Water Balance Results.....	40
8.2 Chemical and Isotopic Results .....	43
9. SENSITIVITY ANALYSIS.....	45
9.1 Methodology & Results.....	45
9.2 Discussion.....	47
9.3 Chemical/Isotopic Sensitivity Analysis.....	49
10. MANUAL CALIBRATION, RESULTS & DISCUSSION.....	50
10.1 Results & Discussion: Water Balance.....	51
10.2 Results & Discussion: Chemical/Isotopic Composition.....	53
11. QUANTIFYING STREAM CHANNEL RECHARGE:	
OVERALL SUMMARY & CONCLUSIONS.....	60
12. IMPLICATIONS FOR FURTHER RESEARCH ...	65

TABLE OF CONTENTS – *Continued*

APPENDICES.....	66
APPENDIX A: FIGURES.....	67
APPENDIX B: TABLES .....	110
APPENDIX C: CONDITION SCORE BIOINDICATORS.....	120
APPENDIX D: MODEL ENTRENCHMENT DEPTHS .....	121
APPENDIX E: PALOMINAS RIVER WATER QUALITY DATA.....	122
APPENDIX F: HEREFORD RUNOFF SAMPLE DATA.....	125
APPENDIX G: NEAR-RIPARIAN BASIN GROUNDWATER DATA.....	126
APPENDIX H: MODEL CODE .....	127
REFERENCES.....	150

## ABSTRACT

Streams and groundwaters interact in distinctly different ways during flood versus base flow periods. Recent research in the Upper San Pedro River using isotopic and chemical data shows that (1) near-stream, or ‘riparian,’ groundwater recharged during high streamflow periods is a major contributor to streamflow for the rest of the year, and (2) the amount of riparian groundwater derived from this flood recharge can vary widely (10-90%) along the river. Riparian groundwater in gaining reaches is almost entirely basin groundwater, whereas losing reaches are dominated by prior streamflow.

This description of streamflow gives rise to the questions of (1) how much flood recharge occurs at the river-scale, and (2) subsequently, what is the relative importance of flood recharge and basin groundwater in maintaining the hydrologic state of the riparian system. To address these questions, a coupled hydrologic-solute model was constructed for 45 km of the Upper San Pedro riparian system—one of only a few free-flowing riparian systems remaining in the Southwest. The model domain is divided into segments, with each segment representing a distinctly gaining or losing reach. Surface-subsurface water exchange is regulated by hydraulic properties of the system calculated based on observed groundwater level response to flood waves. Daily discharge data at three points and chemical/isotopic river and groundwater data at various locations along the river were used to calibrate the model from 1995 to the present.

Model results indicate good agreement between our model and the overall

hydrologic and chemical/isotopic riparian system behavior. Less than 52% of total summer flood recharge occurs in the most upstream ~70% of the river, where gaining conditions dominate. The summer recharge in this upper section of the river accounts for more than 30% of groundwater contributions to the river during lower flow periods.

Total recharge along the lower losing reaches is almost equally divided between flood and baseflow recharge, thus indicating that both recharge components are equally important in maintaining the shallow riparian water tables essential to the riparian forest below Charleston.

## 1. INTRODUCTION

Groundwater-surface water interactions have been the focus of numerous previous studies. Some of this research has dealt with groundwater contributions to surface flow during periods of both high (Pearce et al., 1986; McDonnell, 1991) and low flow (Peters and Ratcliffe, 1998; Baillie et al., 2007). Other research has focused on channel infiltration (Cox and Stephens, 1988; Gillespie and Perry, 1988; Stephens, 1988; Goodrich et al., 1997; Ponce et al., 1999; Harrington et al., 2002; Plummer et al., 2004) particularly as it relates to ephemeral channels in arid and semi-arid regions. Models have been designed to better understand and quantify this recharge (Osterkamp et al., 1994; Marie and Hollett, 1996; Sorman et al., 1997; Sanford et al., 2004; Waichler and Wigmosta, 2004). Most channel infiltration studies are focused on channel recharge flux as it relates to large scale groundwater flow systems.

This past research has focused on one-directional river-aquifer exchange: either as groundwater sustaining baseflow in gaining streams or as streamflow recharging groundwater in losing streams. However, both of these processes can occur in different sections in a river system (Rushton, 2007), and more importantly, a given system or reach may be losing during high flow/river stage but become gaining as flow declines and the hydraulic gradient shifts toward the channel. Studies have shown that such two-way exchange does occur and that it can impact riparian groundwater and streamflow chemical composition long after floodwaters recede (Squillace, 1996; Whitaker, 2000; Baillie et al., 2007). Chemical and isotopic signatures of the Upper San Pedro River (Figure 1) and adjacent “riparian

groundwater” (Baillie et al., 2007) suggest that it is a gaining/losing stream, and that riparian groundwater with a distinct component of flood recharge can be detected at great distances from the river’s edge long after flood waters recede.

The influence of flood recharge on riparian groundwater implies that floodwater infiltrating during high flow can have substantial implications for both the quantity and quality of river baseflow and riparian groundwater. Data collected along the Upper San Pedro River suggests that flood recharge with high nitrate concentrations could serve as a post-flood nutrient source for in-stream and riparian environments (Figure 2, also Brooks and Lemon (2007)). Quantifying the volume of summer flood recharge and tracking the movement of this water through the riparian system after flood recession is the first step in understanding the role of nutrient-rich floodwater on riparian biogeochemistry and hydrology.

Developing a detailed river-aquifer exchange model is the most logical means to quantify recharge at the river scale, particularly in a gaining/losing river where hydrologic conditions (such as the degree of interaction between the basin and riparian aquifers, transpiration flux) vary along the river. Construction of such a model will allow the following questions to be answered:

- 1) How much summer flood recharge occurs along the river? How does this compare to phreatophyte transpiration and groundwater discharge to the river?
- 2) Where is flood recharge highest along the river?
- 3) How much riparian groundwater and streamflow is flood recharge at

different points along the river? How does this change with increasing time after floods?

## 2. STUDY AREA / BACKGROUND

The Upper San Pedro River originates in Sonora, Mexico, and flows northward into southeastern Arizona, where much of the riparian corridor is contained within the San Pedro Riparian National Conservation Area (SPRNCA, Figure 1). The entire San Pedro River Basin is part of the Basin and Range geologic province, which is characterized by roughly parallel mountain ranges resulting from expansion of the earth's crust. The basins between each pair of adjacent ranges (including the San Pedro Basin) are typically filled with alluvial deposits of varying thicknesses. The major water-bearing units of the basin aquifer in the Upper San Pedro Basin are these alluvial deposits, which are divided between Upper and Lower Basin Fill (Pool and Coes, 1999). Depth to bedrock gradually decreases along the river for roughly 15 km upstream of Charleston (Figure 3), forcing water from the basin aquifer toward the surface and into the riparian system (pl. 1, Pool and Coes (1999)). This upward flux of water results in the strongly gaining, perennial stream reaches observed along this portion of the river. Not far downstream of Charleston the depth to bedrock increases dramatically resulting in a losing, ephemeral stream reach as observed at the downstream gauge near Tombstone.

Most of the annual discharge of the Upper San Pedro occurs during the summer as a result of short-duration, high-intensity rainfall events characteristic of the North American Monsoon. Winter rainfall is typically less intense, resulting in less streamflow generation. However, winter precipitation makes up approximately 75% of recharge to the basin aquifer based on isotopic analyses (Wahi et al., 2007),

with the remaining 25% originating as summer precipitation. Isotopic and anion chemical signatures between average basin groundwater and summer precipitation allowed for the assessment of the relative contributions of each component to riparian groundwater and baseflow in Baillie et al. (2007).

### 3. FIELD SAMPLING & ANALYTICAL METHODS

Three surface and groundwater sampling campaigns were conducted to supplement the available USGS-NWIS database (available through [water.usgs.gov](http://water.usgs.gov)) and data collected by Baillie et al. (2007). Four monitoring well transects were chosen: two in predominantly gaining/perennial reaches (Lewis Springs, Moson) and two in losing/intermittent reaches (Palominas, Contention). Before sampling, depth to groundwater was measured and, with prior knowledge of total well depth, water volume within the casing was calculated. At least three times the well volume was pumped before sample collection. During each visit a duplicate sample was collected at each site. River water samples were collected at each transect four times (Aug. 5, Oct. 7, Oct. 27, and Dec. 9, 2006), with three of these dates (all except Oct. 27, 2006) coinciding with well sampling campaigns.

Samples were filtered in the lab in a timely manner after collection with 0.45  $\mu\text{m}$  MCE membrane filters and analyzed for a suite of seven anions ( $\text{F}^-$ ,  $\text{Cl}^-$ ,  $\text{NO}_2^-$ ,  $\text{Br}^-$ ,  $\text{NO}_3^-$ ,  $\text{SO}_4^{2-}$ , and  $\text{PO}_4^{3-}$ ) using a Dionex Ion Chromatograph (IC) located at the University of Arizona. Analytes were separated using an AS17 analytical column and a KOH gradient produced by an EG 50 eluent generator and a GS50 gradient pump. The KOH eluent was removed using an ASRS suppressor column, allowing anion concentrations to then be quantified using a CD25 conductivity detector. Detection limits were approximately 0.025 ppm for all anions except  $\text{PO}_4^{3-}$ , which had a detection limit of roughly 0.1 ppm. Replicate analysis of samples and standard typically agree within 5% or better for concentrations greater than 1 ppm and 10% or

better from samples less than 1 ppm. Isotopes of hydrogen and oxygen were analyzed at the Laboratory of Isotope Geochemistry at the University of Arizona. Water stable isotope measurements ( $\delta^2\text{H}$  and  $\delta^{18}\text{O}$ ) were made on a gas-source Finnigan Delta S Isotope Ratio Mass Spectrometer (IRMS) following reduction by Cr metal at 750°C (Gehre et al., 1996), or  $\text{CO}_2$  equilibration at 15°C (Craig, 1957), respectively. Results are reported in per mil (‰) relative to VSMOW (Gonfiantini, 1978) with precisions of at least 0.9‰ for  $\delta^2\text{H}$  and 0.08‰ for  $\delta^{18}\text{O}$ . The laboratory also uses the SLAP international standard (Coplen, 1995) during analysis.

#### 4. MODEL STRUCTURE: WATER BALANCE

The explanation of the water balance component of the model structure will be developed in the same manner that the model was developed: starting with the prior understanding of the system and how that influenced the partitioning of the riparian system into hydrologically similar reaches. The interaction of each of these reaches—based on the gaining/losing reach division—with the basin aquifer, and the role riparian evapotranspiration plays in determining basin exchange, will follow. Thereafter, the justification for the model’s treatment of river-aquifer exchange and transfer of streamflow downstream will conclude the discussion of water movement within the model.

##### 4.1 Background

Stromberg et al. (2005) developed a vegetation-based model for assessing hydrologic conditions along the San Pedro River. This model used a series of nine bioindicators (listed in Appendix C) to assign condition scores to 26 sites within SPRNCA. Each site was placed within one of three condition classes based on these scores and the river was divided into reaches based on these classes. Class 1 (‘dry’) reaches were characterized by deep riparian groundwater with large intra-annual water table fluctuations and streamflow present less than 50% of the year (Table 1). Class 2 (‘intermediate’) reaches exhibited a shallower, more stable water table and more permanent streamflow than class 1. Class 3 (‘wet’) reaches were characterized by shallow and stable water tables, while exhibiting near-permanent surface flow

(>99% of the year).

The correlation between the bioindicator classification and riparian characteristics (e.g. perennial and gaining—with respect to basin groundwater—versus intermittent and losing) was confirmed by Baillie et al. (2007). Using  $\delta^{18}\text{O}_{\text{H}_2\text{O}}$ ,  $\delta^2\text{H}_{\text{H}_2\text{O}}$  and  $\text{SO}_4/\text{Cl}$  ratios in basin groundwater, streamflow and riparian groundwater samples along the river, Baillie found that riparian groundwater from Stromberg's class 3 reaches were predominantly basin groundwater ( $\geq 60\%$ ), consistent with the predominantly gaining conditions. In contrast, riparian wells located within class 2 reaches all contained  $>70\%$  monsoon floodwaters (e.g.  $<30\%$  basin groundwater), consistent with predominantly losing conditions in the river. The strong agreement between the chemical/isotopic water source characterization and condition class reach characterizations suggests that the more spatially-complete condition class system can be used to determine the degree to which the river is gaining or losing along its length. Thus, changes in vegetation along the river were used to divide the river into the series of reaches (or segments) necessary for the model developed in this study.

#### 4.2 Model Domain Partitioning

The domain of the model is bounded by the USGS stream gage at Palominas, AZ (9470500), and the USGS well transect near Contention, which is just north of the USGS gage near Tombstone, AZ (9471550, Figure 3). This distance spans all or part of 12 reaches as defined by Stromberg et al. (2005). These 12 reaches were

consolidated into nine model segments, as shown in (Figure 3), in the interest of reducing model run time and creating roughly equal length segments. Each model segment is composed of three reservoirs: a riparian groundwater (RGW) reservoir, a smaller near-stream zone (NSZ) (after Chanat and Hornberger, 2003) and a river channel (Figure 4). Water and solutes are exchanged only between adjacent reservoirs.

The hydrologic response of the system to changes in river discharge is governed by the state of the riparian aquifer system. Thus, the processes affecting riparian groundwater levels need to be clearly defined in order to better reproduce the state of the system and subsequent behavior. The dominant processes (Figure 4) controlling the overall water balance of the Upper San Pedro's riparian aquifer are: (1) basin groundwater exchange to the riparian aquifer (magnitude and direction), (2) groundwater losses to phreatophyte transpiration, and (3) river/aquifer exchange (magnitude and direction, which depend on relative water levels in the river and adjacent riparian aquifer). The methodology used to define each of these interdependent processes/fluxes within the model are described below. A summary of the parameters and state variables used to describe the behavior of the system are defined in Table 2.

#### 4.3 Basin/Riparian Groundwater Exchange and Evapotranspiration

Additions or subtractions from the riparian aquifer with respect to basin groundwater (Figure 4) vary between river segments and are treated as constant in

time. This assumption of time-invariability was made because of the lack of data to suggest that changes in groundwater flux are significant at the scale of the model time step, which is one day.

#### 4.3.1 Gaining River Reach ET and Groundwater Estimates

Perennial streamflow in the gaining ('wet') reaches of the river (which correspond to model segments 2, 4, 5, and 6) suggests that, in order for the river to remain gaining year round, the basin groundwater influx to the riparian system must exceed losses to phreatophyte ET from the riparian aquifer during the period of greatest ET flux (e.g. June or July, depending on monsoon onset).

Baird et al. (2005) determined daily ET rates for the four phreatophyte types found along the San Pedro (mesquite, cottonwood, tamarisk and sacaton grass) as a function of water table depth and the time of year (Figure 5A-C). With these ET versus depth curves, vegetation maps (Kepner et al., 2003) and depth to groundwater data (based on land surface and water level elevations near the river from Leenhouts et al., 2005), daily ET losses are calculated for each model segment.

##### *Example ET flux calculation (model segment 4):*

According to the EPA/USDA-ARS vegetation survey conducted in November 2000 (Kepner et al., 2003), the area defined as segment 4 has phreatophyte cover within 100 m of the active river channel as follows: 39.3% cottonwood ( $FracCot=0.393$ ), 6.9% mesquite ( $FracMes=0.069$ ), 25.9% sacaton ( $FracSac=0.259$ ) and 0% tamarisk (see Table 3, in bold). A reasonable depth to groundwater for a day

in June (e.g. pre-monsoon) is 1.78 m below land surface based on data from the USGS well transect near Lewis Springs (Figure 6). The ET for a unit canopy area under these conditions could then be represented as the cumulative ET from each phreatophyte group based on (1) the fraction of each segment covered by each group (e.g.  $FracCot$ ) and (2) the depth-to-water-dependent ET flux for each group (e.g.  $ET_{COT}(t,d)$ , see Figure 5), or:

$$ET(t,d,veg) = FracCot \cdot ET_{COT}(t,d) + FracMes \cdot ET_{MES}(t,d) \dots \\ \dots + FracSac \cdot ET_{SAC}(t,d) + FracTam \cdot ET_{TAM}(t,d),$$

where  $t=June$ ,  $d=1.78$  m,  $FracCot=0.393$ ,  $ET_{COT}(June,1.78m)=4.20$  mm H<sub>2</sub>O,  $FracMes=0.069$ ,  $ET_{MES}(June,1.78m)=0$ ,  $FracSac=0.259$ ,  $ET_{SAC}(June,1.78m)=3.34$  mm H<sub>2</sub>O, and  $FracTam=0$  (Figure 5b, Table 3). This converts to

$$ET(June,1.78m,veg) = [0.3934 \cdot 0.00420 \text{ m/day} + 0 \dots \\ \dots + 0.259 \cdot 0.00334 \text{ m/day} + 0] = \mathbf{0.00252 \text{ m/day}}.$$

This result of 0.00252 m/day (2.52 mm/day) represents the phreatophyte ET flux from one representative square meter of riparian forest.

Within the model, all calculations with respect to the inputs from basin groundwater ( $Q_{bgw}$ ) and equations of state and exchange for the RGW and NSZ reservoirs are made on a *per-meter of river length* basis, and thus expressed in units of m<sup>2</sup>/day. Thus, to remove the proper amount of water from the RGW tank, the ET flux calculated above must be multiplied by the width of the RGW tank (100 m). Thus, the amount of water lost to ET from a single, representative meter of the riparian system during greatest water stress is **0.252 m<sup>2</sup>/day**. Segment 4 has shown

perennial flow, so this value is treated as a lower limit when selecting an input value from basin groundwater ( $Q_{bgw}(4)$ ). Identical calculations were also made for the other segments with perennial flow (2, 5 and 6).

#### 4.3.2 Losing River Reach ET and Groundwater Estimates

For losing reaches, water isotope data collected at the USGS Palominas well transect during this study indicated the likely influence of basin groundwater (Figure 7). One possible explanation for this is that the transect is downstream from a gaining reach, which contributes surface flow with a basin groundwater isotopic composition that is then lost to the riparian aquifer near Palominas. However, there is no evidence to suggest significant gaining conditions upstream and, when considering that annual groundwater fluctuations at Palominas do not differ greatly from those in confirmed gaining reaches such as Moson and Lewis Springs (Leenhouts et al., 2005), it appears most likely that there is a positive gradient toward the river from the basin aquifer. The intermittence of streamflow implies that the magnitude of this flux must fall between zero and the pre-monsoon phreatophyte ET flux. For segment 1, this perimeter ET flux was calculated (as shown in the example ET calculation for segment 4 on pages 22-23) to be  $0.183 \text{ m}^2/\text{day}$ , which is the upper limit for the basin groundwater input (or,  $0 < Q_{bgw}(1) < 0.183 \text{ m}^2/\text{day}$ ).

Basin groundwater input is more difficult to approximate in segment 3 because of the influence of an upstream gaining reach and very little existing data. Based on streamflow permanence data from Leenhouts et al. (2005), the river stopped

flowing at the Hunter transect (located in segment 3) during November of 2001 and 2002 (the only two years for which there is streamflow permanence data). This same data shows that the river flows in segment 2 every November. This implies that the river must be losing at least as much water in segment 3 as it gains from segment 2. Well hydrographs at the Hunter transect (Figure 8) indicate that during November the water table rises slightly which necessarily means an increase in riparian groundwater storage volume ( $\Delta S_{RGW} > 0$ ). There are only three fluxes relative to the RGW reservoir: basin groundwater ( $Q_{bgw}$ ), ET, and exchange with the river/NSZ ( $q_{surface}$ ). Since the riparian aquifer is gaining with respect to the river (e.g. since the river is losing), the three quantities are positive. Thus, knowing  $\Delta S_{RGW} > 0$  and requiring the conservation of mass,

$$\Delta S_{RGW}(3) = q_{surface} + Q_{bgw} - ET > 0 \quad (1a)$$

$$Q_{bgw}(3) > ET - q_{surface} \quad (1b)$$

Using the equation at the top of page 23, the per-meter ET flux for segment 3 in November was found to be  $0.071 \text{ m}^2/\text{day}$ . The Hunter transect is approximately 2.4 km downstream from the boundary between segments 2 and 3 (e.g. where the river switches from perennial to intermittent and begins to lose flow), thus the outflow from segment 2 ( $Q_{out}(2) = 1656 \text{ m}^3/\text{day}$ ) must be lost over no more than 2.4 km of river length. Therefore the amount of water lost per meter of this 2400 m reach ( $q_{surface}$ ) equals  $1656 \text{ m}^3/\text{day} \div 2400 \text{ m} = 0.690 \text{ m}^2/\text{day}$ . Equation 1b then becomes

$$Q_{bgw}(3) > 0.071 - 0.690 = \mathbf{-0.619 \text{ m}^2/\text{day}} \quad (1b\text{-ii})$$

Considering (1) the similar groundwater response pattern observed at the Hunter and Palominas transects (Figure 8), and (2) that Hunter is downstream from a strongly gaining reach and maintains streamflow only intermittently, it appears reasonable that there is less basin groundwater influence at Hunter than at Palominas. Therefore, it is a necessary condition within the model that

$$-0.619\text{m}^2/\text{day} < Q_{bgw}(3) < Q_{bgw}(1).$$

Segment 7 has similar characteristics to segment 3. Both are directly below perennial, gaining reaches and have identical condition scores (Figure 9). Therefore, the same approach was used in determining the basin groundwater flux for segment 7 as was used for segment 3.

$$Q_{bgw}(7) > ET - q_{\text{surface}} = 0.094 - 0.568 = \mathbf{-0.474 \text{ m}^2/\text{day}} \quad (1b-3)$$

As previously noted, Pool and Coes (1999) showed smaller depths to bedrock in the perennial reaches (represented by model segments 4-6) than in the intermittent reaches below them (segments 7-9). The decrease in streamflow permanence (Leenhouts et al., 2005) from Boquillas (segment 7) downstream to Contention (at the end of segment 9) suggests consistently losing conditions (even during winter when ET is zero). Therefore, the model requires that basin groundwater fluxes in segments 8 and 9 are always negative. The complete model requirements regarding basin groundwater flux can be found in table (Table 4).

After exchange of water between basin and riparian groundwater (and again after ET removal), water table elevation in the RGW reservoir is recalculated for each segment using the relation:

$$GWElev_{Final} = GWElev_{Initial} + (Q_{BGW}/Width_{RGW}) * S_y, \quad (2)$$

where  $GWElev_{Final}$  is the groundwater elevation after either groundwater exchange or ET removal,  $GWElev_{Initial}$  is the groundwater elevation before the water exchange,  $Width_{RGW}$  is the width of the RGW reservoir, and  $S_y$  is the specific yield of the riparian aquifer. To avoid adding any further complexities (or uncertainties) to the model, the specific yield is assumed to be the drainable porosity ( $S_y = \theta_r - \theta_s$ ), thus neglecting any impact of the unsaturated zone. Initial saturated and residual water content ( $\theta_s$  and  $\theta_r$ , respectively) values of 0.37 and 0.05 were chosen. These estimates are based on data collected near the Lewis Springs well transect (Whitaker, 2000).

#### 4.4 River/Aquifer Exchange

The direction of exchange between the river/near-stream zone and the riparian aquifer is determined by the elevations of the river surface and water table in the RGW reservoir (Figure 4). At each time step, river surface elevation is calculated based on the river bottom elevation and stage/discharge curves specific to transects in each river segment (Figure 10). River bottom elevation is calculated using the river stage at which no flow occurs (y-intercept of stage/discharge curves), streambank surface elevation and the depth to groundwater in wells next to the river (Figure 11). The groundwater depths next to the river at low/zero flow are presumed to be the depth of riverbank entrenchment as defined in Figure 11. These entrenchment depths for each segment are based on surface surveys of thirteen transects between and

including Palominas and Contention (based on Leenhouts et al. (2005), values in Appendix D). An example of this data and depth to water near zero-flow conditions at the Lewis Springs well transect is shown in Figure 6. Water table elevation estimates at each survey point on each transect were made by Leenhouts et al. (2005) using piezometer(s) and/or stream stage. Due to the restriction in the model of a single depth-to-water value for each segment cross-section, the average depth-to-water during low-flow conditions (September 2002) is used as the ‘Entrenchment Depth’ as defined in Figure 11. For segments containing more than one transect with this water table depth data, the average entrenchment from all transects within the segment is used as the single entrenchment depth.

The river bottom elevation then is calculated using the relation:

$$\text{River Bottom Elev.} = \text{Surface Elev.} - \text{Entrenchment Depth} - \text{Zero flow River Stage}$$

The amount of water exchanged between the river and RGW reservoir is determined by a form of Darcy’s Law:

$$q = T \cdot dh/dl, \quad (3)$$

where  $q$  is the volume of water gained/lost per meter of river length per day [ $\text{m}^2/\text{day}$ , or  $\text{m}^3/\text{m}\cdot\text{day}$ ];  $dh$  = (groundwater elevation – river surface elevation), [m]; and  $dl$  is half the width of the RGW reservoir [m] (Figure 12). When the groundwater elevation is greater than the river surface elevation,  $q$  is positive and the river gains flow from the near-stream zone, which gains an equal amount from the riparian aquifer. When the water table is lower than the river surface,  $q$  is negative and the river loses flow to the near-stream zone, which loses the same amount to the riparian

aquifer. In equation 3,  $T$  represents the near-stream aquifer transmissivity [ $\text{m}^2/\text{day}$ ], which is based on the aquifer diffusivity calculated using the iterative curve matching method developed by Pinder et al. (1969).

#### 4.4.1 Diffusivity Estimation

Pinder et al. (1969) used a finite step equivalent of Duhamel's formula to determine aquifer diffusivity (the ratio of transmissivity to storage coefficient) based on paired river stage data and well hydrographs in a floodplain aquifer. For a semi-infinite aquifer, such as those along the Upper San Pedro (with no known impermeable aquifer boundary), the formula simplifies to equation 4:

$$h_p = \sum_{m=1}^p \Delta H_m \left\{ \text{erfc} \frac{u}{2\sqrt{p-m}} \right\}, \text{ where } u = \frac{x}{\sqrt{D\Delta t}} \quad (4)$$

where  $h_p$  is the head [L] at a distance  $x$  [L] from the river at time  $t=p\Delta t$ ;  $p$  is the integer time step for which  $h_p$  is being calculated;  $\Delta H_m$  is the instantaneous change in river stage between times  $m-1$  and  $m$  for a given value of  $p$ ; and  $D$  is the aquifer diffusivity. The value of  $D$  is iteratively changed until the rising limb of the calculated (or, 'predicted') well curve closely matches that of the observed well hydrograph (Figure 13). Only the rising limb and peak are used because the saturated thickness of an unconfined aquifer (and thus the transmissivity and diffusivity) does not remain constant during the propagation of a flood pulse into the streambank.

This method has been applied effectively to settings with semi-infinite aquifers similar to the Upper San Pedro (Reynolds, 1987).

Once a suitable value of diffusivity is obtained, a transmissivity value ( $T$ ) can be calculated for equation 3 by the relation  $T = D \cdot S$ , where  $S$  is the dimensionless aquifer storativity (Freeze and Cherry, 1979). The floodplain/riparian aquifer in the Upper San Pedro is unconfined, thus the unconfined storativity (more commonly called specific yield,  $S_y$ ) is used.

A series of nine flood pulses observed at the Lewis Springs transect between Aug. 4, 2006 and Sept. 8, 2006 were used to calculate diffusivity values across a range of antecedent moisture conditions (Figure 14). The range of values found is a testament to the impact of differing antecedent conditions and/or hydraulic properties between different layers of the aquifer. For lack of any coupled river and well hydrograph data other than that from Lewis Springs, the diffusivity (and subsequent transmissivity) values were applied to all model segments despite the uncertainty in applying the values to the entire model domain.

After exchange of water between the river and RGW reservoirs, groundwater elevations are again recalculated by equation 2, with  $q$  substituted for  $Q_{bgw}$ . The resulting  $GWElev_{Final}$  value is used as the  $GWElev_{Initial}$  for the next time step.

#### 4.5 Transfer of Water Downstream

After exchange with the RGW and near-stream reservoirs, the per-meter flux of water into or out of the river [ $m^2/day$ ] is multiplied by the segment length [ $m$ ] to

give the flow volume [ $\text{m}^3/\text{day}$ ] gained or lost along the entire reach:

$$Q_{out} = Q_{in} + q \cdot SegLength \quad (5)$$

The change in flow volume is then added or subtracted from the surface flow entering the segment. In the case of segment 1, this inflow is the USGS-gaged flow data from Palominas. For all other segments, surface inflow is the outflow from the segment immediately upstream calculated during the same time step. Thus, travel time within the stream is ignored. This approach is not unreasonable given the daily time step of the model and the observed range of peak flow travel times from Palominas to Tombstone (11.5-13.75 hours) for four storms of varying size in 2006.

Adjoining model segments are only connected through the river, which is to say there is no groundwater flow parallel to the river. This assumption is made because (1) the alternating gaining/losing character of the river and longitudinally-variable groundwater fluctuations (Leenhouts et al., 2005) do not suggest significant longitudinal hydrologic connection within the riparian aquifer, and (2) groundwater flow parallel to the river (based on the complete range of  $T$  values calculated above and the elevation and UTM coordinates of the Palominas and Contention transects, which resulted in a  $dh/dl$  value of approximately 0.003) would be 9.80 to 245  $\text{m}^3/\text{day}$ —more than two to four orders of magnitude less than the observed average streamflow during the time domain of the model at all three discharge-rated USGS gages (Palominas=67,800  $\text{m}^3/\text{day}$ ; Charleston=79,100  $\text{m}^3/\text{day}$ ; Tombstone=89,600  $\text{m}^3/\text{day}$ ). Thus, at any given point, the river has far greater influence on the behavior of the riparian system than does the riparian aquifer up-gradient. Despite this

assumption, however, the use of water table and river surface elevations (rather than relative heights) in all water exchange calculations provides the potential for later alteration of the model to include riparian groundwater flow parallel to the river should it be deemed significant.

## 5. MODEL STRUCTURE: CONSERVATIVE TRACERS

As noted in Section 4.1 (Model Structure: Water Balance Background), prior research has found that the ratio of sulfate to chloride ( $\text{SO}_4/\text{Cl}$ ) and water isotopes ( $\delta^{18}\text{O}$ ,  $\delta^2\text{H}$ ), when combined, are good indicators of the source of water in the Upper San Pedro riparian system. Therefore, these conservative hydrologic tracers are used in the model presented here. The methodology used for the chemical/isotopic component will be outlined similarly to the water balance portion: riparian exchange with the basin aquifer followed by chemical changes to the riparian aquifer resulting from phreatophyte evapotranspiration, river/aquifer exchange, and river flow downstream. A conceptual model of how water moves through the system will precede the more detailed tracer methodology. A flow diagram of this conceptual model is provided in Figure 15.

### 5.1 Summary: Tracking Water Movement Through The Model

For a given parcel of water entering the system, there are a number of potential fates. Surface flow, whether entering at Palominas or farther downstream within the model domain, can either be added to groundwater discharged to the river (when groundwater elevation is greater than river surface elevation), remain in the channel with volume and chemical/isotopic composition unchanged (when groundwater elevation is equal to river surface elevation), or lost to the NSZ/RGW reservoirs (when groundwater elevation is less than river surface elevation). In either

of the first two cases, the water parcel is conveyed to the next segment downstream where it encounters the same three potential fates.

If surface flow is lost to the groundwater system during elevated flows, it will have the net effect of adding the water volume lost from the river to the RGW reservoir, by way of the constant-volume, continually-saturated NSZ. The existence of the NSZ has no impact on the water partitioning—only on the chemical/isotopic composition of each reservoir. Once in the groundwater system, the parcel of water mixes with the reservoir volume from the previous time-step. If the segment where the water parcel recharged has a regional gradient toward the river (e.g.  $Q_{bgw}$  flux is positive, and thus *into* the RGW reservoir), the RGW water volume containing the original parcel of water will be mixed with this basin groundwater addition. If the segment's overall gradient is away from the river ( $Q_{bgw} < 0$ ), a portion of the original water parcel will be lost to the basin aquifer.

In either case, following the basin aquifer exchange, a portion of the original parcel will be lost to phreatophyte ET—this amount will depend on vegetative cover and depth to groundwater as discussed above. After ET removal from the RGW reservoir, the direction of exchange between the river and groundwater system will dictate whether the entire residual portion of the original water parcel will remain in the RGW reservoir or if a portion of it will re-enter the NSZ and/or the river.

## 5.2 Basin/Riparian Groundwater Exchange

The chemical and isotopic compositions of basin groundwater are only needed

for those model segments that gain water from the basin aquifer (segments 1, 2, 4-6 and potentially segment 3). For these basin groundwater-gaining segments, basin wells with at least one sample analyzed for  $\text{SO}_4$ , Cl,  $\delta^{18}\text{O}$ , and  $\delta^2\text{H}$  are used as chemical inputs to the model (Figure 3). Following addition of basin groundwater, the resulting riparian groundwater chemistry is calculated using the relation:

$$C_{new} = (C_{in}V_{in} + C_{prev}V_{prev}) / V_{tot} \quad (6)$$

where  $C_{new}$  is the desired RGW concentration after basin groundwater addition,  $C_{in}$  is the basin groundwater concentration,  $V_{in}$  is the volume added (e.g.  $Q_{bgw}$ ),  $C_{prev}$  is the initial concentration in the RGW reservoir,  $V_{prev}$  is the initial volume of the RGW reservoir and  $V_{tot} = V_{in} + V_{prev}$ . In the case of  $^{18}\text{O}$  and  $^2\text{H}$ , per-mil ( $\delta$ ) values are used rather than concentrations. Segments that lose riparian groundwater to the basin aquifer (segments 7-9 and potentially segment 3) do not require basin groundwater data and these recalculations are omitted.

### 5.3 Evapotranspiration

ET is removed exclusively from the riparian aquifer and is treated as a process that does not isotopically fractionate or remove any conservative solutes. Therefore, ET only decreases the volume of water in the RGW reservoir and results in an increase in the concentrations of sulfate and chloride (however, the  $\text{SO}_4/\text{Cl}$  ratio remains the same). Resulting  $\text{SO}_4$  and Cl concentrations in the RGW reservoir are determined using the relation

$$C_{PostET} = (C_{PreET} \cdot V_{PreET}) / V_{PostET} \quad (7)$$

#### 5.4 River/Aquifer Exchange

When the river is losing, river chemistry is unaltered, whereas RGW and NSZ chemistry changes. For the RGW reservoir, resulting concentrations are:

$$C_{RGW(final)} = (C_{NSZ(initial)} \cdot \mathbf{q} + C_{RGW(Initial)} V_{RGW(Initial)}) / V_{RGW(final)} \quad (8)$$

For the constant-volume NSZ:

$$C_{NSZ(final)} = ((C_{River} \cdot \mathbf{q} + C_{NSZ(initial)}(V_{NSZ} - \mathbf{q})) / V_{NSZ} \quad (9)$$

For cases when the river is gaining, riparian groundwater chemistry does not change. River and NSZ chemistry do, however, and concentrations/per-mil values are recalculated by the relations

$$C_{RiverOutflow} = (C_{RiverInflow} Q_{RiverInflow} + C_{NSZ} V_{NSZ}) / Q_{RiverOutflow}, \quad (10)$$

$$C_{NSZ(final)} = (C_{RGW} \cdot \mathbf{q} + C_{NSZ(Initial)}(V_{NSZ} - \mathbf{q})) / V_{NSZ}, \quad (11)$$

In instances when more water is exchanged between the river and aquifer than is contained in the NSZ reservoir (e.g.  $\mathbf{q} < V_{NSZ}$ , which occurs only during—and potentially shortly after—the highest river flows), a different set of equations are implemented to account for the addition of water with the chemical composition from two chemically- and isotopically-distinct reservoirs. When the river loses more water than can be stored in the NSZ, the expressions are

$$C_{RGW(final)} = (C_{NSZ(Initial)} \cdot V_{NSZ} + C_{River} \cdot (\mathbf{q} - V_{NSZ}) + C_{RGW(Initial)} V_{RGW(Initial)}) / V_{RGW(final)} \quad (12)$$

$$C_{NSZ(final)} = C_{River} \quad (13)$$

Under gaining conditions when the river is gaining water from both the NSZ

and RGW reservoirs, the expressions are

$$C_{RiverOutflow} = (C_{NSZ(Initial)} \cdot V_{NSZ} + C_{RGW} \cdot (q - V_{NSZ}) + C_{RiverInflow} Q_{RiverInflow}) / Q_{RiverOutflow} \quad (14)$$

$$C_{NSZ(final)} = C_{RGW} \quad (15)$$

For each segment, the final RGW and NSZ concentrations for each time step are stored and used as the initial concentrations for the following time step (day).

### 5.5 Transfer of Water Downstream

After all appropriate recalculations are completed following solute exchange, final streamflow chemistry from one segment is stored and implemented as the river inflow chemistry to the next segment for the same time step.

## 6. MODEL INPUTS

Both water and chemical/isotopic inputs are critical parts of the model because of the input-dependence of the state and outputs of the model, on which model performance will ultimately be judged. This section will outline both the water volume and chemical/isotopic data implemented in the model, whether observed or inferred, for streamflow and basin groundwater entering the model domain.

### 6.1 Streamflow Volume

Mean daily river discharge gauged at the USGS gage near Palominas, AZ, is the main input of surface water to the model domain. These data have been reviewed and approved for publication by the USGS through September 30, 2006, and values after that date are provisional. Flow at the Palominas gage is periodically measured and there is good agreement between the measured and stage-based estimates during this provisional period.

Hydrographs from all four USGS gages within the model domain were analyzed to account for surface flows entering the river downstream from Palominas ('intra-domain inflow'). For a given portion of the river the nearest upstream and downstream hydrographs were compared to determine when and approximately where intra-domain additions must enter the stream (example: Figure 16). At times when it is determined that flow necessarily enters the river between gages, the addition of flow is made to the model segment containing the ephemeral channel with the largest contributing area, and thus where flow is most likely to have entered the

river. The amount of flow added to the river is the difference in flow volume between the downstream and upstream gages. This approach is taken in the interest of making more conservative estimates of elevated flows and subsequent flood recharge.

This method of intra-domain flow addition results in a total of  $3.60 \times 10^6 \text{ m}^3$  of water added to the river between 10/1/95 and 12/31/04. During the same period, cumulative flow at the outlet of the Walnut Gulch Experimental Watershed (Flume 1) near Tombstone, AZ, was  $3.78 \times 10^6 \text{ m}^3$ —comparable to the flow added to the river in the model. However, the contributing area to Walnut Gulch is approximately 149  $\text{km}^2$ , whereas the entire contributing area to the Upper San Pedro between Palominas and Tombstone (e.g. area within the model domain) is nearly 2,600  $\text{km}^2$ —more than 17 times that of Walnut Gulch alone. Thus, it is reasonable to say that the model underestimates surface flows entering the river downstream of Palominas.

## 6.2 Surface Flow Chemistry

Daily estimates of river chemistry and isotopic composition at Palominas had to be made due to the daily time step ( $n=4223$ ) of the model and the existence of only 24 days with  $\text{SO}_4$  and Cl data and 75 days with water isotope data from Palominas (data in Appendix E).  $\delta^{18}\text{O}$ ,  $\delta^2\text{H}$ ,  $\text{SO}_4$  and Cl values on days for which no data exists were estimated based on either recent samples or sample averages from similar times of year and hydrograph condition (Table 5, Figures 17 & 18). For example, model

input  $\delta^{18}\text{O}$  and  $\delta^2\text{H}$  values for the period between 7/15/96 and 8/12/99 are based on the shape of the hydrograph (e.g. elevated vs. low flow) and time of year. However, for the period from 11/30/00 to 8/1/02, when there is more available data, all dates are given values identical to the nearest data point. The same was done for  $\text{SO}_4$  and Cl values, although their input values rely more heavily on the averaged values due to the smaller number of samples.

Surface flows added within the model domain are given the same chemical and isotopic composition as a runoff sample collected near Hereford, AZ, on July 15, 2004 (data in Appendix F) during the Baillie et al. (2007) study. This sample is used because it is the only sample that could be definitively defined as predominantly overland flow entering from side channels within the model domain.

### 6.3 Groundwater Flux and Chemistry

The volumes of basin groundwater added to the RGW reservoir of each segment were estimated as outlined in Sections 5.2-5.3 ('Basin/Riparian Groundwater Exchange' and 'Evapotranspiration'). The chemical and isotopic composition of these inputs are based on basin wells up-gradient from each model segment with a positive flux from basin groundwater (as noted in Section 5.2). The model requires concentrations of  $\text{SO}_4$  and Cl for each member—not simply the  $\text{SO}_4/\text{Cl}$  ratio since the ratio does not necessarily mix linearly as do the two species. The variations in  $\text{SO}_4$  (1.5 to 20 ppm) and Cl (4.5 to 50 ppm) concentrations—as well as  $\delta^{18}\text{O}$  per-mil

values (-6.75 to -9.60‰) —in these up-gradient basin (‘near-riparian’) wells made use of segment-specific groundwater values more judicious than using a single basin groundwater end member for the entire domain. Therefore, for segments 1-6 (e.g. all segments which can potentially be gaining with respect to the basin aquifer) a single well was chosen which had Cl, SO<sub>4</sub>, δ<sup>18</sup>O and δ<sup>2</sup>H data for the same sample. When this criterion did not eliminate all but a single sample for each segment, either the most recent sample or the sample from a well 200+ ft deep was chosen. Data for these ‘near-riparian’ basin wells can be found in Appendix G.

## 7. MODEL OUTPUTS

For each segment and time step the following quantities are determined: river discharge flow volume ( $\text{m}^3/\text{day}$ ); ET flux ( $\text{m}^2/\text{day}$ ); groundwater elevation (m above mean sea level); per-meter groundwater storage volume ( $\text{m}^2$ ); river, near-stream zone and riparian groundwater chemistry (ppm, per mil); direction and magnitude of gradient [-] and water volume exchanged ( $\text{m}^2/\text{day}$ ).

Available data for streamflow at two downstream locations (Charleston (9471000), at the end of segment 6, and Tombstone (9471550), near the end of segment 9) can be compared to model discharge results.

Chemical and isotopic data in the river and riparian aquifer is far less complete through time. In addition to the temporal incompleteness of this data, the existing data are distributed spatially across a range of distinct points throughout the domain. The fact that water sample collection sites rarely coincide with the boundaries between model segments does not allow for any more than a qualitative comparison between the tracer data and model predictions.

## 8. RESULTS: BASE-CASE MODEL SIMULATION

A base set of parameters was selected as a starting point for model performance assessment and subsequent sensitivity analysis and optimization. These parameter values are listed in Tables 6a and 6b and were selected based on the criteria outlined for each parameter in Sections 4.3-4.4. As with model development, the results of the model simulation using this ‘base case’ parameter set is first outlined in terms of water flow through the system (‘Water Balance Results’) and then in terms of the chemical and isotopic signatures of the system resulting from the water balance portion.

### 8.1 Water Balance Results

The basin groundwater fluxes ( $Q_{bgw}$ ) were selected based on the requirements from Table 4. For those segments without either an upper or lower bound (depending on the segment), 1 m<sup>2</sup>/day and -1 m<sup>2</sup>/day were chosen arbitrarily as limits of the maximum groundwater volume exchanged per meter of river length. A diffusivity ( $D$ ) value of 3090 m<sup>2</sup>/day was chosen from those values calculated by the Pinder method (Pinder et al, 1969) using Lewis Springs well and stage data. As noted previously, a porosity of 0.37 and residual water content of 0.05 were chosen, resulting in a specific yield value of 0.32. The specific yield is the only one of these three values ( $\theta_s$ ,  $\theta_r$ ,  $S_y$ ) used in any model calculations; thus only the difference, and not the actual values, of the porosity and residual water content estimates have any impact on the model. The riparian groundwater reservoir width ( $RGWwidth$ ) was

chosen to be 100 meters, which is a rough approximation of the average floodplain width along the model domain. A riparian aquifer reservoir depth (*RGWdepth*) of 10 meters was also chosen as a groundwater data-based best guess of the maximum depth of floodwater influence. A volume of 10 m<sup>2</sup> for the near-stream zone was also chosen as a best guess of the cross-sectional area of a potentially-active surface/subsurface mixing zone.

To establish the initial state of the groundwater system, a preliminary simulation was run with the water table elevations for each segment equal to the zero-flow elevation of the river. Groundwater levels from day 4019 (10/1/06) of this initial simulation were used as the initial state of the system (10/1/95) for the ‘base case’ results presented here. This initial state was chosen because (1) it was the same day-of-water year as day 1, and (2) it is likely closer to the post-monsoon water level conditions on 10/1/95 than the initial assumption of groundwater levels being such that the entire river is neither gaining nor losing.

The discharges at the end of each model segment from the base case simulation are shown in Figure 19. Note that the perennial segments (2, 4, 5 and 6) do not cease flowing and that ephemeral segments (1, 3, 7, 8 and 9) go dry. Also note that at higher flow there appears to be greater correlation of downstream discharge with the input at Palominas than at lower flow. The simulated and observed hydrographs at the two discharge-rated USGS gages below Palominas (Charleston and Tombstone) are compared in Figure 20. In general the model does not appear as well-behaved during low flow as in subsequent, more optimized simulations

presented below.

The simulated and observed discharge time series at Charleston and Tombstone show that, because of the daily time-step and subsequent omission of travel time within the model, a given floodpeak is not always simulated on the same day(s) that it is observed at the Charleston and/or Tombstone gauges. This appears to be the source of at least some of the scatter about the 1:1 lines when comparing modeled versus observed discharges (Figure 21).

Simulated groundwater levels for each segment are shown in Figure 22. Greater fluctuations are seen at points along the river with lower condition scores (segments 1, 8 and 9), most notably during the pre-monsoon, low-flow/high phreatophyte ET flux periods. There is less groundwater level fluctuation below the baseline at these segments following large monsoons than smaller monsoon periods (e.g. water year (WY) 2001 compared to WY 2003). Gaining reaches do not experience water table fluctuations as great as do losing reaches.

The volumes of water gained or lost from each river segment are shown in Figure 23, in which positive values represent gaining river conditions and negative values represent losing river conditions. To make (1) all gaining conditions positive, (2) all losing conditions negative, and (3) small exchanges and gradual shifts from gaining to losing (or vice versa) visually noticeable, the following manipulations were made to the data shown in Figure 23:

For gaining conditions:

$$\log_{10}(\text{Volume Exchanged}) = \log_{10}(\text{Volume Exchanged} + 1),$$

and for losing conditions:

$$\log_{10}(\text{Volume Exchanged}) = -\log_{10}(|\text{Volume Exchanged}| + 1).$$

This results in (1) comparable values for both river conditions, and (2) values of zero (Figure 23) when the volume exchanged in either direction is less than 1 m<sup>3</sup>/day per river segment. Worthy of note are (1) the losing character of segments 3, 7, 8 and 9 during low flow, (2) the gaining character of segments 2, 4, 5 and 6 during low flow, and (3) the alternation between gaining and losing of segment 1, and (4) the losing character of all reaches during high flow and gaining character immediately thereafter are all.

## 8.2 Chemical and Isotopic Results

The riparian groundwater and near-stream zone reservoirs were composed entirely of basin groundwater in the preliminary simulation. Riparian groundwater chemistry from 10/1/06 of this simulation was used as the initial state of the system in the 'base case' (again because it was the same day of year and represented the best estimate of actual conditions on day 1 (10/1/06)). Simulated river, near-stream zone and riparian and basin groundwater SO<sub>4</sub>/Cl and δ<sup>18</sup>O values are shown in Figures 23-28. Flat portions of these figures indicate when the river stops flowing at a particular segment. As noted previously, river chemistry is not well-behaved during periods of low flow, but this proves to be a result of the parameter set chosen for the base case and was greatly improved during optimization.

The near-stream zone chemical/isotopic signature is almost always bounded by the riparian groundwater and river signatures. When this is not the case, the near-stream zone resembles that of prior streamflow. Riparian groundwater in losing segments is a running, volume-weighted average of prior streamflow, whereas in gaining segments riparian groundwater chemistry generally trends toward the basin groundwater end-member with punctuated departures from this trend induced by short, elevated high-flow and recharge events with distinctly monsoonal-looking high  $\text{SO}_4/\text{Cl}$  ratios and  $\delta^{18}\text{O}$  values.

## 9. SENSITIVITY ANALYSIS

### 9.1 Methodology & Results

Twenty-one parameters (Table 7) were altered separately across their observed ranges. In cases where parameters were necessarily inferred (e.g. basin groundwater flux— $Q_{bgw}$ ), the range of values allowable as defined during model development (see Section 4) were used. These ranges are shown in Table 7. The number of values chosen for each parameter perturbation varied based on the perceived importance and behavior of that parameter at the time: twenty values, evenly-spaced across the entire parameter range, were chosen for water balance parameters used across the entire domain ( $D$ ,  $S_y$ ,  $RGWwidth$ ,  $RGWdepth$  and the coefficient for ET,  $ETMult$ ). Six evenly-spaced values were used for each basin groundwater flux ( $Q_{bgw}$ ) and nine multipliers (0.5 to 1.5) were chosen for the Palominas river input values of  $SO_4$  and  $\delta^{18}O$ . Four additional values were chosen for each of the basin groundwater compositions: one for each of the combinations of  $\pm 1\sigma_{SO_4}$  and  $\pm 1\sigma_{\delta^{18}O}$ . The standard deviation ( $\sigma$ ) for both  $SO_4/Cl$  and  $\delta^{18}O$ , based on the basin groundwater end-member data from Baillie et al (2007)), is 0.4.

The difference in number of perturbations should not affect the overall assessment of parameter sensitivity because of the objective function created to rank sensitivity. The function (after van Griensven and Meixner (2006)) used to determine the relative sensitivity of each output to each parameter is:

$$\text{Score} = \frac{\sum_{n=1}^{N=N_{\text{pert}}} \sum_{t=1}^{t=t_{\text{max}}} [O_{\text{pert}} - O_{\text{base}}]^2}{N_{\text{pert}} [\text{Par}_{\text{MAX}} - \text{Par}_{\text{MIN}}]}$$

In this “Score” function,  $O_{\text{base}}$  is a given output (e.g. river discharge leaving segment 4, ET flux from segment 7, etc.) from the base case model simulation and  $O_{\text{pert}}$  is the same output for a model run using a different value of parameter,  $Par$ . These departures from the base case are squared (to ensure no cancellation of errors), summed for the entire model time-domain (e.g. from  $t=1$  to  $t=t_{\text{max}}$ ), and averaged for all the perturbations ( $N=N_{\text{pert}}$ ) of parameter  $Par$ . This quantity is then divided by the range of values across which parameter  $Par$  is altered ( $Par_{\text{MAX}}-Par_{\text{MIN}}$ ) in an attempt to prevent the order of magnitude of a parameter from impacting the perceived sensitivity of the model. The above “score” function results in a single value for each model output for each perturbed parameter, making it possible to rank the sensitivity of each output to each parameter. All parameters to which a given output is shown to be sensitive are subsequently given a score-based rank: the parameter with a rank of one corresponding to the most sensitive (e.g. with the highest score), with rank increasing with decreasing sensitivity.

To compare the same output across all nine model segments to provide the overall sensitivity of the model to a given parameter, these ranks are used in a second function:

$$\text{Importance} = \frac{\sum_{s=1}^9 \left( \frac{R}{R_{MAX}} \right)}{9}$$

where  $R$  is the rank based on the “Score” function described above and  $R_{MAX}$  is the total number of parameters to which a given output is sensitive. For instance,  $Rank_{MAX}$  for the river discharge leaving segment 1 ( $Q_{out}(1)$ ) is six, because it is not impacted by 15 of the 21 parameters: all seven chemical parameters (Table 7) and the eight groundwater fluxes downstream from segment 1. The  $Rank \div Rank_{MAX}$  formulation results in values for each parameter between 0 and 1, with values near zero indicating greater sensitivity than values closer to one. These values are then averaged over all nine segments (e.g. from  $s=1$  to  $s=9$ ), resulting in a single value (between 0 and 1) for six general output classes: river discharge ( $Q$ ), phreatophyte ET flux ( $ET$ ), groundwater level/elevation ( $GWElev$ ), riparian groundwater chemical/isotopic composition ( $RGW$ ), near-stream zone chemical/isotopic composition ( $NSZ$ ), and river chemical/isotopic composition ( $River$ ). All six of these classes, their corresponding importance values (0-1) and importance ranks (0-14 for water balance outputs, 0-21 for chemical/isotopic outputs) are shown in Table 7.

## 9.2 Discussion

The sensitivity of any of the hydrologic outputs to riparian aquifer depth

(*RGWdepth*) is an artifact of the lower limit value (1m) chosen and the ET calculation function of the model. When the *RGWdepth* parameter is less than the entrenchment depth of the river (see Table 6a-b, Figure 11), the bottom of the RGW reservoir is perched above the zero-flow river stage elevation, thus creating an unrealistically shallow water table and the accompanying high gradient and discharge toward the river. The shallow water table also impacts the phreatophyte ET flux, which is directly dependent upon the depth to water. It should be noted, however, that the orders of magnitude of the ‘scores’ of the three hydrologic output classes for *RGWdepth* perturbation were 17 to 23 orders of magnitude lower than the next-least sensitive parameter (diffusivity,  $D$ ). The ‘importance’ value of 1.0 for all three hydrologic output classes indicates that the perturbation of *RGWdepth* had the least effect for each output.

A number of interesting results are shown in Table 7. The importance of aquifer specific yield ( $S_y$ ) was initially surprising given the greater relative certainty (e.g. within a factor of eight, as opposed to  $Q_{bgw}$  and  $D$ ) with which it was known. However, upon further analysis it becomes apparent that the importance of  $S_y$  is not unreasonable; it is used to formulate the transmissivity ( $T$ ) of the entire model domain and in determining the change in groundwater levels after basin groundwater exchange, ET, and river discharge or recharge. Considering that (1) riparian aquifer diffusivity,  $D$ , impacts the water balance of all nine model segments, (2)  $D$  is assumed to be time-constant, and (3) the lack of coupled well and river stage data at more than one location (and thus any idea of the representativeness of the chosen

value and range), it is surprising that for each of the six output classes  $D$  is the least important parameter excepting one parameter (segment 1 basin groundwater chemistry, *BGWChem1*).

Overall river discharge and groundwater levels are generally more sensitive to upstream than downstream groundwater fluxes ( $Q_{bgw}$ ). This result is not surprising since it is the nature of the model (and of the natural system) that upstream changes necessarily impact the flow and the state of the system downstream. It is also not surprising that this trend of decreasing importance downstream is more pronounced in river discharge than in groundwater levels since changes in river stage hydrographs are always greater than the accompanying changes observed in well hydrographs.

### 9.3 Chemical/Isotopic Sensitivity Analysis

Most notable of the results of the chemical and isotopic sensitivity analysis are (1) the importance of the input chemistry at Palominas (“*PALRivChem*”) on the composition of all three reservoirs, and (2) the relative insensitivity to changes in diffusivity and gaining reach basin groundwater chemistry.

The importance of river input chemistry is not surprising given that the state of the river (physically and, therefore, also chemically) is the primary driving force behind the direction and magnitude of water movement through the riparian system. The impact of  $S_y$  on the chemistry of the system appears to be a result of its significance for the hydrologic behavior of the system.

## 10. MANUAL CALIBRATION, RESULTS & DISCUSSION

The model was manually calibrated based upon the results of the sensitivity analysis, with the parameters that were altered from the base case being those identified as most important through the sensitivity analysis. Diffusivity, specific yield and basin groundwater fluxes ( $Q_{bgw}$ ) were altered to better estimate the hydrologic and chemical behavior of the model. More specifically, these parameters were altered within the allowable ranges outlined in Table 7 to best match groundwater levels, discharge at Charleston and Tombstone and (more roughly) the chemistry of the river and riparian groundwater. It should be noted that  $D$ ,  $S_y$  and the 9  $Q_{bgw}$  values were the only ones altered because (1) the values of  $D$  and  $S_y$  used in the base case were skewed toward the higher end of observed values, and (2) they are the three most poorly-defined hydrologic parameters. Following many iterative changes to one or more of these 11 parameters, an optimal set was chosen which gave reasonable results. This ‘optimal’ parameter set is provided in Table 8 for reference.

During the final stages of this study Wahi et al. (accepted) was consulted to roughly gauge the accuracy of the estimated groundwater flux ( $Q_{bgw}$ ) to the riparian system within the model. Wahi et al. estimated the range of mountain system recharge, which includes both mountain front and mountain block recharge, as  $2 \times 10^6 \text{ m}^3/\text{year}$  to  $9 \times 10^6 \text{ m}^3/\text{year}$ . The cumulative annual basin groundwater flux to the riparian system for segments 1-6 (which corresponds to the area of the Wahi et al. study) is approximately  $4.4 \times 10^6 \text{ m}^3/\text{year}$ , or within the estimated range of mountain system recharge. The independent agreement of the model’s inferred values with the

Wahi et al. estimates (and assuming discharge equals recharge) suggests that the post-optimization  $Q_{bgw}$  values are reasonable.

### 10.1 Results & Discussion: Water Balance

A comparison of simulated versus observed discharge at Charleston and Tombstone is shown in Figure 30. Comparison of Figure 30 with Figure 20 indicates that the model is more well-behaved with respect to discharge in the optimized case than the base case. For both locations, the model generally underestimates streamflow on the receding limb of high flows. This result is most evident during late fall and winter following the wetter years of 2000-2001 and 2005-2006 (indicated in Figure 30 by blue arrows). The simulation also underestimates winter baseflow, when phreatophyte transpiration is zero and stream discharge is determined predominantly by the cumulative upstream basin groundwater fluxes. Conversely, the model overestimates streamflow (1) in autumn after all but the wettest monsoons (e.g. 2001-2004, green arrows in Figure 30), and (2) every spring/pre-monsoon period at Charleston. Observations indicate that the river at Tombstone ceases flow every spring during the model time domain, which the model predicts. However, the model predicts zero discharge earlier than is observed every year except during spring 2006.

Charleston is located at the bottom of a gaining reach. Therefore, the model is currently incapable of producing discharge values below some threshold, which is  $6048 (10^{3.78}) \text{ m}^3/\text{day}$  (Figure 31). However, the model is able to produce zero discharge at Tombstone due to the predominantly losing river conditions between the

two gauges. After optimization, the correlation coefficients at Charleston (0.7552) and Tombstone (0.6422) are noticeably improved over the base case ( $r^2=0.4110$  and 0.5684, respectively: see Figures 20 and 30).

Observed and simulated data from the 1997 monsoon season indicate a variety of processes that might be degrading model performance (Figure 32). The scatter in Figure 31 appears to be at least partly an artifact of two things. First, the daily time step and lack of any in-stream travel time component to the model are the cause of at least some of the observed/modeled differences. This is the situation on 10/7/97, when a floodwave is observed at Palominas, and subsequently predicted at Charleston (Figure 32, top) on the same day. However, the same flood wave was not observed at Charleston until sometime the following day, and the comparison of simulated high flow and observed pre-floodwave low flow on 10/7/97 results in one of the greatest departures from the 1:1 line on Figure 31. The model makes a much more reasonable prediction of discharge after arrival of the flood wave on 10/8/97.

An example of a second source of observed/modeled differences is indicated by the observed peaks at Charleston and Tombstone on 8/15/97, and again at Charleston on 8/1/97 (Figure 32). These disparities between observed and simulated discharge are due in large part to the uncertainty of surface flow additions within the model domain. When hydrographs were analyzed for time-steps when intra-domain surface flow would be added to the model, gauges were analyzed sequentially along the stream: Palominas was compared to Lewis Springs, Lewis Springs to Charleston and Charleston to Tombstone. The Lewis Springs gauge is not discharge-rated,

therefore nothing quantitative could be determined about any change in discharge between Palominas and Lewis Springs and between Lewis Springs and Charleston. As a result, only those floodwaves observed at a lower gauge that were not observed at the immediately upstream gauge could be conclusively defined as having entered the river between within the domain. This lack of quantitative information to define side-channel flow additions between Palominas and Charleston (e.g. the upper two-thirds of the model) almost certainly led to conservative recharge estimates; upstream of Charleston surface flow from side channels only enters the river on 18 of the 4223 days of simulation. Comparatively, it could be conclusively determined that significant surface flow entered the river between Charleston and Tombstone (e.g. the lower third of the model) on 22 days—4 more days than flow entered an area roughly twice as large.

## 10.2 Results & Discussion: Chemical/Isotopic Composition

The chemical and isotopic results for streamflow entering each segment ('Upstream Flow'), streamflow leaving each segment ('Downstream Flow'), the RGW and near-stream reservoirs and basin groundwater are compared to all available samples from the river and riparian wells in Figures 32-37. Both upstream and downstream  $\text{SO}_4/\text{Cl}$  and  $\delta^{18}\text{O}$  values are shown because the data for each segment spans the entire segment. Thus, most samples were not collected at the upstream or downstream end of the segment, but at intermediate sites (and thus intermediate

chemical composition) between these two discrete points.

The model treatment of the RGW reservoir as a well-mixed tank rather than a distributed aquifer makes comparison of RGW data and simulations less conclusive. However, rough conclusions regarding the riparian groundwater data and simulations can be drawn. All riparian groundwater samples included for comparison (Figures 32-37) were taken at varying depths and distances from the river. It is expected that in losing reaches (such as segment 9), (1) riparian groundwater data close to the river would resemble more recent streamflow, and (2) samples collected in wells farther from the river would appear chemically and isotopically similar to less recent streamflow. Therefore, it is anticipated that the simulated, lumped RGW reservoir of a losing reach would resemble a running, volume-weighted average of past river flow/recharge rather than the continuum of increasingly recent streamflow closer to the river, as is expected of the data.

For gaining reaches, it is expected that (1) riparian groundwater samples collected farther from the river would fall closer to the basin groundwater end-member, and (2) samples from wells closer to the river would appear chemically and isotopically more like the most recent high flow(s). Thus, it is reasonable to expect that some gaining reach riparian groundwater data would fall above and some below the simulated RGW value, dependent on well location.

Comparison of  $\delta^{18}\text{O}$  and  $\text{SO}_4/\text{Cl}$  results for segment 2 (Figure 33 and 36, middle) show better agreement between the model and sample data for  $\delta^{18}\text{O}$  than

SO<sub>4</sub>/Cl; nearly all simulated  $\delta^{18}\text{O}$  river data fall between the up- and downstream river values, whereas many of the simulated SO<sub>4</sub>/Cl ratios fall well outside this range. This difference is likely due to the greater resolution of  $\delta^{18}\text{O}$  data at Palominas (relative to SO<sub>4</sub>/Cl data—see Figures 17-18), particularly given the high sensitivity of model river chemistry to river input chemistry at Palominas (*PALRivChem*).

There is also better agreement of the segment 2 riparian groundwater  $\delta^{18}\text{O}$  simulation with the data than there is for SO<sub>4</sub>/Cl. The riparian groundwater simulation falls within the range of data: above the deepest well (128 ft) furthest from the river and below the shallower wells (20ft, 30ft) closer to the river. The segment 2 RGW SO<sub>4</sub>/Cl simulation does not fall between the data from these same wells. However, since (1) the SO<sub>4</sub>/Cl ratio in streamflow samples in September-October 2002 and both pre-monsoon river and riparian groundwater samples in 2004 fall below even the basin groundwater value, and (2) segment 2 is a strongly gaining reach with respect to basin groundwater (e.g. very positive  $Q_{bgw}$ ), the segment-specific basin groundwater end-member must not be entirely representative of the local basin groundwater entering the riparian system. This trend of model-data chemical/isotopic agreement with  $\delta^{18}\text{O}$  declines with distance downstream, whereas the SO<sub>4</sub>/Cl ratio agreement increases sharply between segments 2 and 4. Modeled river  $\delta^{18}\text{O}$  values fall consistently above the reasonable upstream-downstream range for segment 4. However, the relative behavior of more negative river  $\delta^{18}\text{O}$  values immediately following the monsoon followed by a winter increase and spring, pre-

monsoon decrease is captured by the model at segment 4. The best model-data agreement during this inter-monsoon period is during the winter, although in all cases the model underestimates river  $\delta^{18}\text{O}$  values. The segment 4 underestimation of  $\delta^{18}\text{O}$  is more pronounced during the periods immediately before and after the monsoon. The simulated  $\text{SO}_4/\text{Cl}$  ratios do not exhibit this consistent overestimation, falling instead within the upstream-downstream flow range expected of points within the segment.

The trend of decreasing model ability to simulate river  $\delta^{18}\text{O}$  values and more reasonable  $\text{SO}_4/\text{Cl}$  simulation continues downstream to segment 6. Just as with segment 4, in segment 6 the model (1) captures the seasonal pattern observed in river  $\text{SO}_4/\text{Cl}$  values, (2) does not simulate river  $\delta^{18}\text{O}$  values as well as  $\text{SO}_4/\text{Cl}$  values, with the greatest model-data disagreement in river  $\delta^{18}\text{O}$  is in the spring, pre-monsoon period (see Figure 34 (segment 6, bottom), before 2004 and 2005 monsoons), and (3)  $\text{SO}_4/\text{Cl}$  riparian groundwater samples closest to the river fall between the lumped RGW reservoir value and streamflow. Unlike segment 4, the river  $\text{SO}_4/\text{Cl}$  values do not fall within the upstream-downstream range, however it seems likely that the model's underestimation of river  $\text{SO}_4/\text{Cl}$  could easily be a result of too low a  $\text{SO}_4/\text{Cl}$  ratio in the basin groundwater end-member of segments 4 or 5—the two most strongly gaining reaches of the model. This conclusion is not unreasonable, given that groundwater inputs for each segment during the entire time-domain are based on a small number (1-8, depending on segment and chemical/isotopic species) of

potentially-unrepresentative well samples.

The final segment with enough data from which any meaningful conclusions can be drawn is segment 9. As with segments 4 and 6, segment 9 simulation results show generally better agreement with  $\text{SO}_4/\text{Cl}$  than with  $\delta^{18}\text{O}$ . Specifically, the simulated  $\delta^{18}\text{O}$  values are consistently lower than the data, with the model having better agreement with the data during winter baseflow than during post- and pre-monsoon periods. Although less temporally complete, sample  $\text{SO}_4/\text{Cl}$  ratios exhibit the overall patterns of modeled river and, to a lesser extent, RGW  $\text{SO}_4/\text{Cl}$  values. The consistent underestimation of river  $\text{SO}_4/\text{Cl}$  could again (as with segments 6 and 7—see Figures 37-38) be due to too low a  $\text{SO}_4/\text{Cl}$  ratio in the basin groundwater end-members for segment 4, 5, or 6.

The decreasing model performance in predicting  $\delta^{18}\text{O}$  with distance downstream, especially when taken with the progressively better performance of the model in simulating the behavior of the system with respect to  $\text{SO}_4/\text{Cl}$  suggests two things. First, there could be an issue with the representativeness of the basin groundwater end-members as indicated above, although this appears to only address part of the model's inability to simulate  $\delta^{18}\text{O}$  as well as it simulates  $\text{SO}_4/\text{Cl}$ . Second, there must be some processes occurring in the system that are not accounted for by the model, and these processes must affect  $\delta^{18}\text{O}$  differently than  $\text{SO}_4/\text{Cl}$ . The consistent underestimation of river  $\delta^{18}\text{O}$  values, occurrence of the poorest  $\delta^{18}\text{O}$

agreement of the model with data during the pre- and immediately post-monsoon period coupled with the better  $\delta^{18}\text{O}$  agreement during winter baseflow conditions suggests seasonally-variable isotopic fractionation. There is no published evidence to suggest that the phreatophyte transpiration occurring in the riparian groundwater system is a fractionating process.

Evaporation, however, has been well-documented as a fractionating process. Open-water evaporation from the river channel could help explain (1) the good behavior of the model with respect to  $\text{SO}_4/\text{Cl}$  patterns (which are unaffected by evaporation) and poor behavior with respect to  $\delta^{18}\text{O}$ , (2) the better  $\delta^{18}\text{O}$  model-data agreement during winter baseflow when less evaporation and thus less fractionation would occur, (3) the poorest model-data agreement in both gaining and losing reaches (e.g. segments 6 and 9) during pre-monsoon conditions—when temperatures are high, humidity and flow are both relatively low and evaporation and subsequent isotopic fractionation would both therefore be at their highest—and (4) the observed pre-monsoon cessation of streamflow below a mildly gaining reach (e.g. segment 6 outflow at Charleston).

The amount of open-water evaporation required to produce the observed pre-monsoon differences in  $\delta^{18}\text{O}$  values between Charleston and Tombstone on four dates with samples from both locations (4/29/04, 4/7/05, 5/10/05, 4/5/06) was less than four percent of total flow. According to discharge data at Charleston, this would result in evaporation of 470-898 m<sup>3</sup>/day between Charleston and Tombstone. Based on the

open water area between Charleston and Tombstone (approximately  $1.1 \times 10^5 \text{ m}^2$ , according to Kepner et al., 2003) and the daily open-water evaporative flux estimates for April and May (13.2 and 15.2 mm/day—Leenhouts et al., 2003), the estimated evaporative flux is 1450-1670  $\text{m}^3/\text{day}$ . Therefore, enough evaporation is physically possible for open-channel evaporation to cause the observed isotopic enrichment between Charleston and Tombstone.

The inclusion of open-channel evaporation within the model structure coupled with higher  $Q_{bgw}$  values in upstream gaining reaches would also likely allow for better simulation of the greater observed changes in inter-monsoon streamflow than can be predicted with the current model structure.

## 11. QUANTIFYING STREAM CHANNEL RECHARGE:

### OVERALL SUMMARY & CONCLUSIONS

Variations in the chemical and isotopic compositions of model inputs—streamflow at Palominas and the basin groundwater end-members—complicate the direct usage of  $\text{SO}_4/\text{Cl}$  or  $\delta^{18}\text{O}$  to calculate relative contributions of basin groundwater and summer monsoon floodwater to the riparian system. This complication was eliminated by altering the chemical composition of all inputs to reflect different seasonal sources. Basin groundwater end-members were uniformly given sulfate concentrations of zero and chloride concentrations of one (arbitrary) unit. Streamflow at Palominas (and from side channels) between June 1 and October 31 was given sulfate concentrations of 100 units and chloride concentrations of 1 unit. The portion of the code that concentrates riparian groundwater due to phreatophyte evapotranspiration was removed to maintain chloride concentrations of 1 unit. These adjustments to the model turn all model  $\text{SO}_4/\text{Cl}$  calculations into calculations of percent-floodwater. The use of June 1 instead of a discharge threshold to define monsoon onset is not a problematic assumption considering that the highest discharge during the simulation period at Palominas between June 1 and actual monsoon onset is less than 1 cfs ( $\sim 10^3 \text{ m}^3/\text{day}$ ) and thus represents a very small volume of water compared to later monsoon flows on the order of thousands of cfs ( $\sim 10^6 \text{ m}^3/\text{day}$ ).

Resulting calculations of percent summer floodwater show greater ranges of influence in baseflow (nearly 100% in some segments—see Figure 39) than in the

riparian aquifer (8-79%). Mean flood water influence on baseflow is 79% at Palominas and declines to 40% and 27%, respectively, as it passes through the two most upstream perennially gaining reaches (2 and 4). This value (27%) decreases slightly along the rest of the river. These values should be viewed as underestimations of floodwater influence on baseflow due to the underestimation of surface flow generated and entering the river within the domain. The degree of underestimation likely increases with distance downstream as the contributing area and, presumably, neglected side-channel inflow increases.

Regarding the riparian groundwater system, upstream losing reaches (1 and 3) show the greatest monsoon floodwater influence. This influence decreases as the river flows through segments 2 and 4 (both strongly gaining reaches). However, as basin groundwater input decreases downstream of Lewis Springs (segment 4) monsoon influence increases, which—given the likely underestimation of monsoon influence on the river—is somewhat surprising. This trend indicates that as a given flood propagates through the lower losing reaches of the system, it encounters areas with progressively more ephemeral flow (as evidenced by the observed/predicted hydrograph at Tombstone, Figure 30) and thus less influence of the upstream, perennial reaches.

The lowest values within the riparian groundwater-floodwater influence ranges (e.g. periods of greatest basin influence) fall immediately before each monsoon season, with the lowest values occurring in years following less active monsoons. Conversely, the greatest monsoon influence occurs at the last elevated

flow event of each monsoon, with floodwater becoming gradually less important until the start of the next monsoon.

Riparian groundwater and river data presented in Baillie et al. (2007) all fell between the Palominas and Charleston gages. The reaches in that study with condition scores of less than 2.5 showed greater than 70% summer/monsoon floodwater (see Baillie et al., 2007). These reaches correspond to segments 1 and 3 in the model developed in this study, and there is good agreement between model simulations and the Baillie et al. mixing calculations; the modeled composition of summer floodwater in these segments averages 63% or more. There is better agreement with respect to reaches with conditions scores of 2.6 or more. The Baillie et al. study calculated at least 60% basin groundwater in the riparian groundwater of such reaches (which correspond to segments 2, 4, and 5). The model presented here produces a range of percent-floodwater values for these locations, and all such values in these reaches fall below 40% (i.e. greater than 60% basin groundwater).

A cumulative, river-scale water balance of the riparian groundwater system is shown in Table 9. At this scale, collective basin groundwater inputs exceed phreatophyte evapotranspiration. The remainder of this flux compensates for the deficit between aquifer recharge and riparian groundwater discharge to the river. Closer examination of the longitudinal variations in these four fluxes ( $Q_{bgw}$ ,  $ET$ , *Groundwater Discharge* and *Recharge*) exposes an interesting trend. The upper ~70% of the river (segments 1-6: Palominas to Charleston) accounts for roughly a

third (36%) of the total river-scale recharge (see Table 9). Of the total recharge in this upper portion of the river, an average of 92.6% takes place during the summer monsoon (averaged across the six river segments, range: 83.7% to 95.9%). The remaining 7.4% (range: 4.1 to 16.3%) occurs during (1) winter or spring floods, and (2) pre-monsoon periods when phreatophyte ET exceeds basin groundwater input in some areas, thus shifting the hydraulic gradient away from the river. The actual volume of water recharged in segments 1-6 ('upstream') during the monsoon only accounts for 52% of the river-scale summer recharge.

The remaining two-thirds (64%) of total river-scale recharge takes place in the lower ~30% (segments 7-9) of the model domain, where losing conditions are almost always present: annual groundwater discharge to the river is only 2% of the entire domain. Nearly half (48%) of the total summer recharge occurs in this lower portion of the river. Therefore, more cumulative recharge takes place along the lower portion of the river than along the upper portion throughout the entire year (Figure 42). The greater proportion of total versus summer recharge in the lower reaches (64% versus 48%) suggests that baseflow recharge below Charleston is significant.

The preponderance of recharge below Charleston throughout the year suggests that the hydrologic state of the river in the downstream losing reaches is dependent on the *annual* streamflow regime at Charleston; not simply on flood recharge or basin groundwater. This further implies that the portion of the riparian corridor most sensitive to (1) changes in flood frequency and magnitude, and (2) basin groundwater inputs in the middle, gaining reaches, are the downstream losing reaches. Changes in

flood volume and frequency are possible, if not likely, with changes in atmospheric circulation patterns and precipitation quantity and timing resulting from climate change. Additionally, the lesser dependence of riparian groundwater in gaining reaches on monsoon recharge and greater groundwater discharge than recharge (e.g. net streamflow source) imply the importance of basin groundwater in maintaining (1) baseflow conditions in the upper portion of the river and, subsequently, (2) more constant flow and stable groundwater levels in the more sensitive downstream losing reaches.

It is evident from this modeling study, and the prior field study by Baillie et al., that summer flood recharge plays a major role in sustaining streamflow and the hydrologic state of the riparian groundwater system in the Upper San Pedro River. Summer flood recharge in the upper portion of the river ( $1.66 \times 10^7 \text{ m}^3$ ) comprises 30.0% of the total groundwater discharge to the river, with much of the remainder originating from basin groundwater (67.2%). The reaches between Charleston and Tombstone show much higher cumulative recharge ( $3.20 \times 10^7 \text{ m}^3$ ) than the upper reaches, with total recharge being roughly equal between monsoon ( $1.54 \times 10^7 \text{ m}^3$ ) and inter-monsoon ( $1.66 \times 10^7 \text{ m}^3$ ) periods.

## 12. IMPLICATIONS FOR FURTHER RESEARCH

The model developed in this study largely agrees with previous discharge and chemical/isotopic data. However, inclusion of an open-channel evaporation component to this model appears to be necessary to test the ability to better match isotopic data. The model shows promise as a useful scenario analysis tool to analyze for changes in streamflow regime and/or interaction between the riparian and basin aquifers. There also appears to be great potential for the coupling of the model presented here with MODFLOW models of the Upper San Pedro Basin. Such coupling would certainly provide better estimates, and allow the more realistic time-variability, of the flux direction and magnitude between the basin and riparian aquifers.

Distribution of the model longitudinally and laterally, attaining greater knowledge of the spatial variability in hydraulic properties (e.g. diffusivity and specific yield) of the riparian system and better definition of surface flow additions below Palominas are the next logical, and most useful, modeling and field-based exercises to better characterize the behavior of the riparian system.

APPENDICES

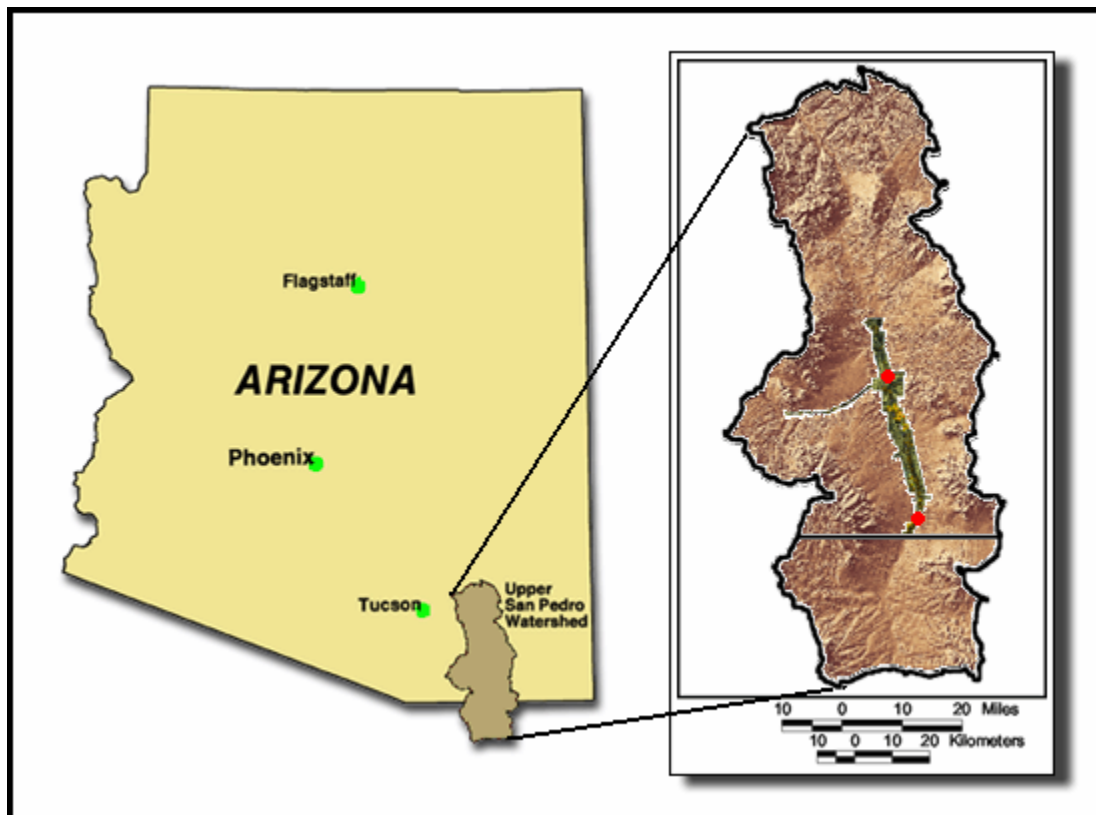
## APPENDIX A: FIGURES

## LIST OF FIGURES

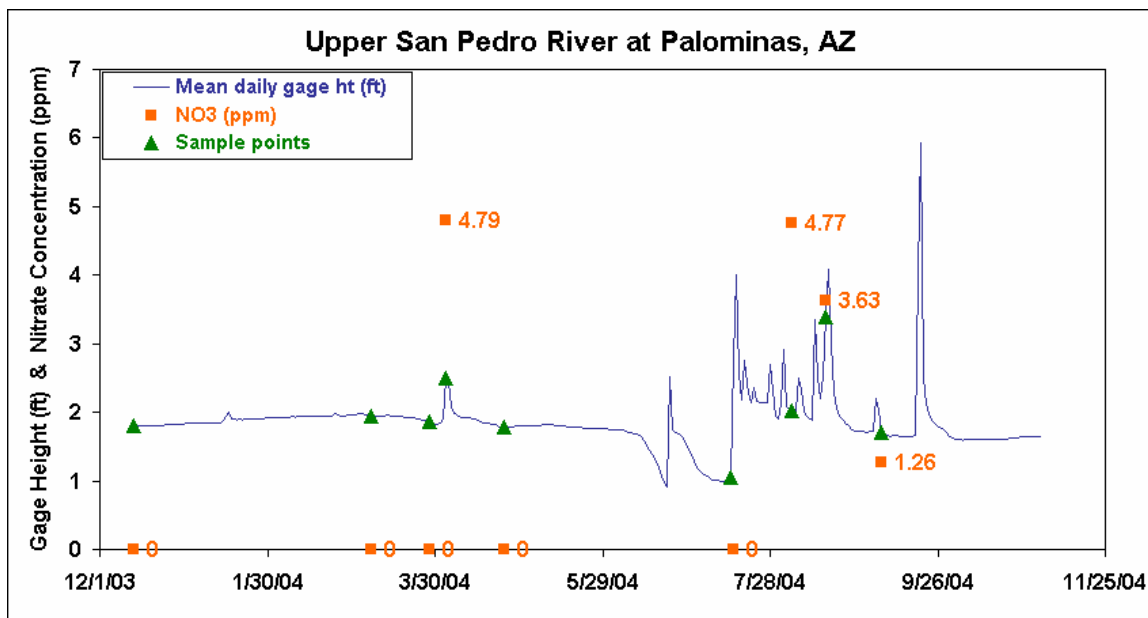
Figure 1: Map of Upper San Pedro Watershed.....	69
Figure 2: Stage hydrograph and [NO <sub>3</sub> ] at Palominas, AZ (2003-2004).....	70
Figure 3: Map of model domain with model segment boundaries.....	71
Figure 4: Conceptual model cross-section.....	72
Figure 5: Seasonal groundwater depth vs. ET flux curves.....	73-74
Figure 6: Example river entrenchment depth determination method .....	74
Figure 7: Palominas river and riparian well isotopic data (2006).....	75
Figure 8: Mean monthly water table elevations at HUN and PAL transects .....	75
Figure 9: Average condition score for each model segment.....	76
Figure 10: Model segment-specific stage-discharge curves.....	77-79
Figure 11: River and surface elevation conceptual diagram.....	79
Figure 12: River-groundwater exchange conceptual diagram.....	80
Figure 13: Example of Pinder curve-matching method for aquifer diffusivity .....	81
Figure 14: Lewis Springs hydrograph and calculated diffusivity values (2006) .....	82
Figure 15: Model flow diagram for water and tracers.....	83
Figure 16: Example of intra-domain inflow addition analysis.....	84
Figure 17: Observed and synthesized river $\delta^{18}\text{O}$ input chemistry.....	85
Figure 18: Observed and synthesized river SO <sub>4</sub> /Cl input chemistry. ....	86
Figure 19: Base case simulation streamflow results (time-series).....	87
Figure 20: Observed versus base case simulation streamflow time-series.....	88
Figure 21: Observed versus base case simulation streamflow.....	89
Figure 22: Simulated groundwater levels.....	90
Figure 23: Water volume exchanged between the river and RGW reservoir .....	91
Figure 24: Base case modeled riparian system $\delta^{18}\text{O}$ signatures (segments 1-3) .....	92
Figure 25: Base case modeled riparian system $\delta^{18}\text{O}$ signatures (segments 4-6) .....	93
Figure 26: Base case modeled riparian system $\delta^{18}\text{O}$ signatures (segments 7-9) .....	94
Figure 27: Base case modeled riparian system SO <sub>4</sub> /Cl values (segments 1-3) .....	95
Figure 28: Base case modeled riparian system SO <sub>4</sub> /Cl values (segments 4-6).....	96
Figure 29: Base case modeled riparian system SO <sub>4</sub> /Cl values (segments 7-9).....	97
Figure 30: Post-optimization simulated streamflow (time-series) .....	98
Figure 31: Observed versus post-optimization simulated streamflow .....	99
Figure 32: Fine resolution observed versus simulated streamflow .....	100
Figure 33: Post-optimization modeled $\delta^{18}\text{O}$ signatures (segments 1-3).....	101
Figure 34: Post-optimization modeled $\delta^{18}\text{O}$ signatures (segments 4-6) .....	102
Figure 35: Post-optimization modeled $\delta^{18}\text{O}$ signatures (segments 7-9) .....	103
Figure 36: Post-optimization modeled SO <sub>4</sub> /Cl values (segments 1-3).....	104
Figure 37: Post-optimization modeled SO <sub>4</sub> /Cl values (segments 4-6).....	105

LIST OF FIGURES - *Continued*

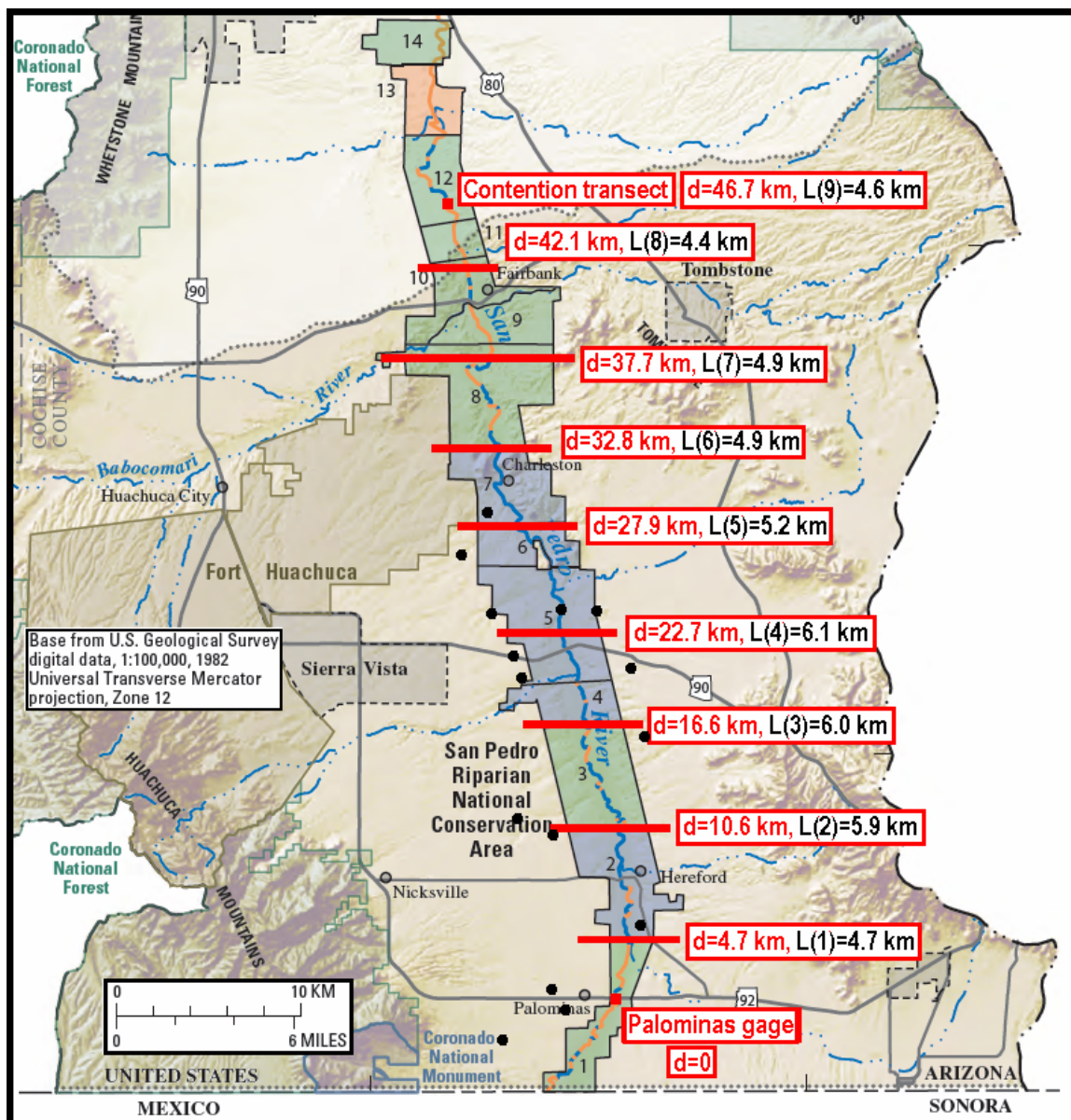
Figure 38: Post-optimization modeled SO <sub>4</sub> /Cl values (segments 7-9).....	106
Figure 39: Percent monsoon floodwater in the riparian system.....	107
Figure 40: Cumulative riparian fluxes: model segments 1-6 .....	108
Figure 41: Cumulative riparian fluxes: model segments 7-9 .....	108
Figure 42: Cumulative, riparian fluxes by model segment (mean annual fluxes) .....	109



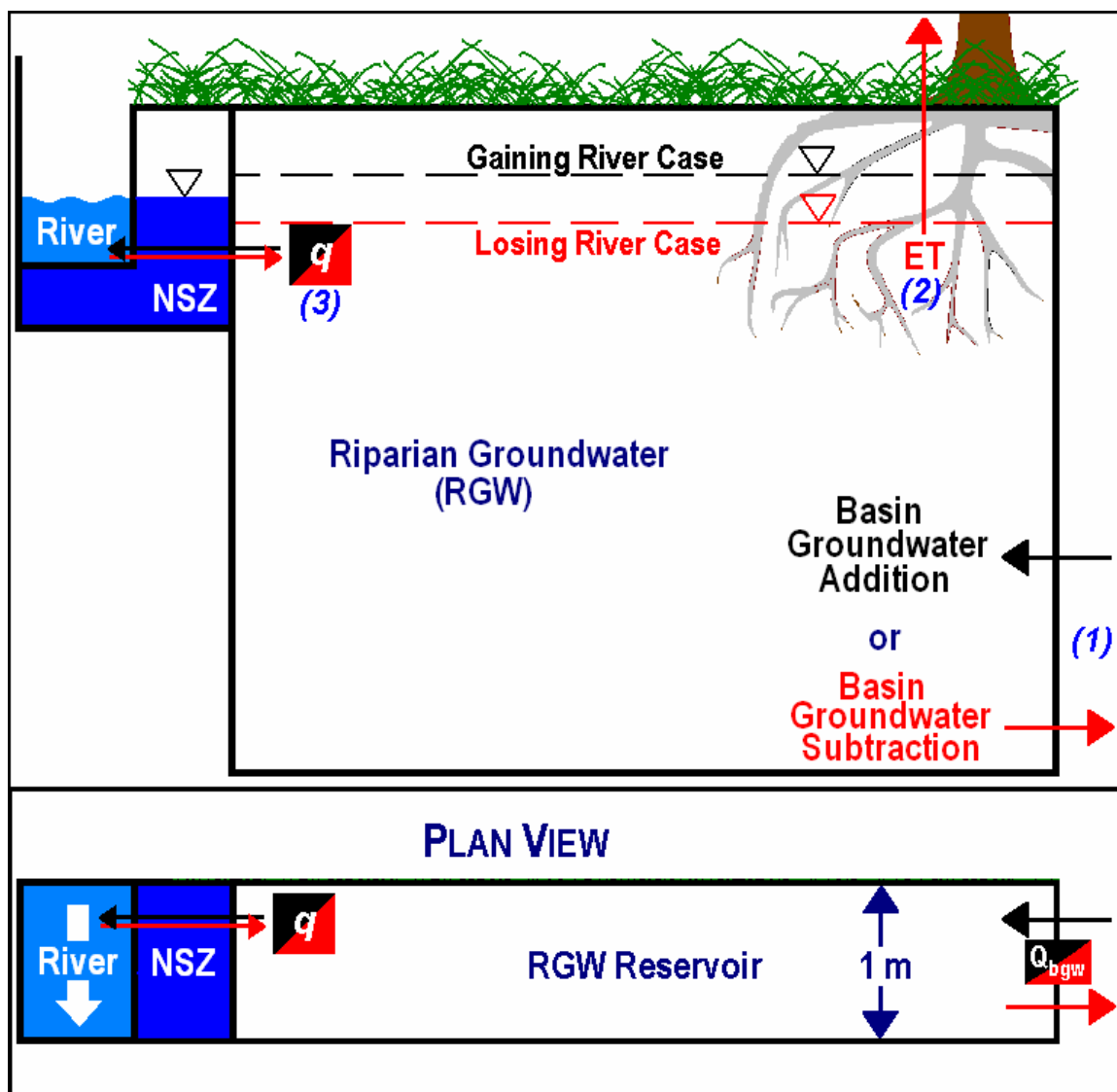
**Figure 1.** Map of Upper San Pedro Watershed (modified from Kepner et al., 2003). SPRNCA shown in green. Locations of USGS gauges at Palominas (bottom) and Tombstone (top) shown in red.



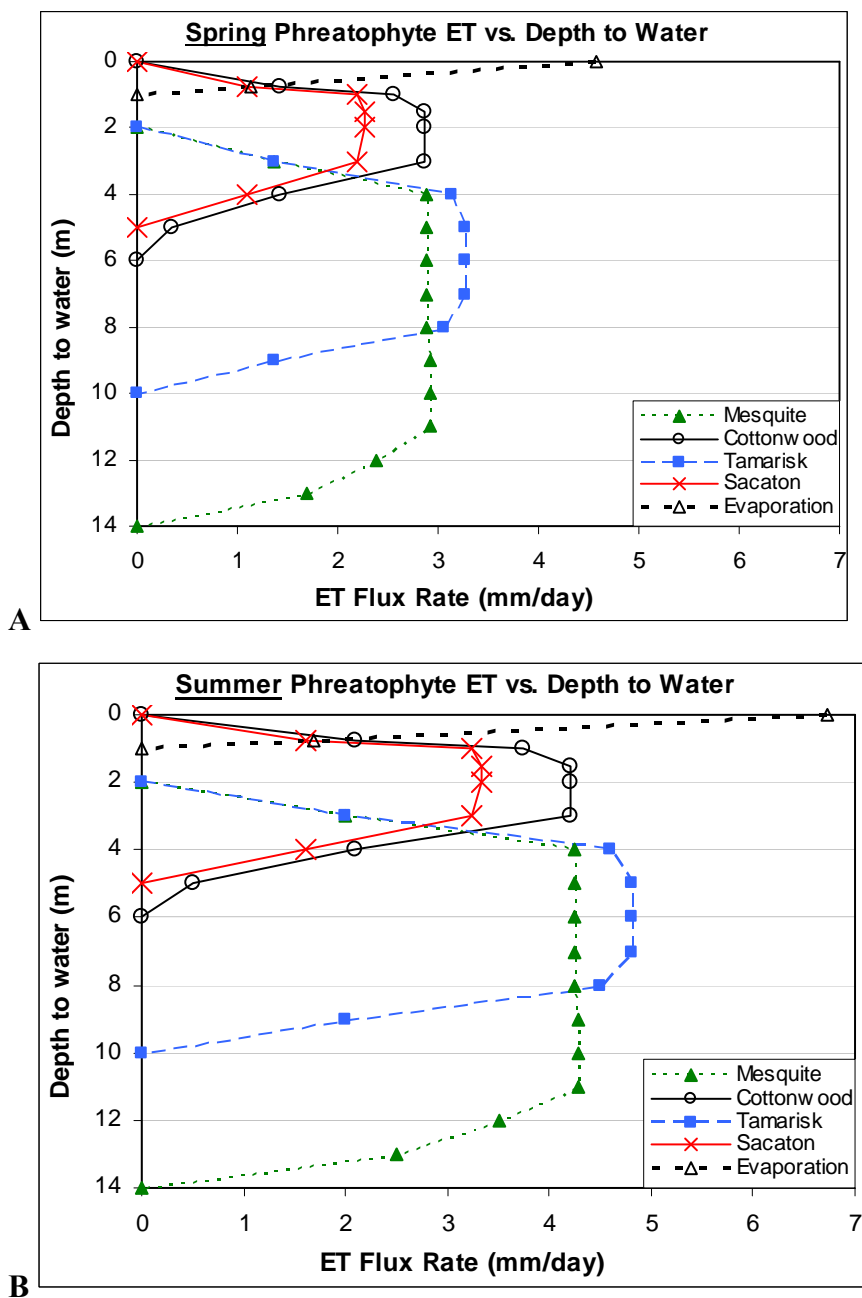
**Figure 2.** Stage hydrograph and NO<sub>3</sub> at Palominas, AZ, before and during the 2004 monsoon season. NO<sub>3</sub> concentrations correspond to the sample points on the hydrograph; zero values are given in place of those samples in which no NO<sub>3</sub> could be detected.



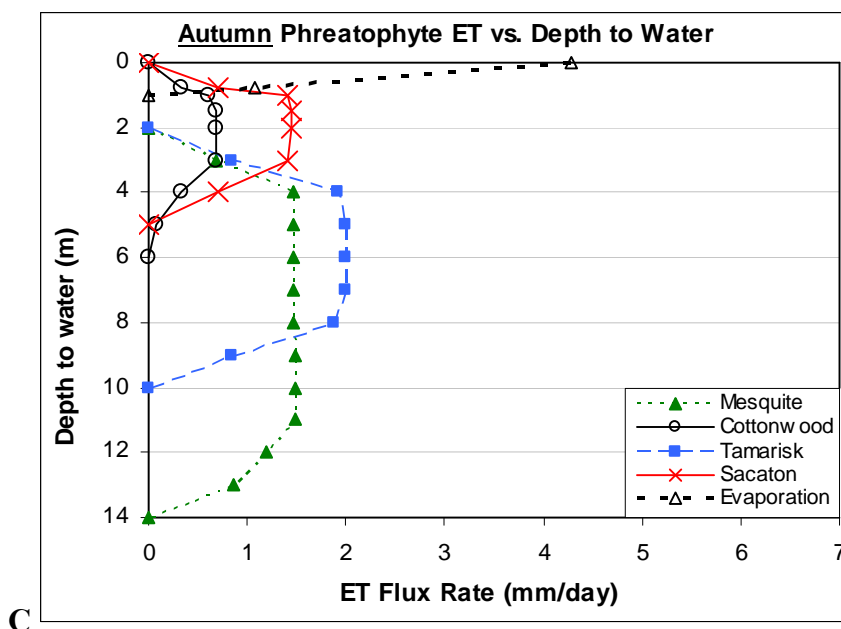
**Figure 3.** Map of model domain (modified from Leenhouts et al., 2005) with model segment boundaries marked in red. Basin wells with available  $\text{SO}_4/\text{Cl}$  and water isotope data used as groundwater chemistry inputs shown as solid black circles. Distances,  $d$ , denote river length from Palominas. Distances  $L(n)$ , denote length of the  $n$ th model segment.



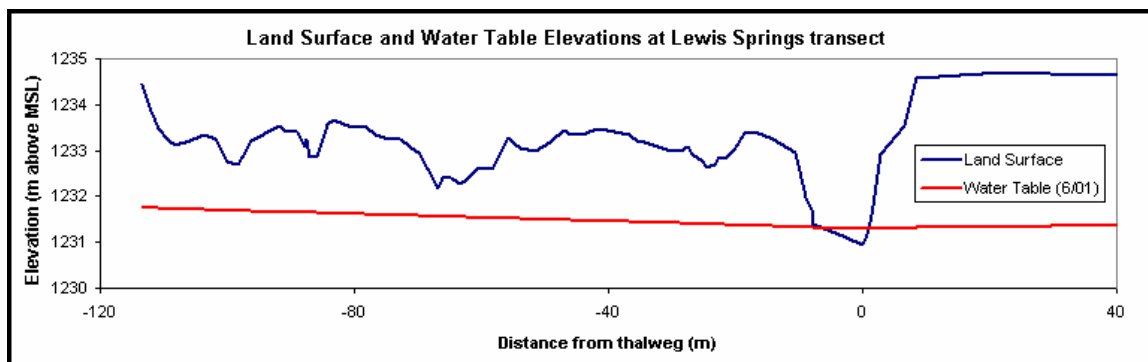
**Figure 4.** Conceptual model cross-section. Blue numbers (1-3) indicate the model-prescribed order of water and solute exchange between reservoirs.



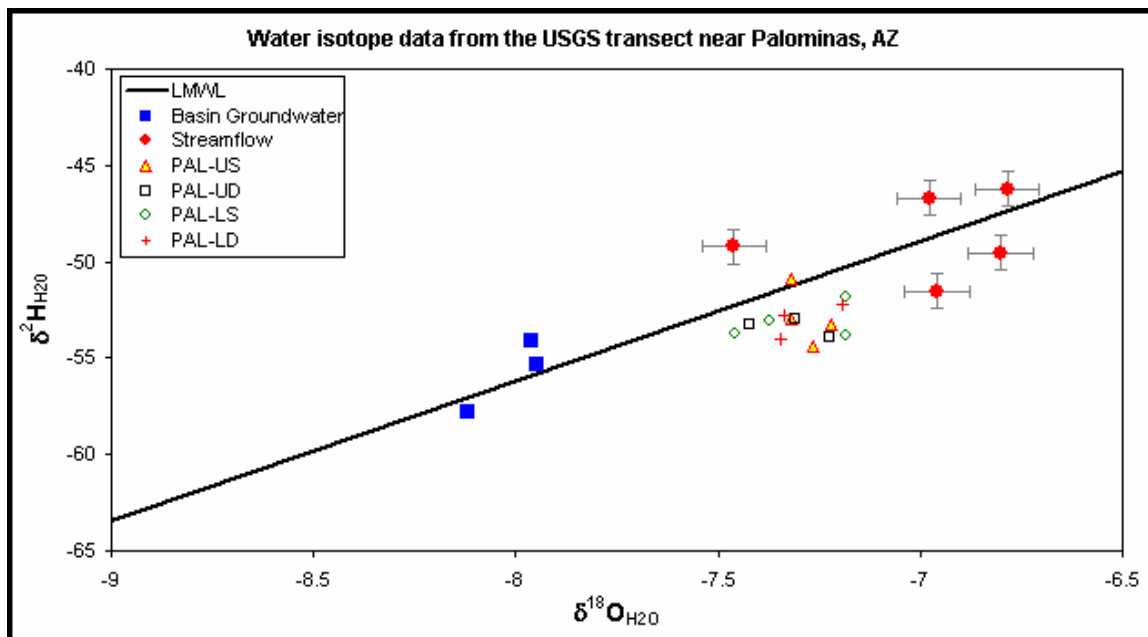
**Figure 5A-B.** Depth vs. ET curves for spring (March/April) and summer (June-Sept.) for the four phreatophyte types found along the San Pedro (after Baird et al., 2005).



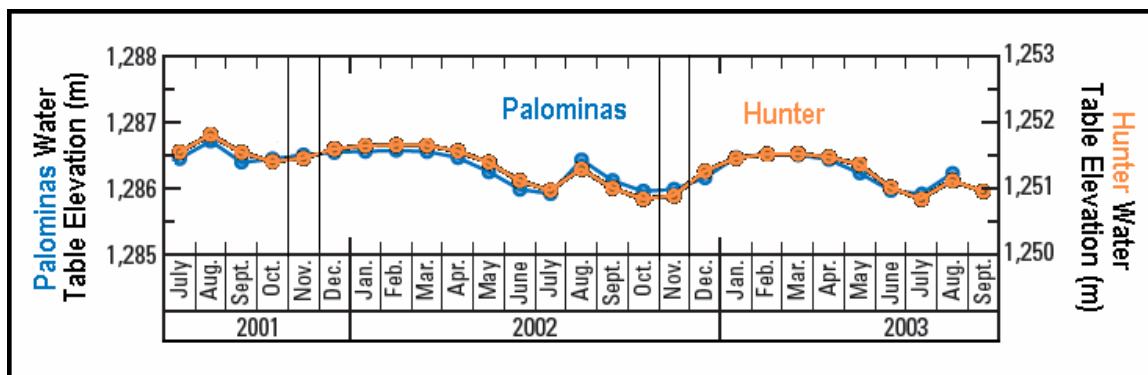
**Figure 5C.** Depth vs. ET curves for autumn (Oct./Nov.) for the four phreatophyte types found along the San Pedro (after Baird et al., 2005).



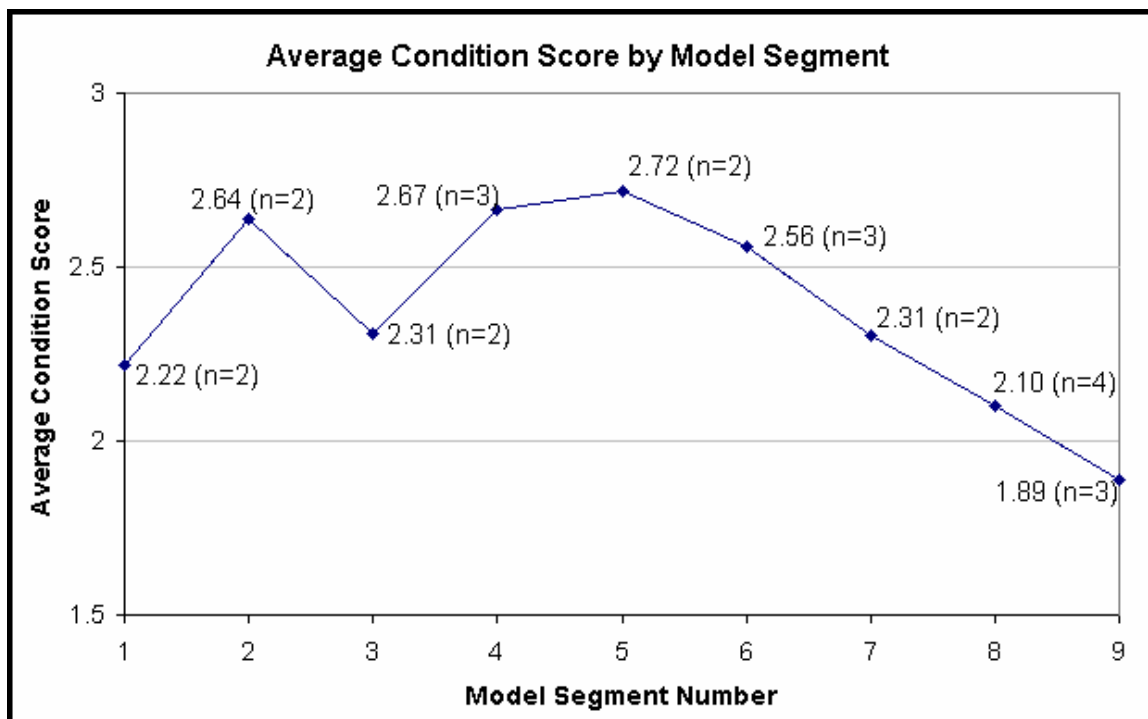
**Figure 6.** Example of data and method used to determine river entrenchment depth (based directly on floodplain depth to water). Land surface elevation data and water table elevation estimates shown are from the Lewis Springs transect, contained within segment 4 of the model. Average depth-to-water is 1.78 m below land surface. Data from Leenhouts et al. (2005).



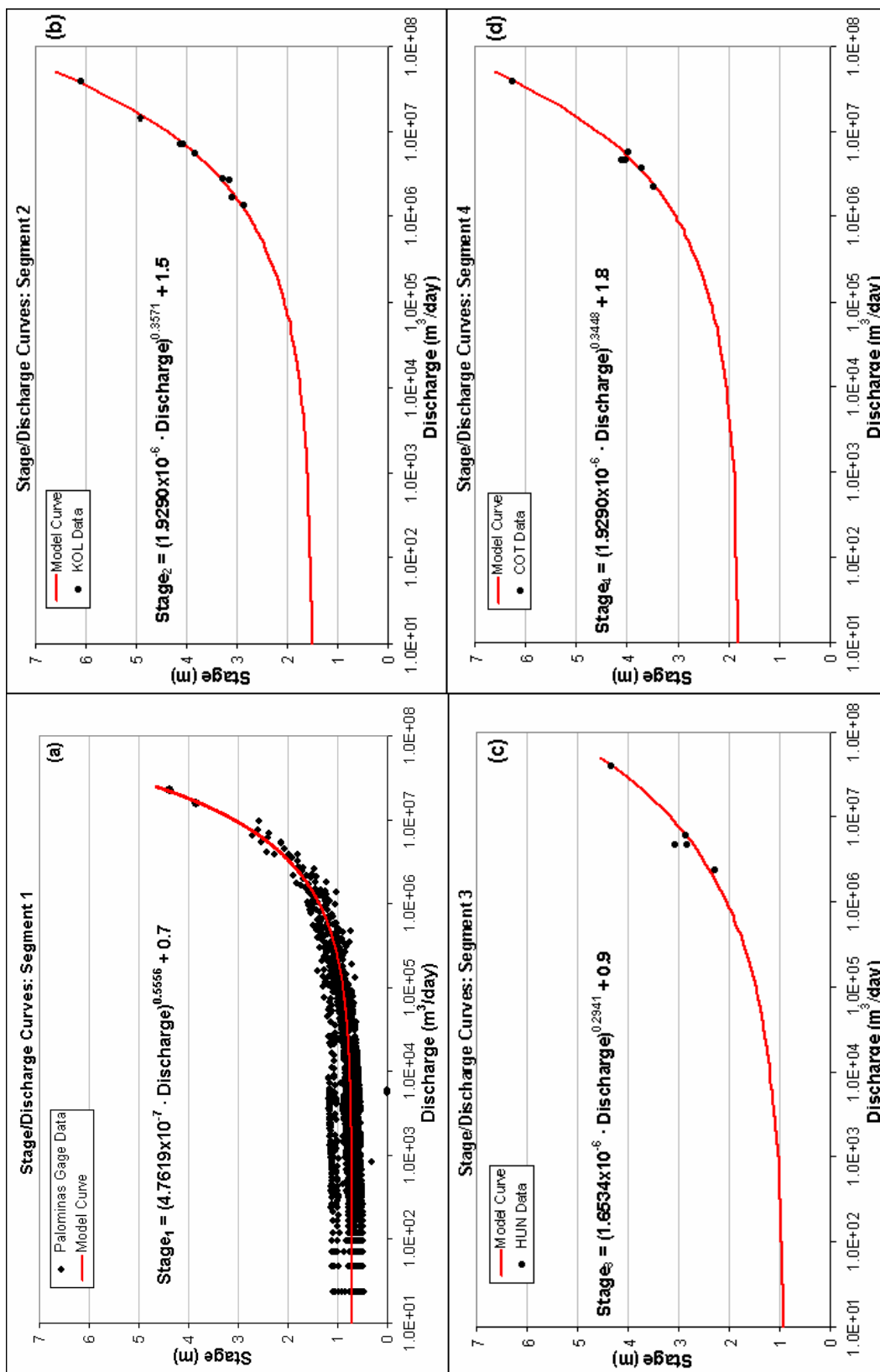
**Figure 7.** Water isotope data (collected between 8/06 and 12/06) from the river and four riparian wells near Palominas, AZ (e.g. PAL-US, -UD, -LS, -LD: all of which are within 100m of main channel). Note that riparian and basin well samples have the same uncertainty as the streamflow samples (see Section 3 for values). Basin groundwater samples are from wells less than 2 km up-gradient from the PAL well transect (collected between 6/96 and 9/99). See Figure 3 for exact basin well locations.

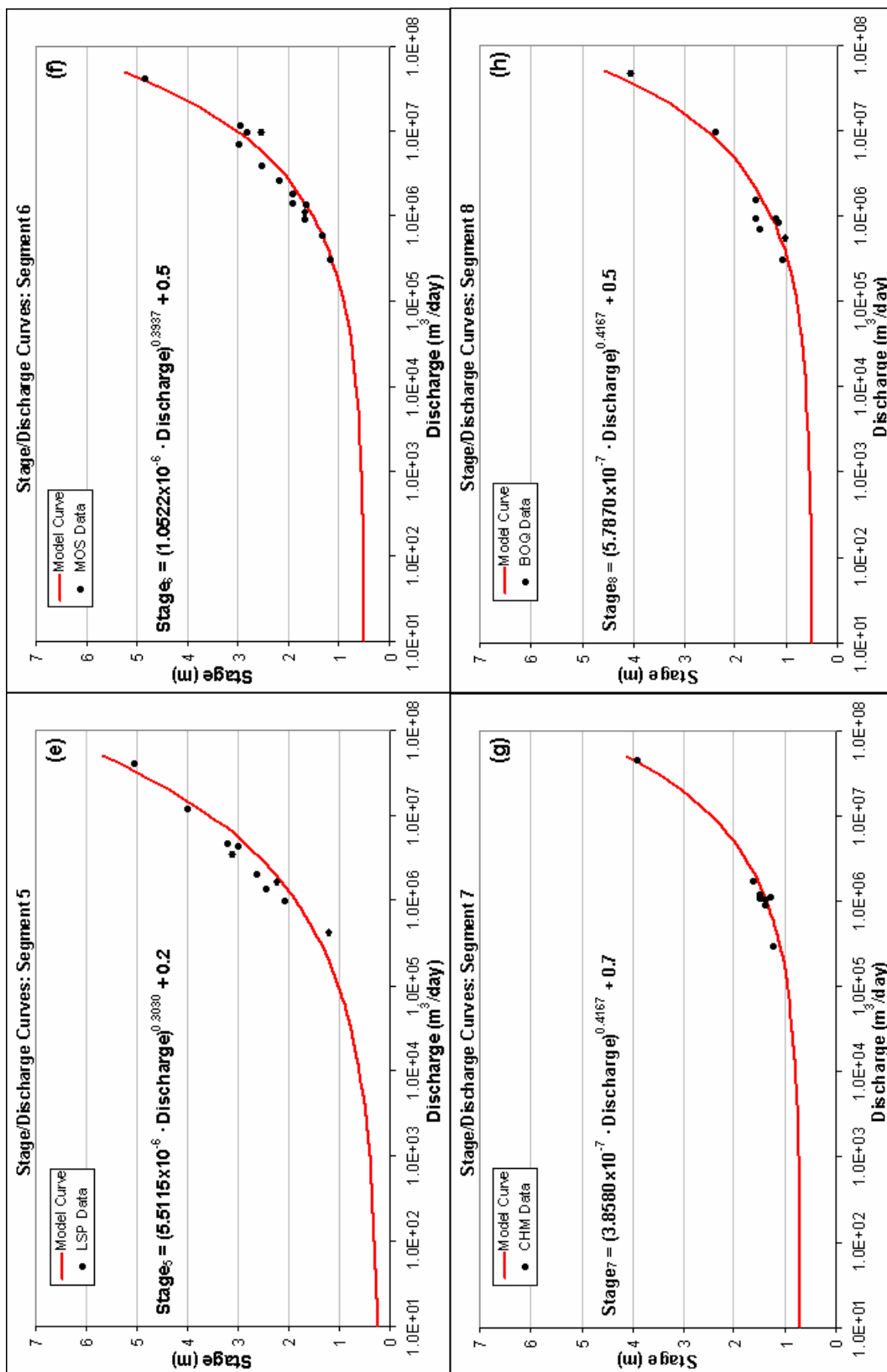


**Figure 8.** Mean monthly water table elevations at HUN (orange) and PAL (blue) transects for the period of overlapping record (modified from Leenhouts et al., 2005). November 2001 and 2002 windows indicate slight increases from the previous month.



**Figure 9.** Average condition score for each model segment. *n* equals the number of transects per segment.





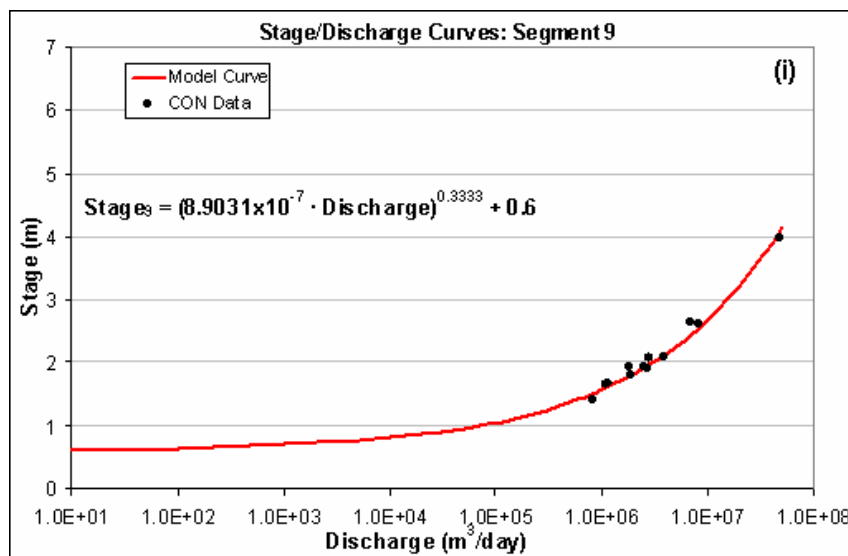


**Figure 10a-i.** Model curves for generating river stage from daily discharge. All site data used for each segment is from a transect within that segment.

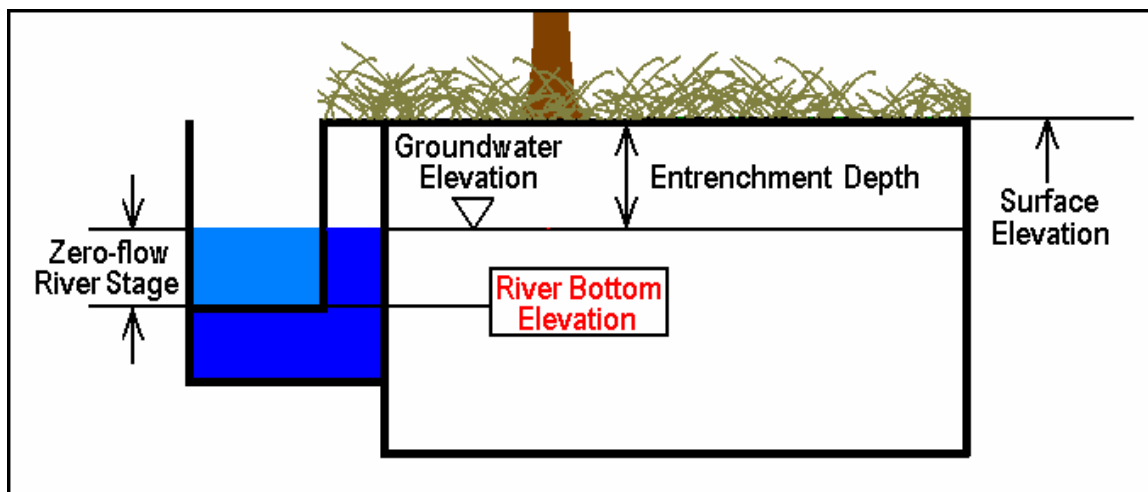


**Figure 11.** Conceptual diagram of how river bottom and surface elevations are determined. Entrenchment depth for each model segment is the depth to groundwater in wells next to the river during low/zero flow conditions (based on river discharge and groundwater level data from nine well transects in Leenhouts, et al., 2005). Zero-flow river stage and the y-intercept of the segment-specific stage/discharge curves (Figure 10) are identical.

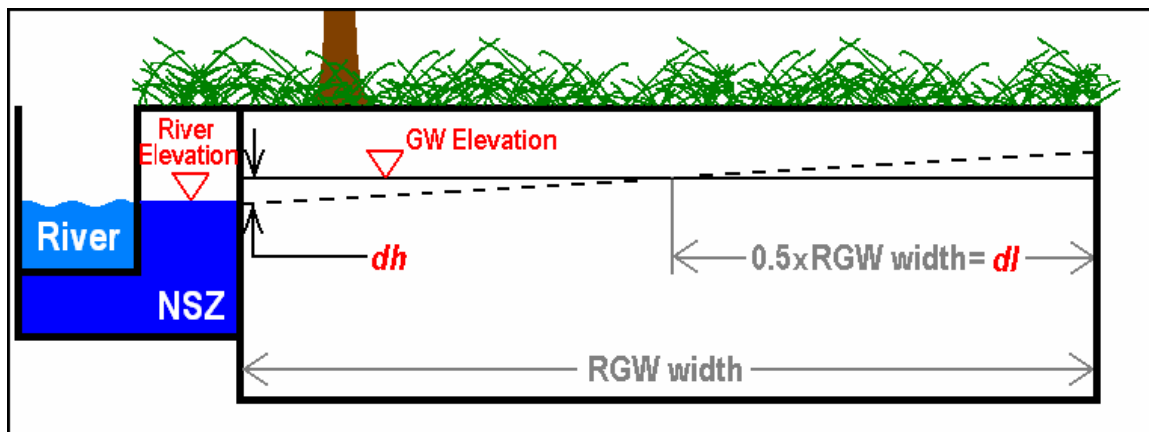


**Figure 12.** Conceptual diagram of river/RGW exchange during gaining river conditions. Dashed line is theoretical water table position, whereas the solid *GW Elevation* line is the water table elevation as represented in the model.

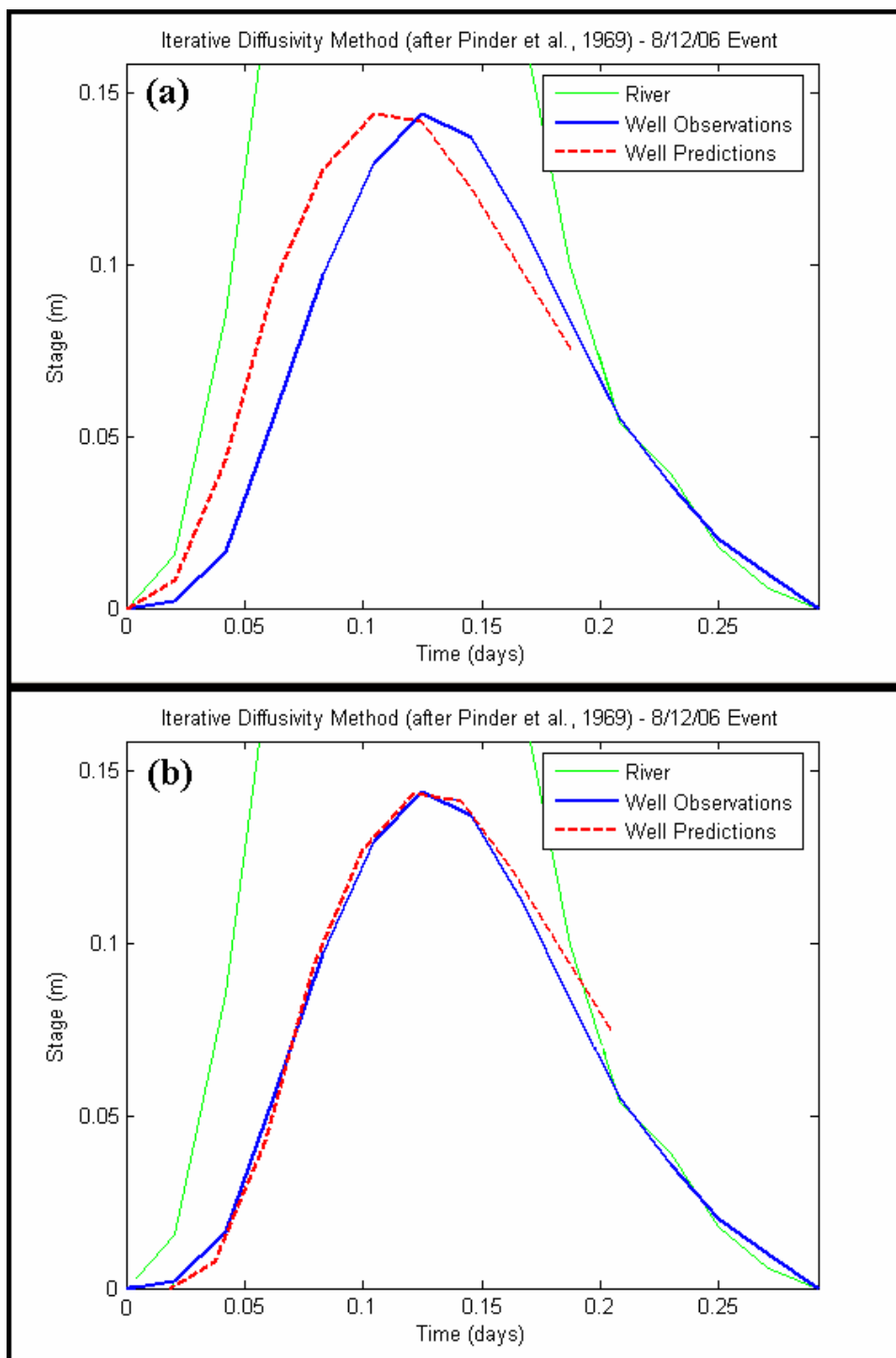


**Figure 13.** Example of one flood event (8/12/06) observed at USGS well transect near Lewis Springs. Iteration shown corresponds to  $D = 4475 \text{ m}^2/\text{day}$ . **(a)** Predicted curve without correction for time lag at observation well ( $x = 31.6 \text{ m}$  from river edge). **(b)** Predicted curve with time shift.

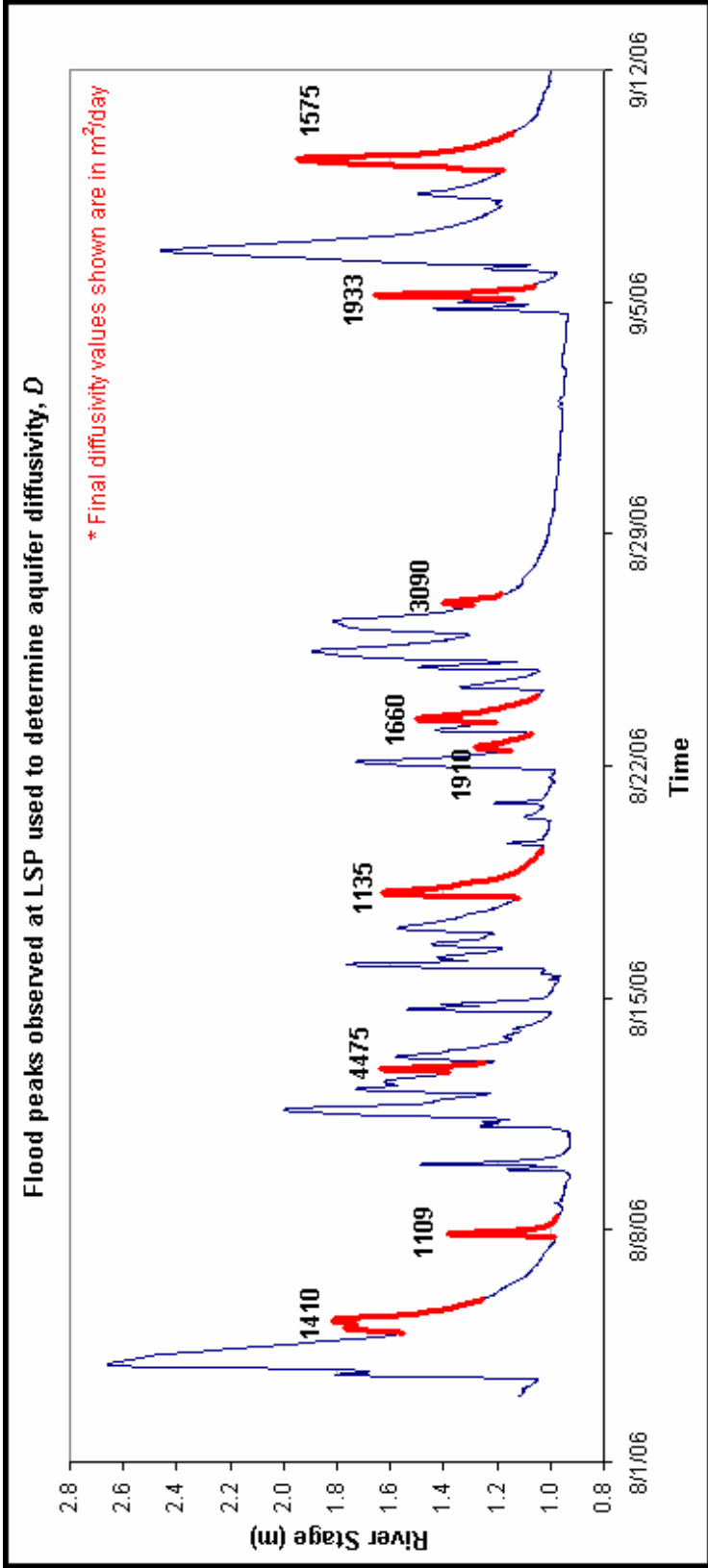


**Figure 14.** Hydrograph with nine diffusivity ( $D$ ) values for different flood waves, calculated after Pinder et al. (1969).

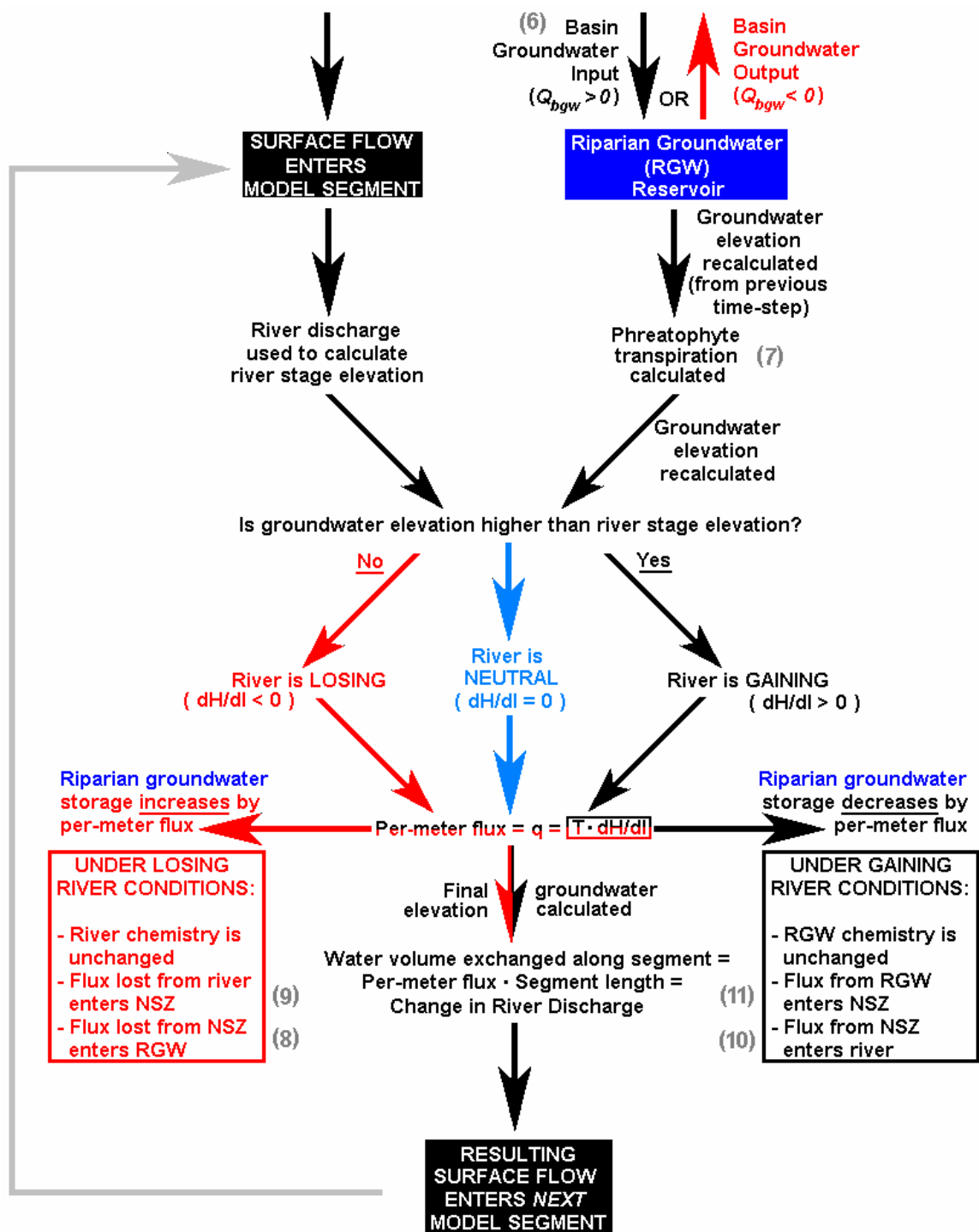


**Figure 15.** Flow diagram of water and tracer movement through the model. Gray numbers in parentheses indicate the equations from sections 5.2-5.5 that are used to calculate changes in tracer values along each trajectory.

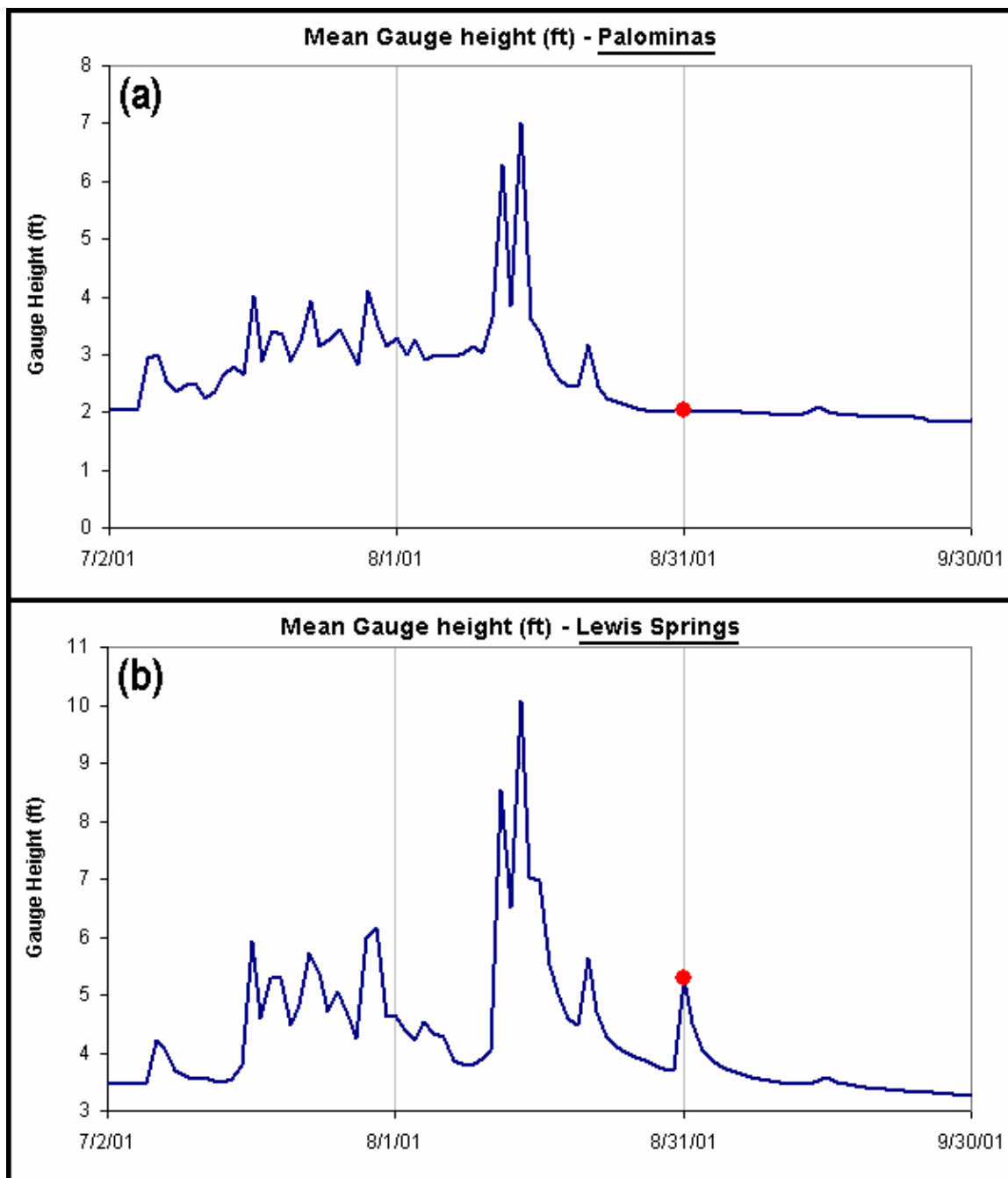
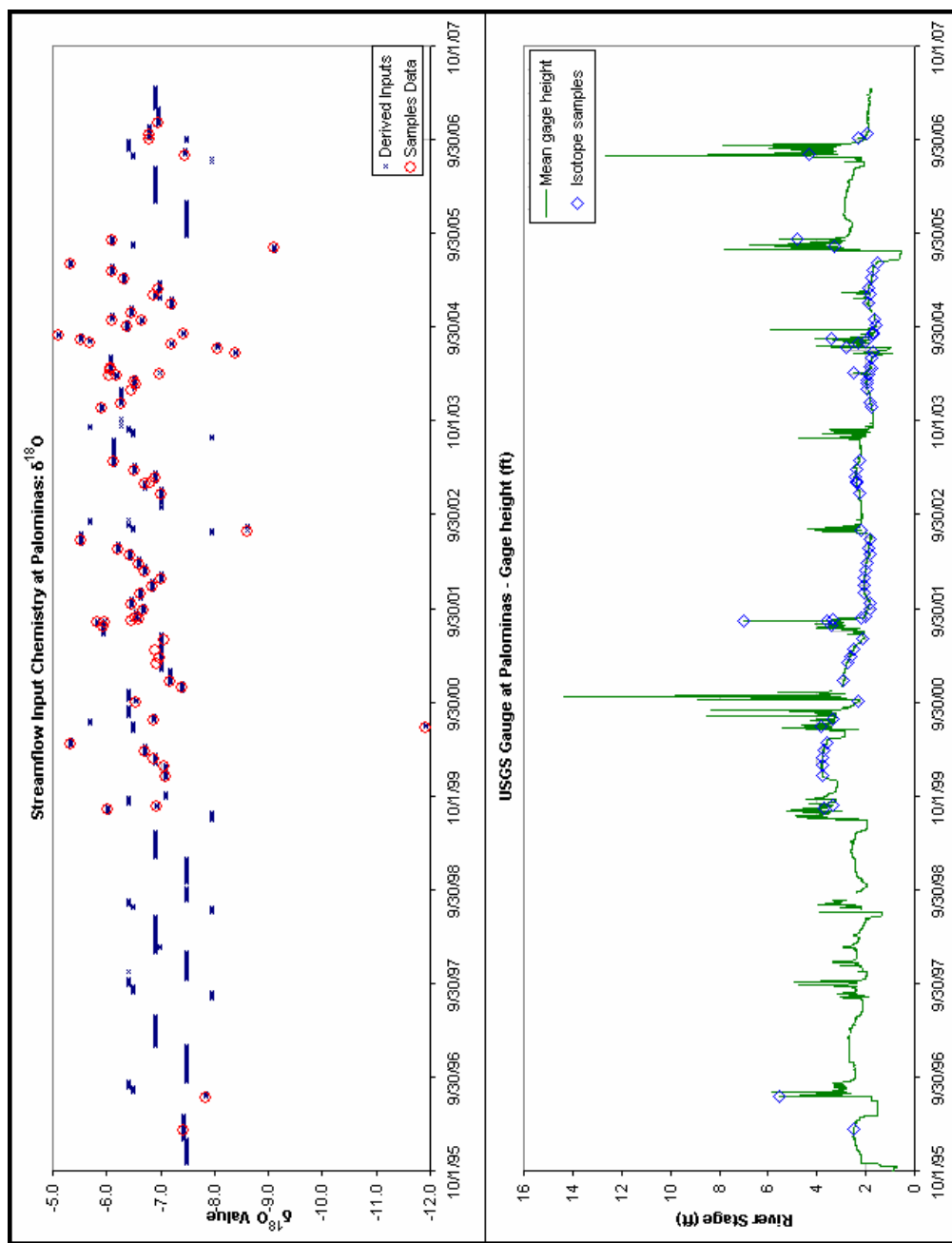
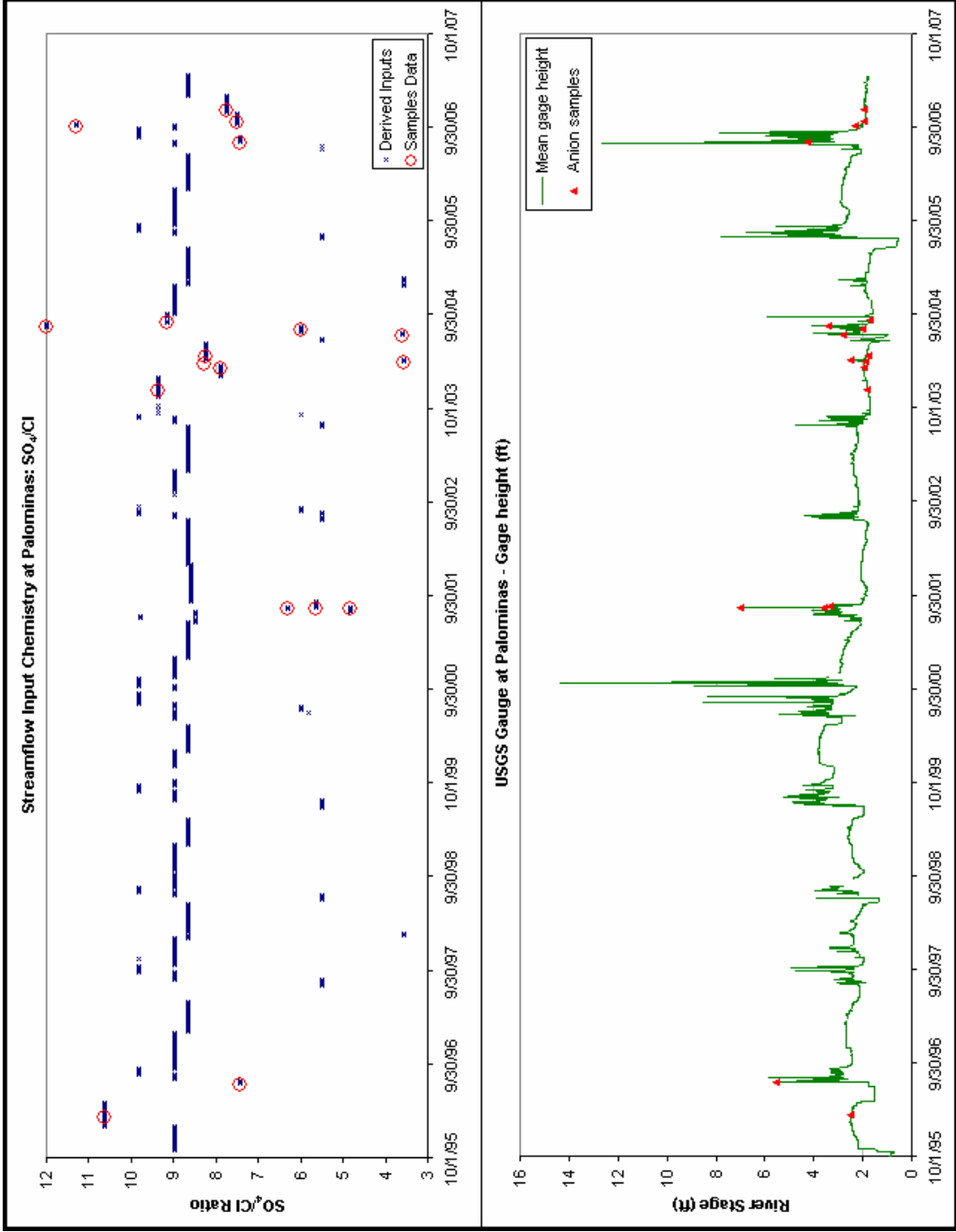


Figure 16. An example of hydrograph analysis for intra-domain flow addition. The 8/31/01 elevated flow event is observed at the Lewis Springs USGS gage (b), but is not observed at the Palominas USGS gage (a), and necessarily enters the river between the two gauges.



**Figure 17.** Top:  $\delta^{18}\text{O}$  per mil values in samples collected at the Palominas USGS gage and derived values for model input. Days with non-zero discharge are shown. Bottom: Stage hydrograph and isotope anion sample dates for the model time domain.



**Figure 18.** Top:  $SO_4/Cl$  ratios in samples collected at the Palominas USGS gauge and derived values for model input. Days with non-zero discharge are shown. Bottom: Stage hydrograph and anion sample dates.

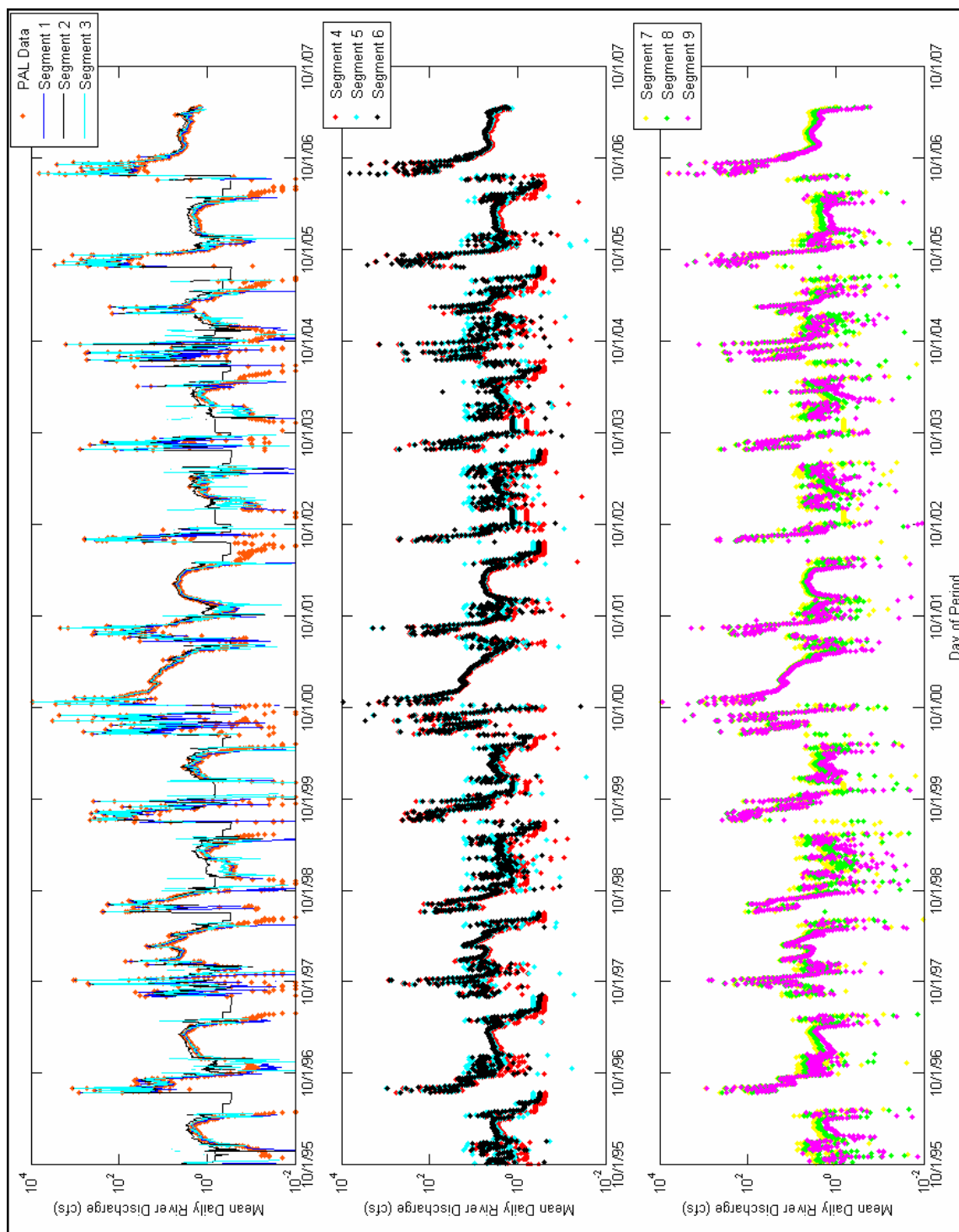


**Figure 19.** Model base-case results: input data at Palominas (top) and simulated streamflow for each model segment.

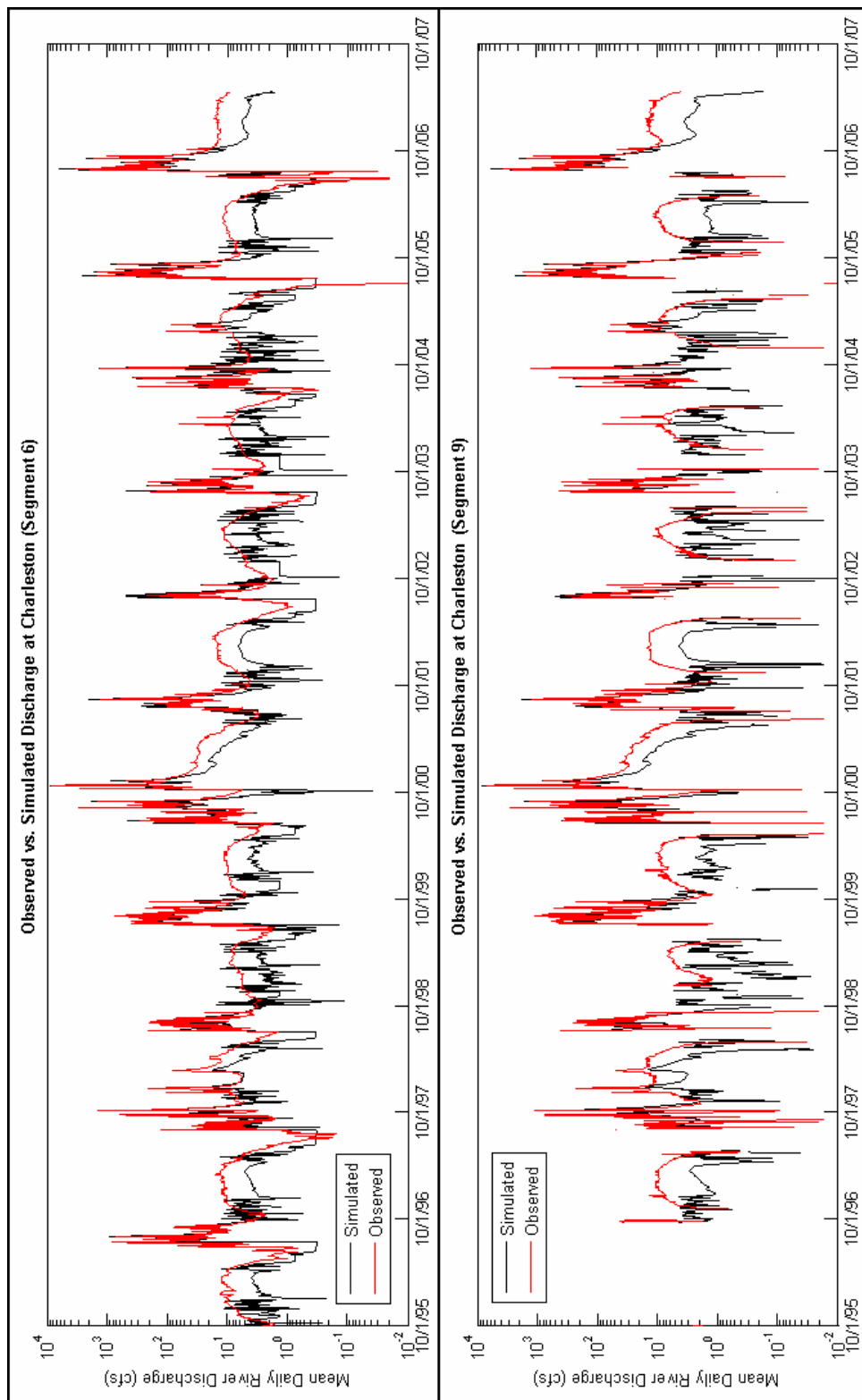


**Figure 20.** Simulated and observed streamflow hydrographs at the two discharge-rated gauging stations within the model domain (Charleston and Tombstone) for the model base case. Discharge observations do not exist at Tombstone between 10/1/95 and 9/20/96.

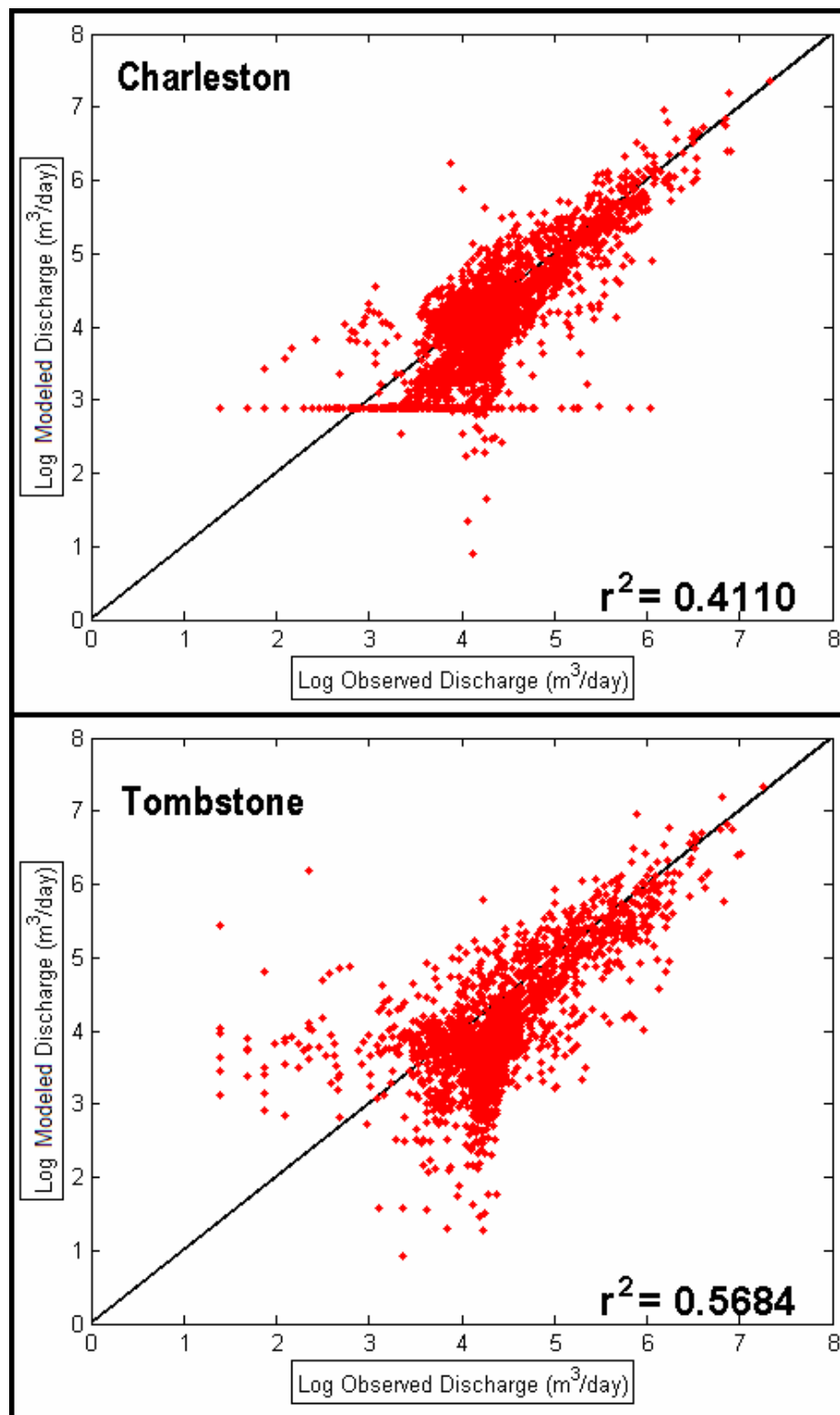


**Figure 21.** Modeled vs. observed discharge (m<sup>3</sup>/day) at Charleston and Tombstone for entire time domain (10/1/95-4/23/07) for 'base case' parameter set.

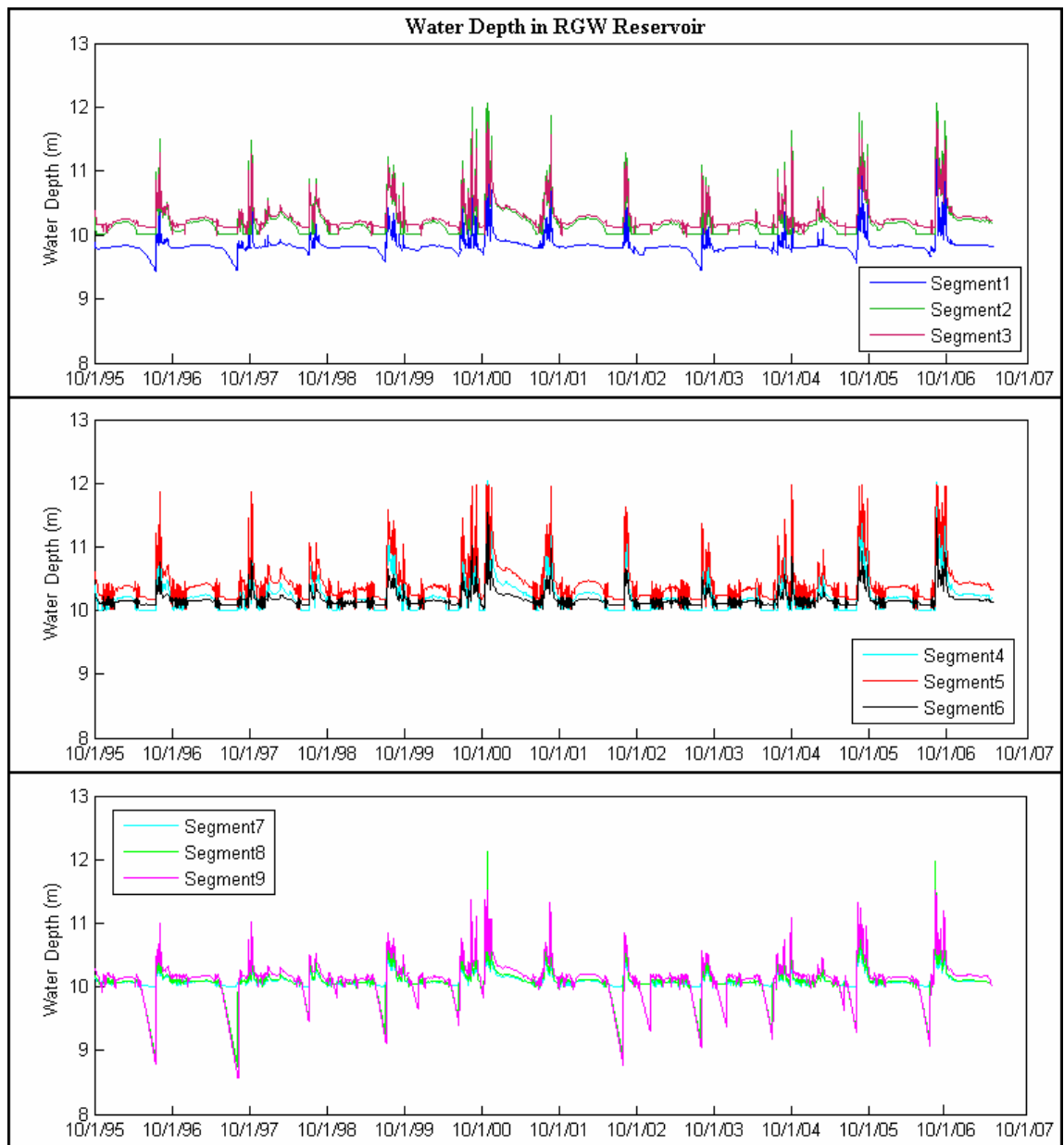


**Figure 22.** Simulated groundwater levels expressed in terms of water depth in RGW reservoir (m).

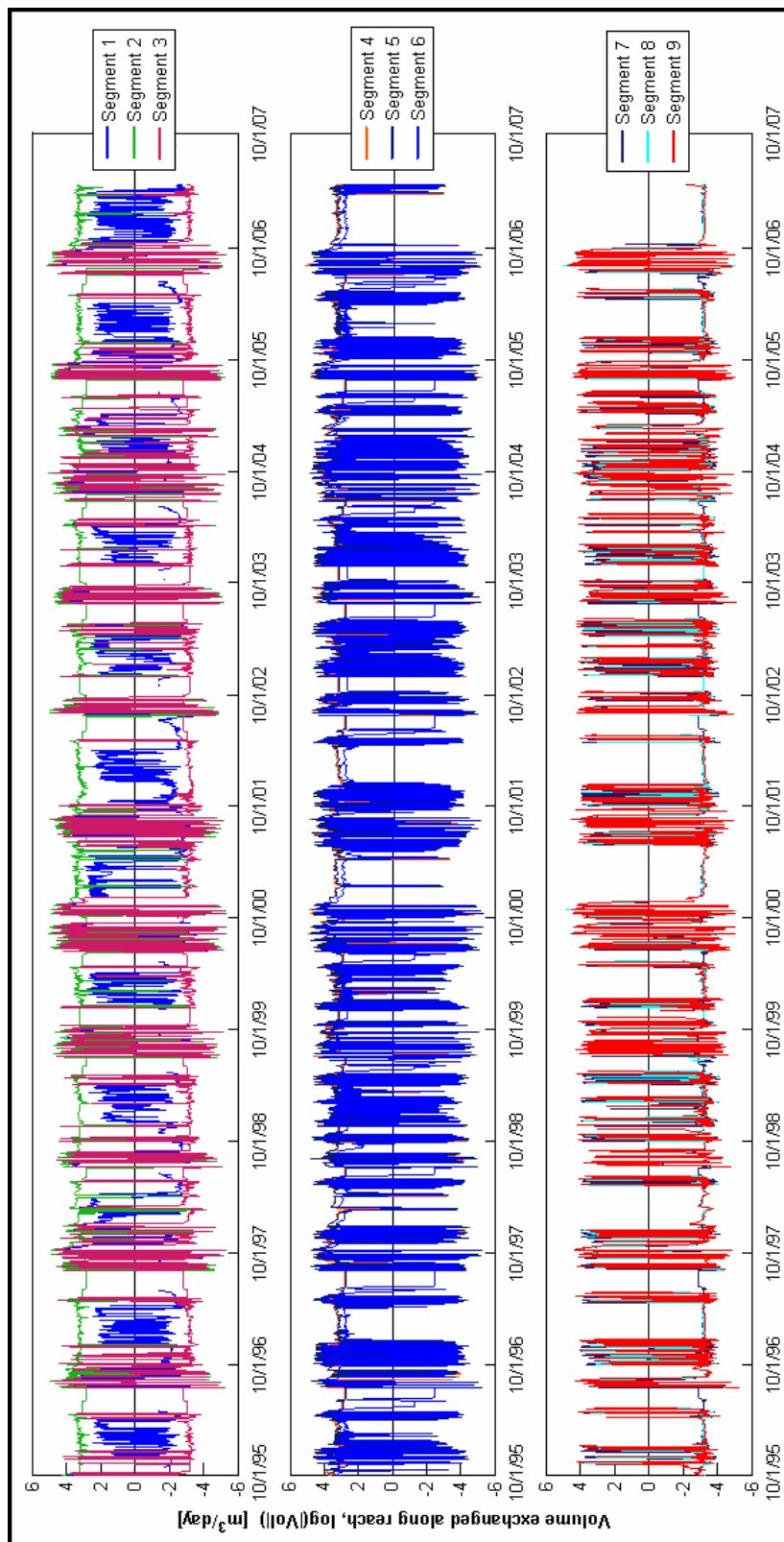


**Figure 23.** Log<sub>10</sub> of water volume exchanged between the river and RGW reservoir along each reach for the base case. Positive values indicate the river is gaining; negative values indicate losing.  
*Note:* 10<sup>4</sup> m<sup>3</sup>/day = 4.08 cfs.

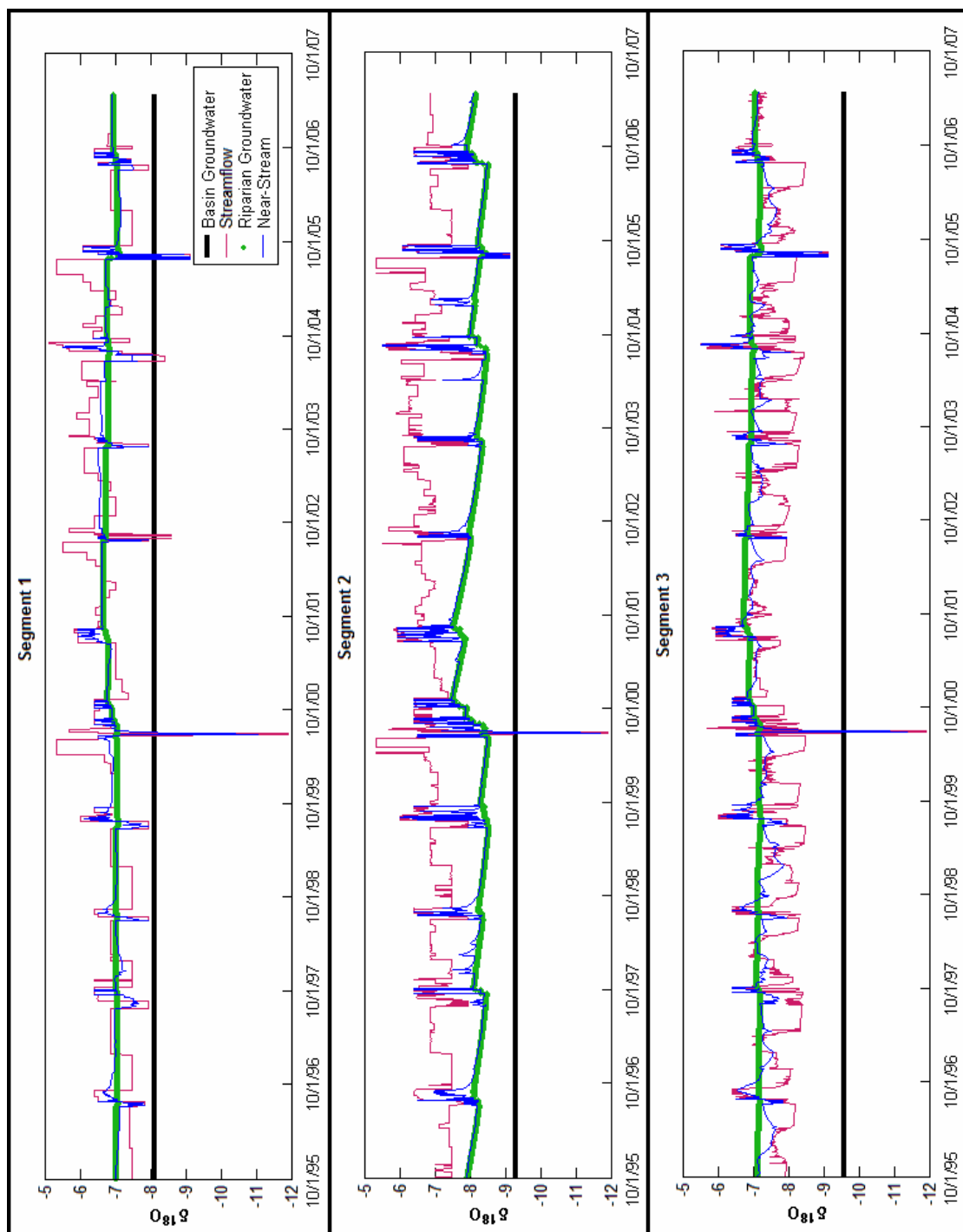


**Figure 24.** Modeled riparian groundwater and near-stream zone  $\delta^{18}\text{O}$  values relative to basin groundwater and modeled river values *entering* segments 1, 2 and 3. For segment 1, streamflow values are river chemistry inputs at the upstream end of the model domain (Figure 17).

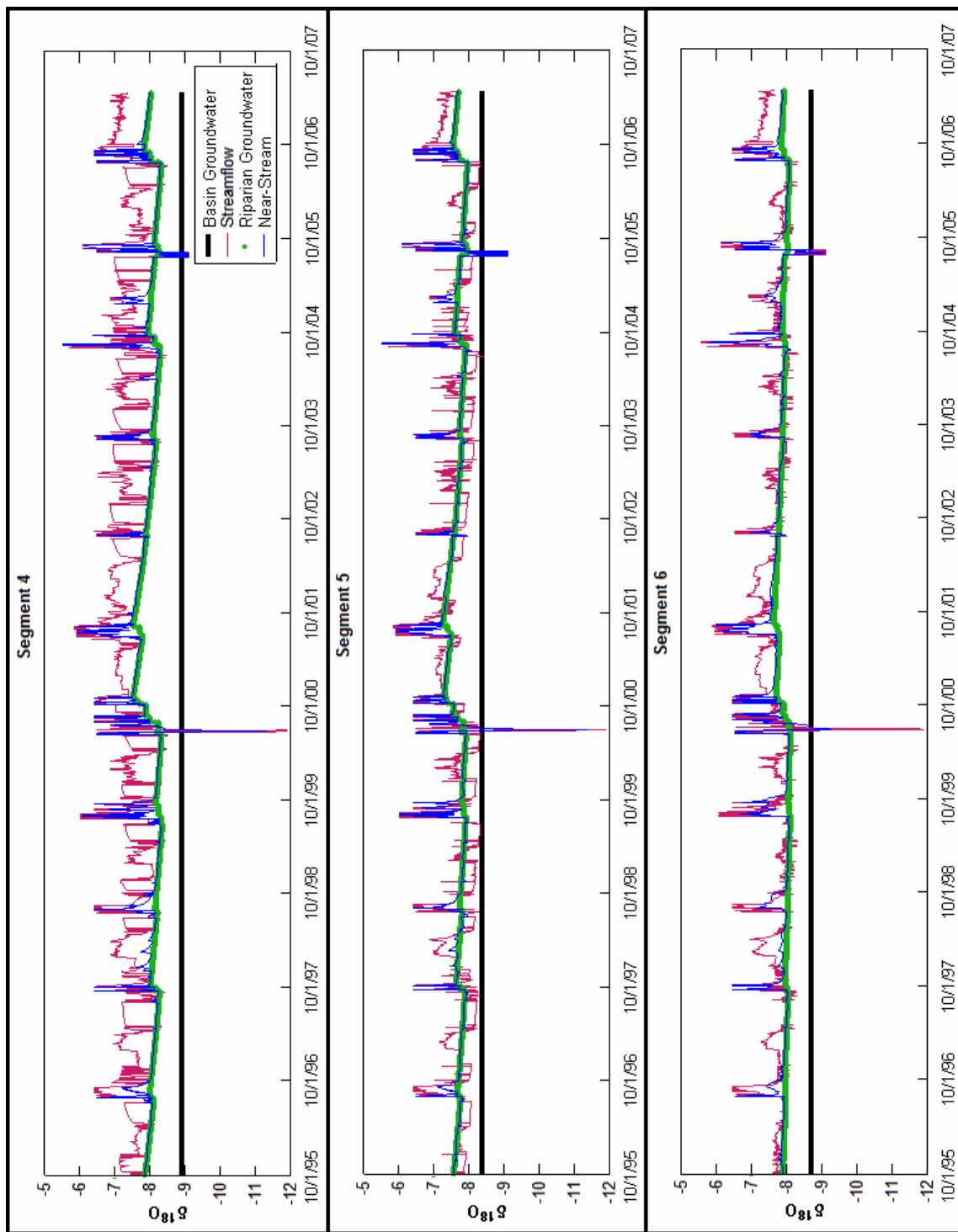


**Figure 25.** Modeled riparian groundwater and near-stream zone  $\delta^{18}\text{O}$  values relative to basin groundwater and modeled river values *entering* segments 4, 5 and 6.

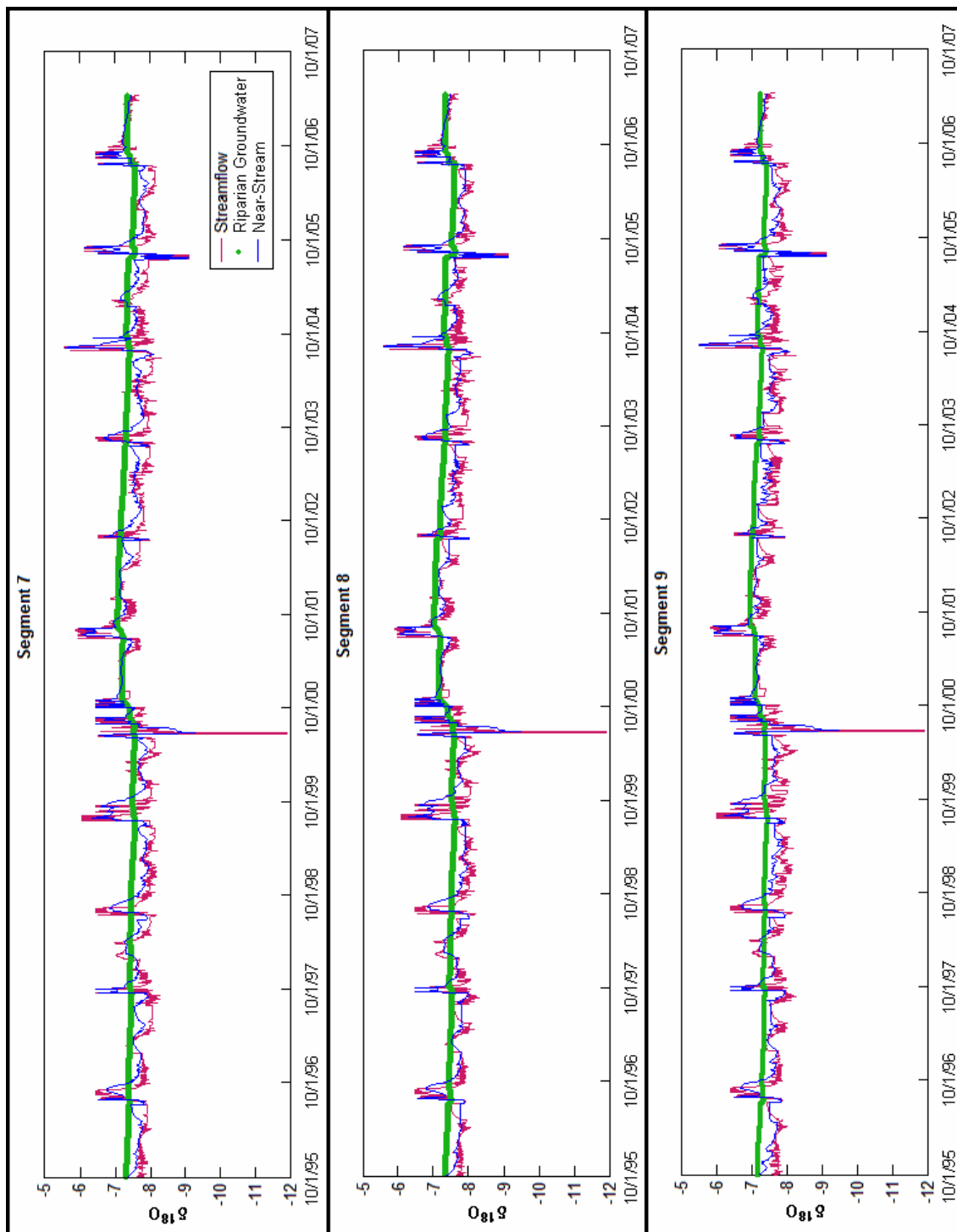


**Figure 26.** Modeled riparian groundwater and near-stream zone  $\delta^{18}\text{O}$  values relative to basin groundwater and modeled river values *entering* segments 7, 8 and 9.

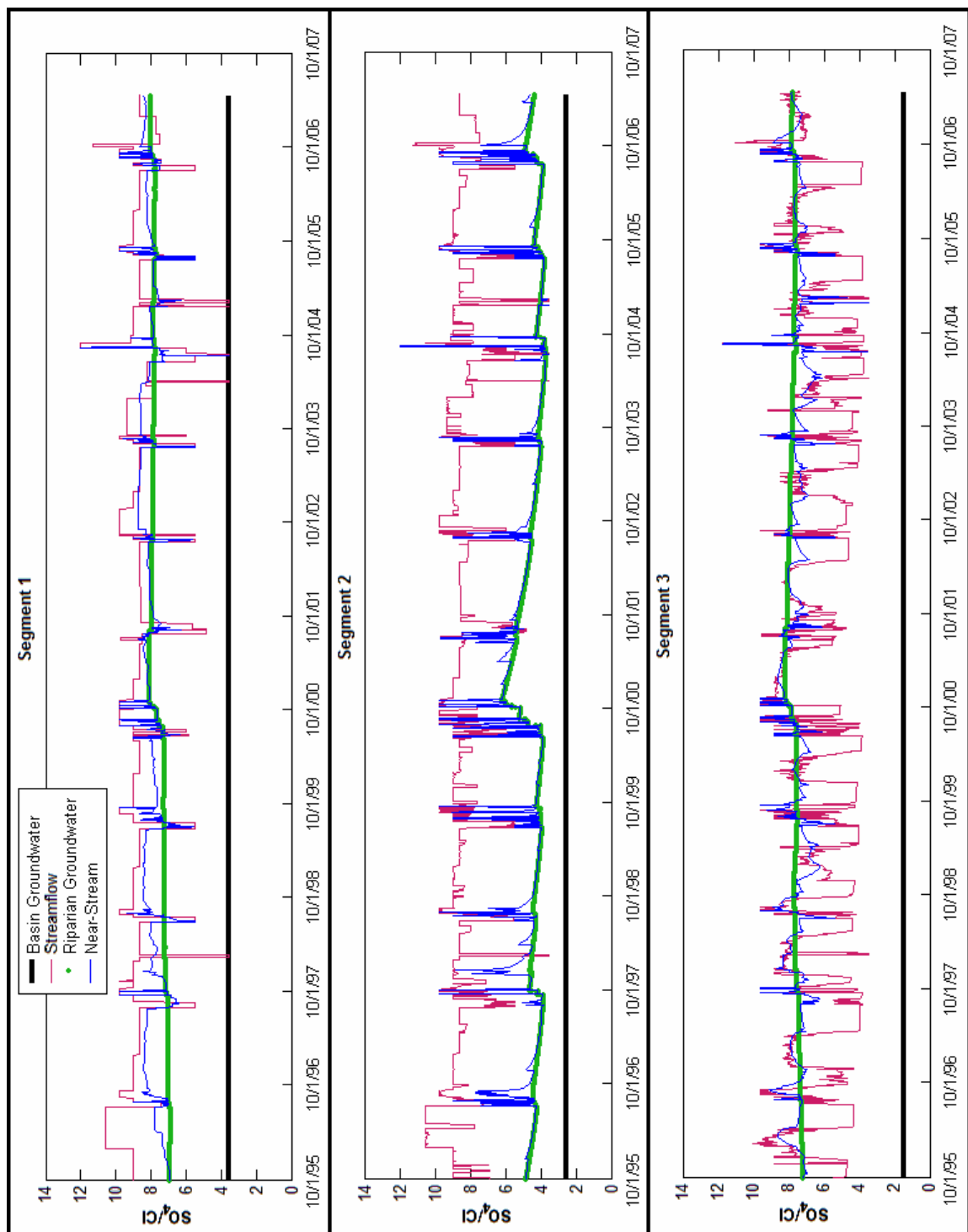


**Figure 27.** Modeled riparian groundwater and near-stream zone  $SO_4/Cl$  values relative to basin groundwater and modeled river values coming into segments 1, 2 and 3. For segment 1, streamflow values are the river chemistry inputs (Figure 18).

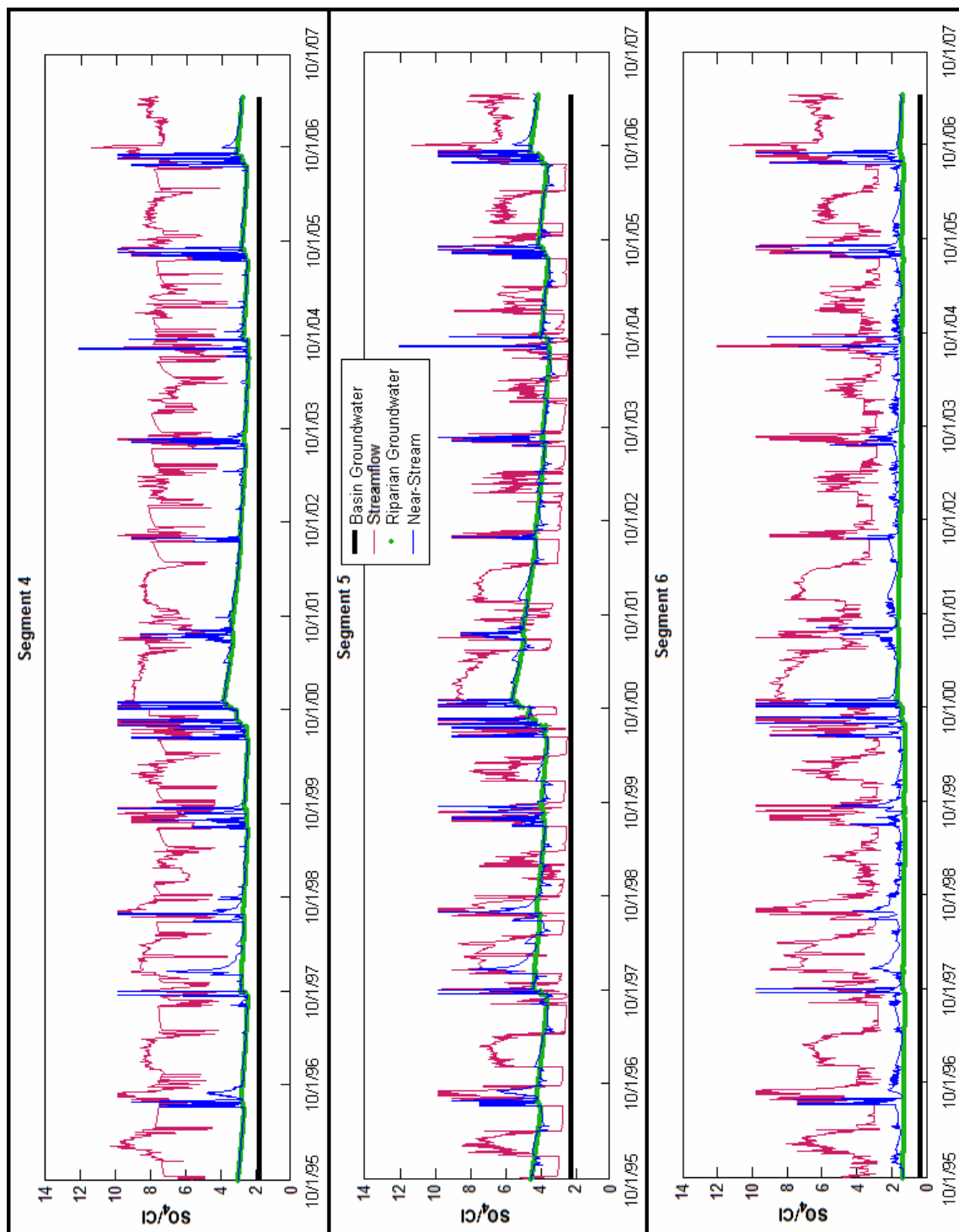


**Figure 28.** Modeled riparian groundwater and near-stream zone  $SO_4/Cl$  values relative to basin groundwater and modeled river values coming into segments 4, 5 and 6.

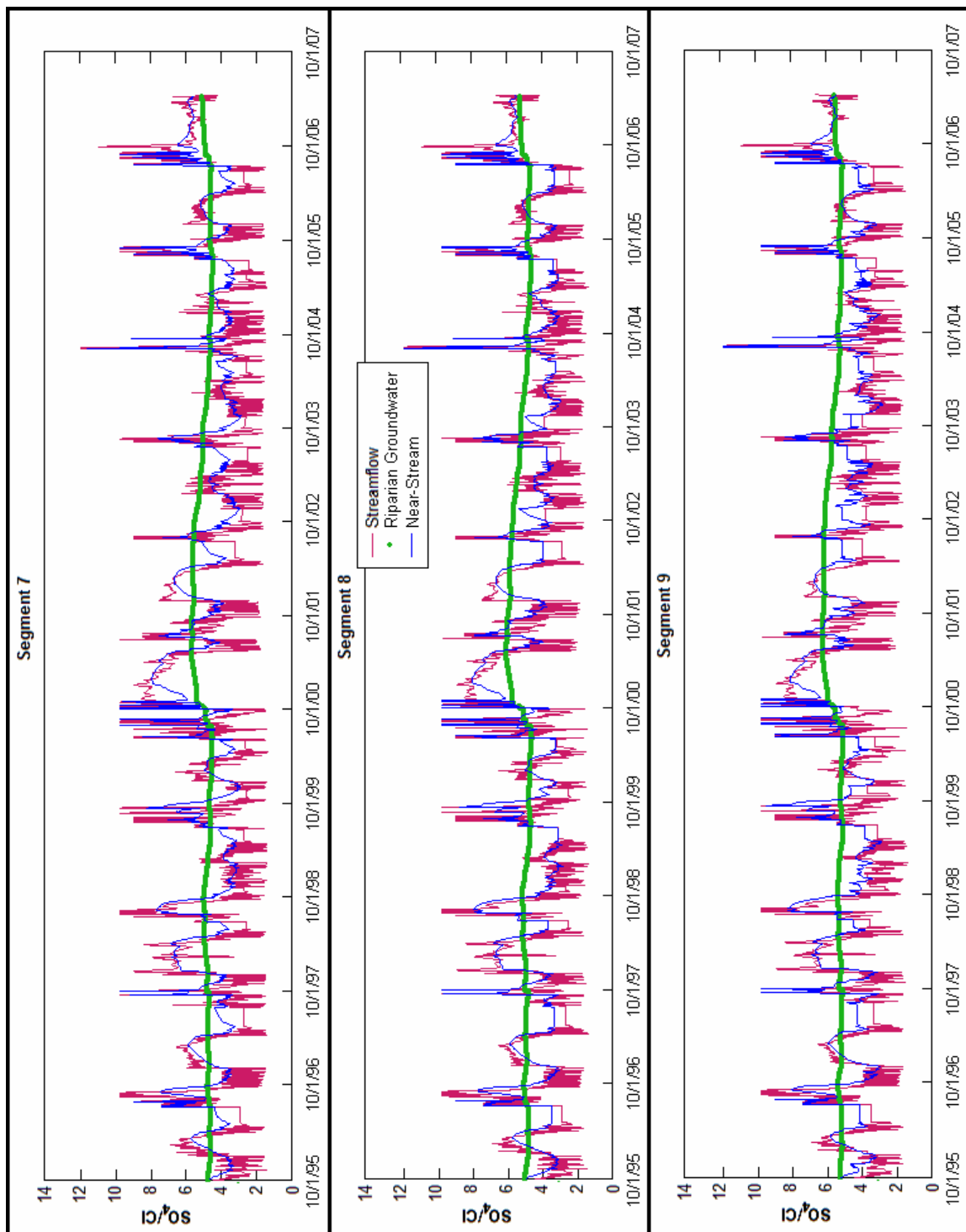


**Figure 29.** Modeled riparian groundwater and near-stream zone  $SO_4/Cl$  values relative to basin groundwater and modeled river values entering segments 7, 8 and 9.

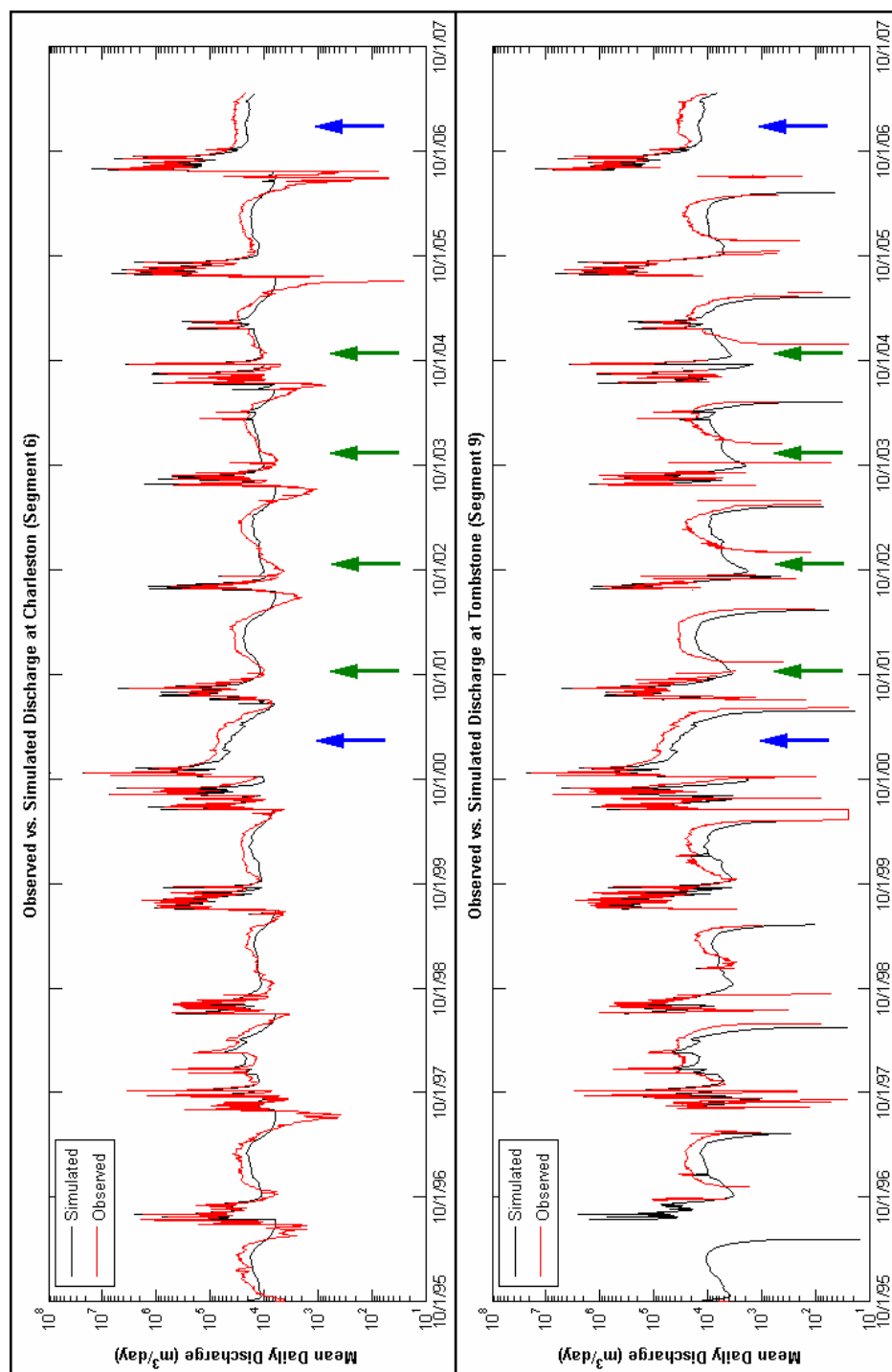


**Figure 30.** Observed and simulated river discharge at Charleston and Tombstone after manual model optimization. Green arrows indicate the consistent overestimation of post-monsoon baseflow following drier summers. Blue arrows indicate the consistent underestimation of post-monsoon baseflow following wetter summers.

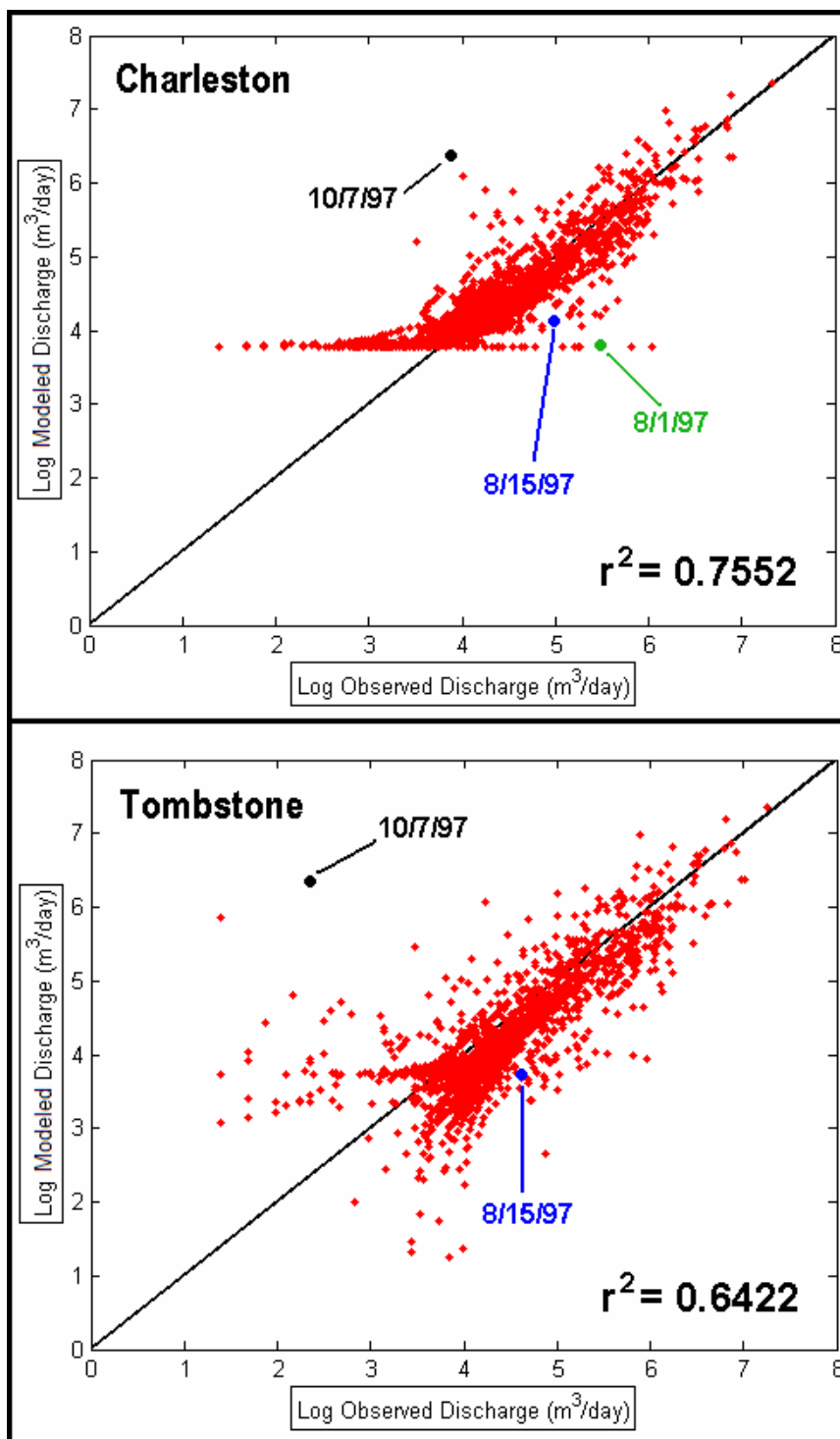


**Figure 31.** Post-optimization modeled vs. observed discharge (m<sup>3</sup>/day) at Charleston (top) from 10/1/95 to 4/23/07 and Tombstone (bottom) from 9/20/96 to 4/23/07. Note that data points and corresponding dates in the upper figure correspond to the dates shown in Figure 32.

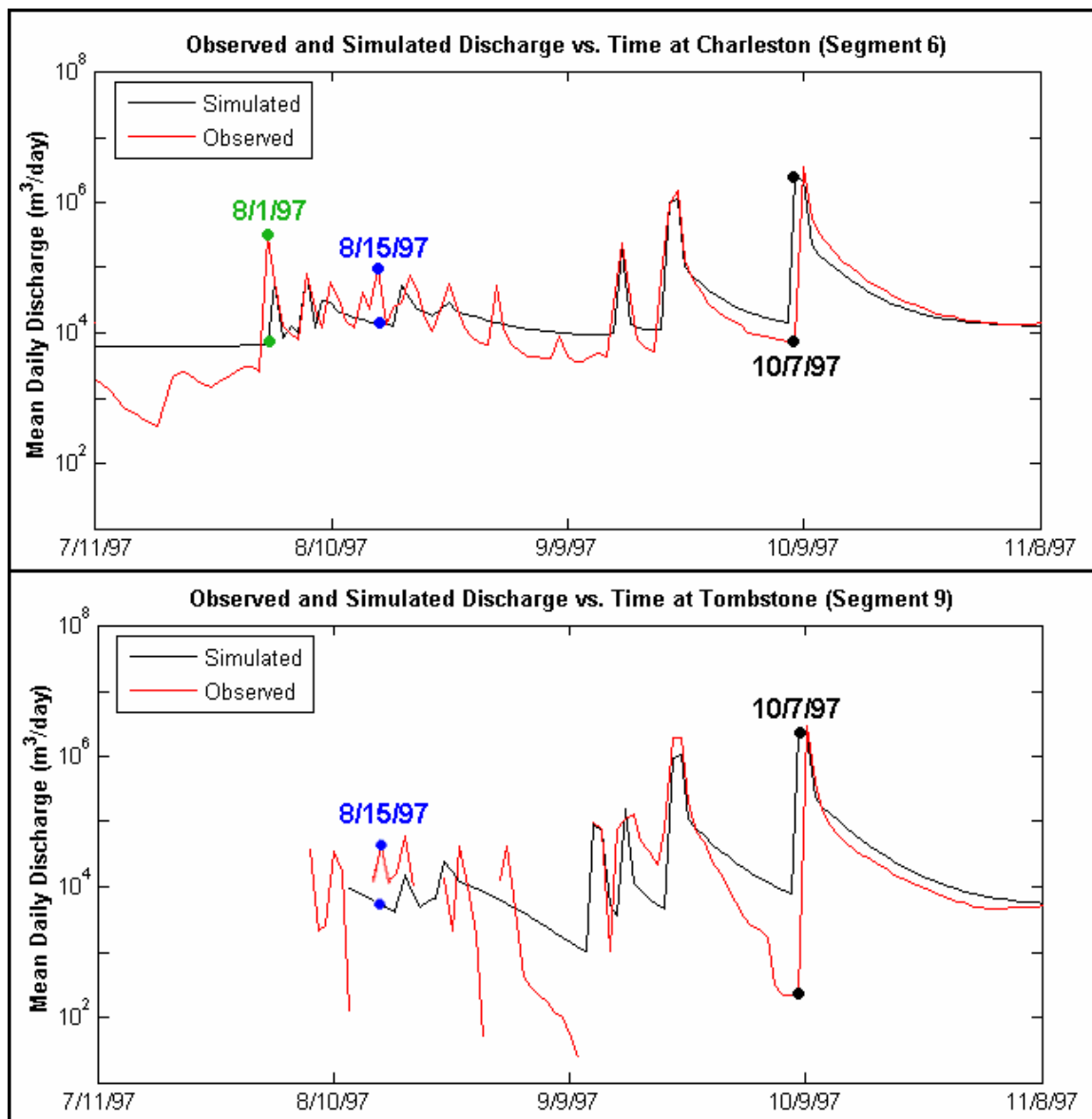


**Figure 32.** Close-up of input river discharge at Palominas and the observed and simulated river discharge at Charleston from 9/9/97 to 11/8/97. Note that the elevated flow event on 8/1/97 was not observed at the Tombstone gauge.

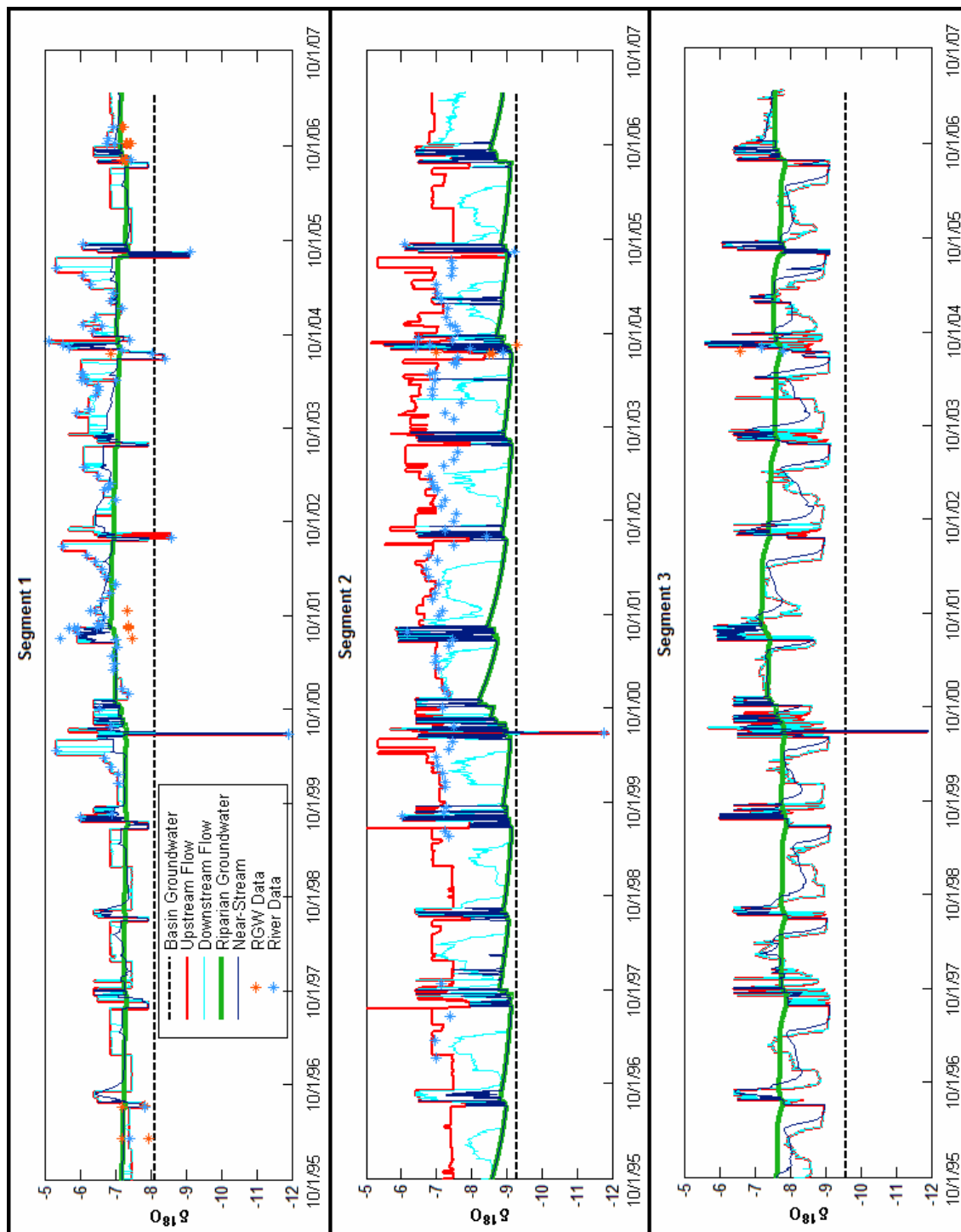


**Figure 33.** Post-optimization modeled riparian groundwater and near-stream zone  $\delta^{18}\text{O}$  values relative to basin groundwater and modeled river values entering and leaving segments 1, 2 and 3. In the case of segment 1, upstream flow values are the river chemistry inputs at the upstream end of the model domain.

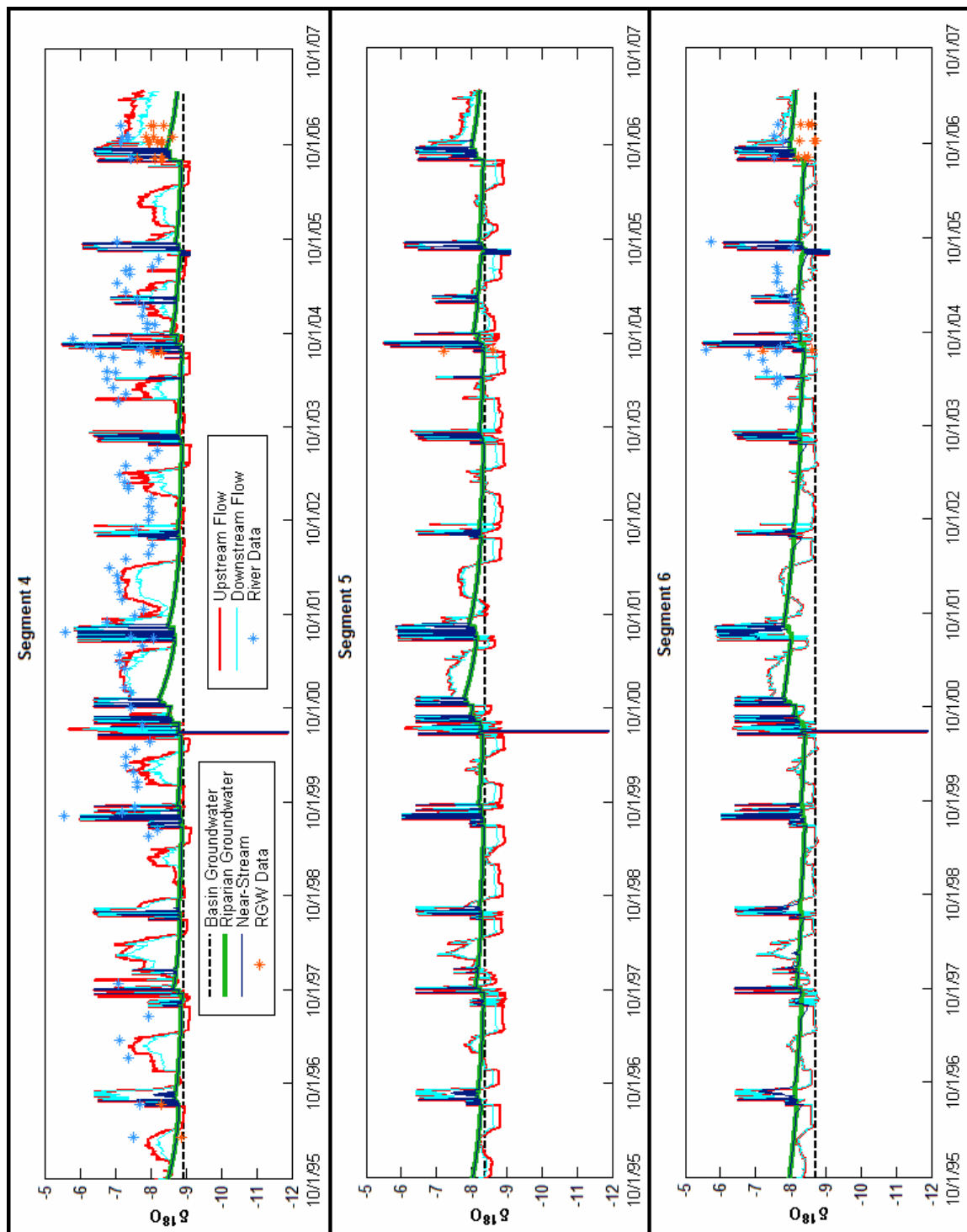


**Figure 34.** Post-optimization modeled riparian groundwater and near-stream zone  $\delta^{18}\text{O}$  values relative to basin groundwater and modeled river values entering and leaving segments 4, 5 and 6.

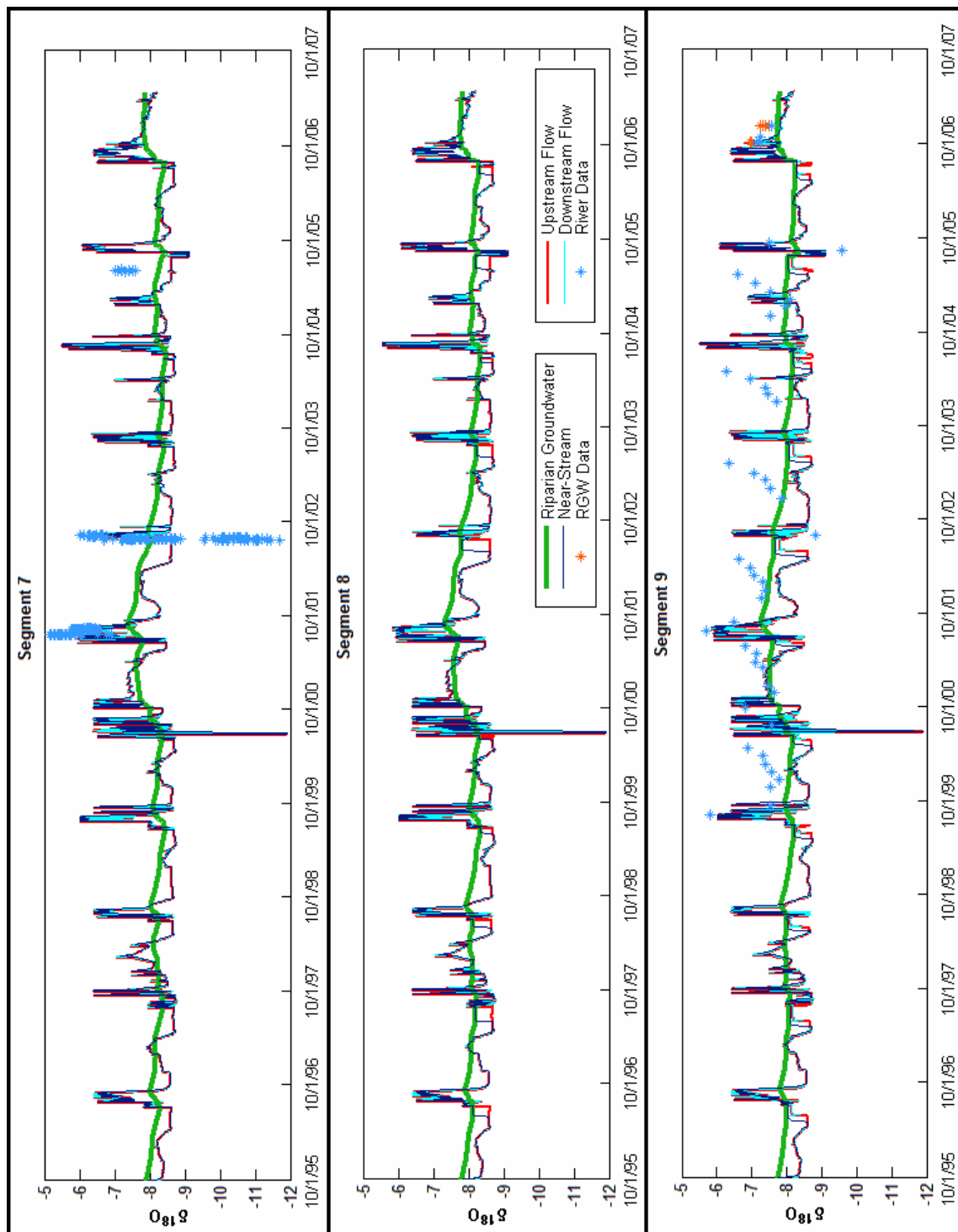


**Figure 35.** Post-optimization modeled riparian groundwater and near-stream zone  $\delta^{18}\text{O}$  values relative to basin groundwater and modeled river values entering and leaving segments 7, 8 and 9.

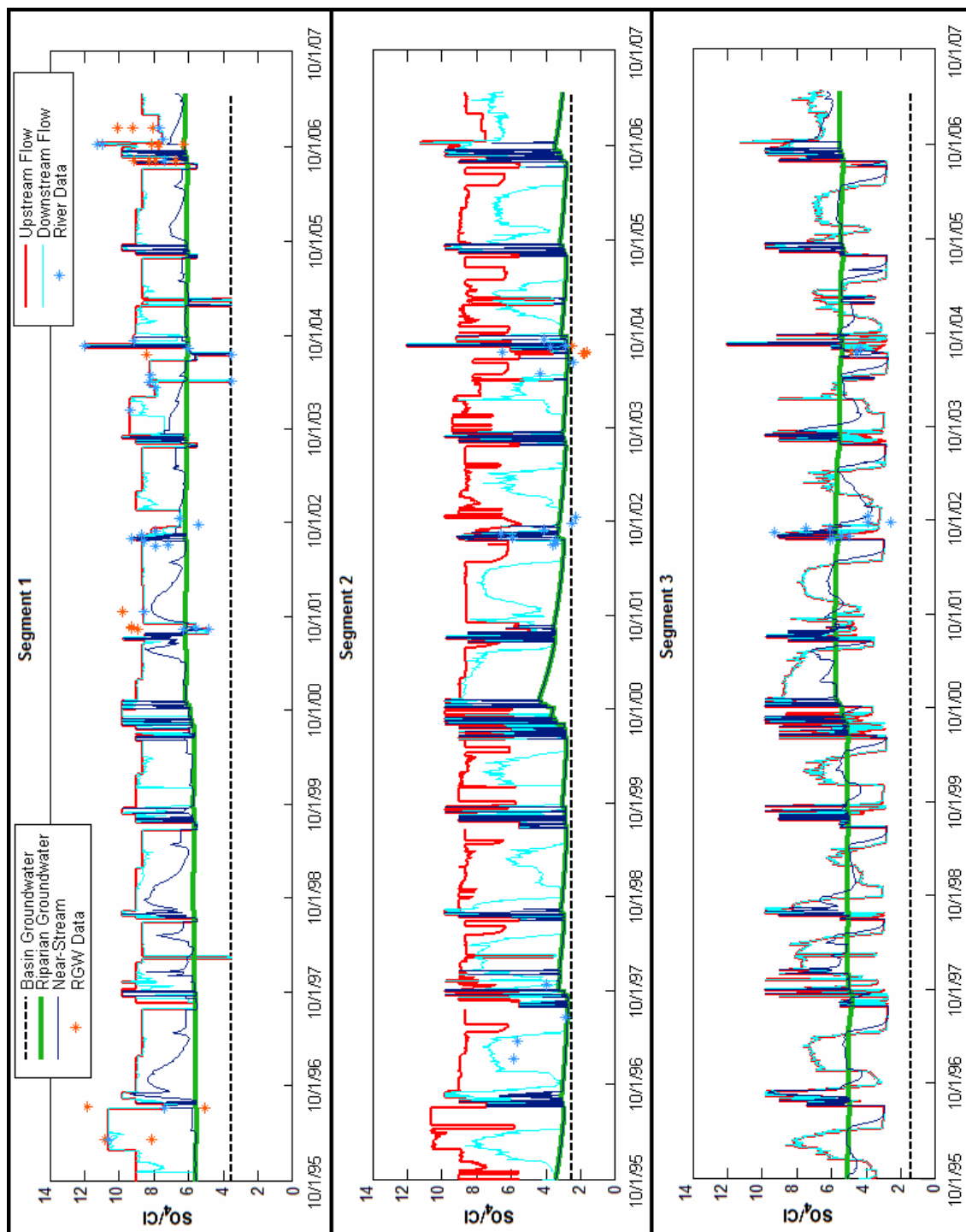


**Figure 36.** Post-optimization modeled riparian groundwater and near-stream zone  $SO_4/Cl$  values relative to basin groundwater and modeled river values entering and leaving segments 1, 2 and 3. In the case of segment 1, upstream flow values are the river chemistry inputs at the upstream end of the model domain.

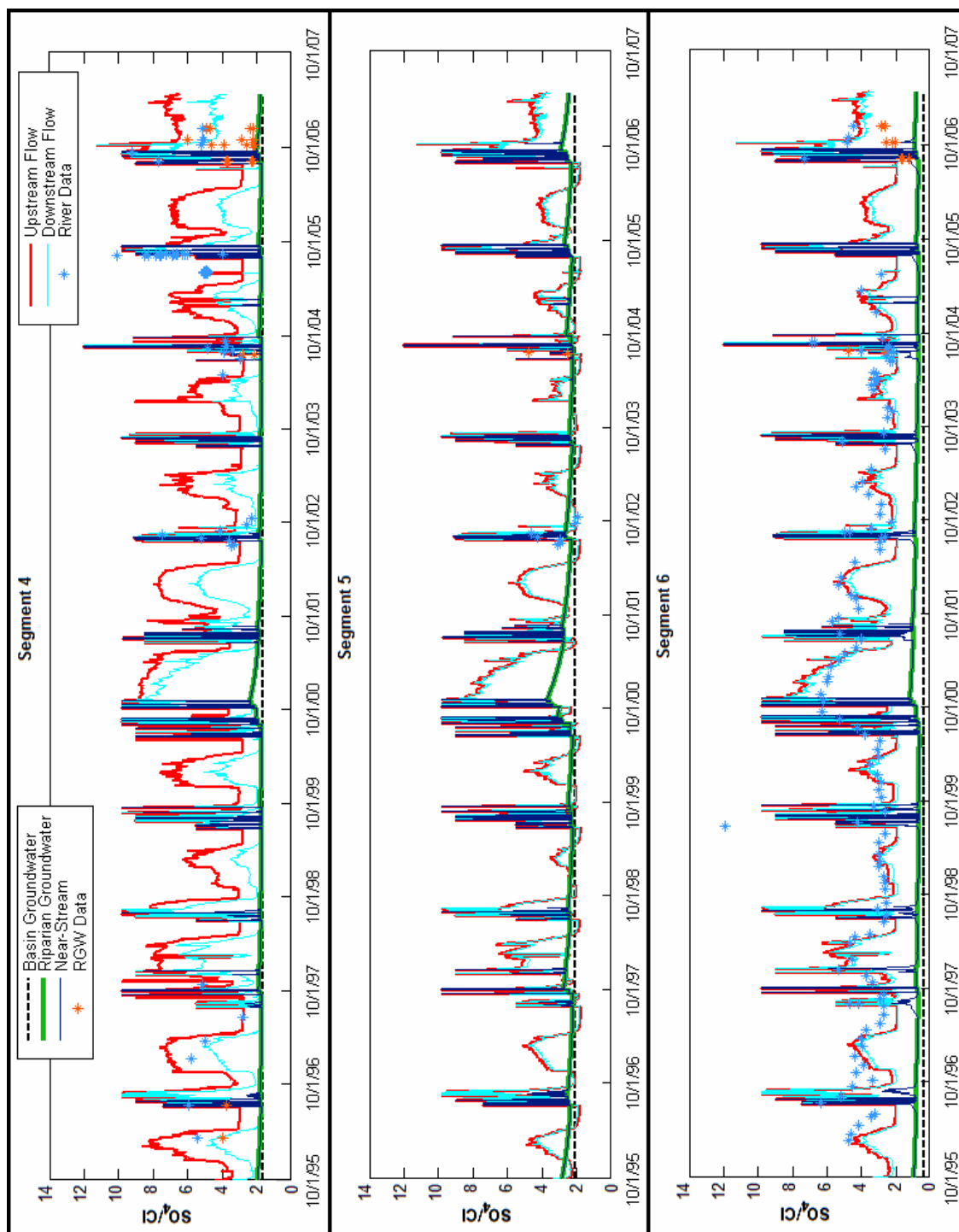


**Figure 37.** Post-optimization modeled riparian groundwater and near-stream zone  $SO_4/Cl$  values relative to basin groundwater and modeled river values entering and leaving segments 4, 5 and 6.

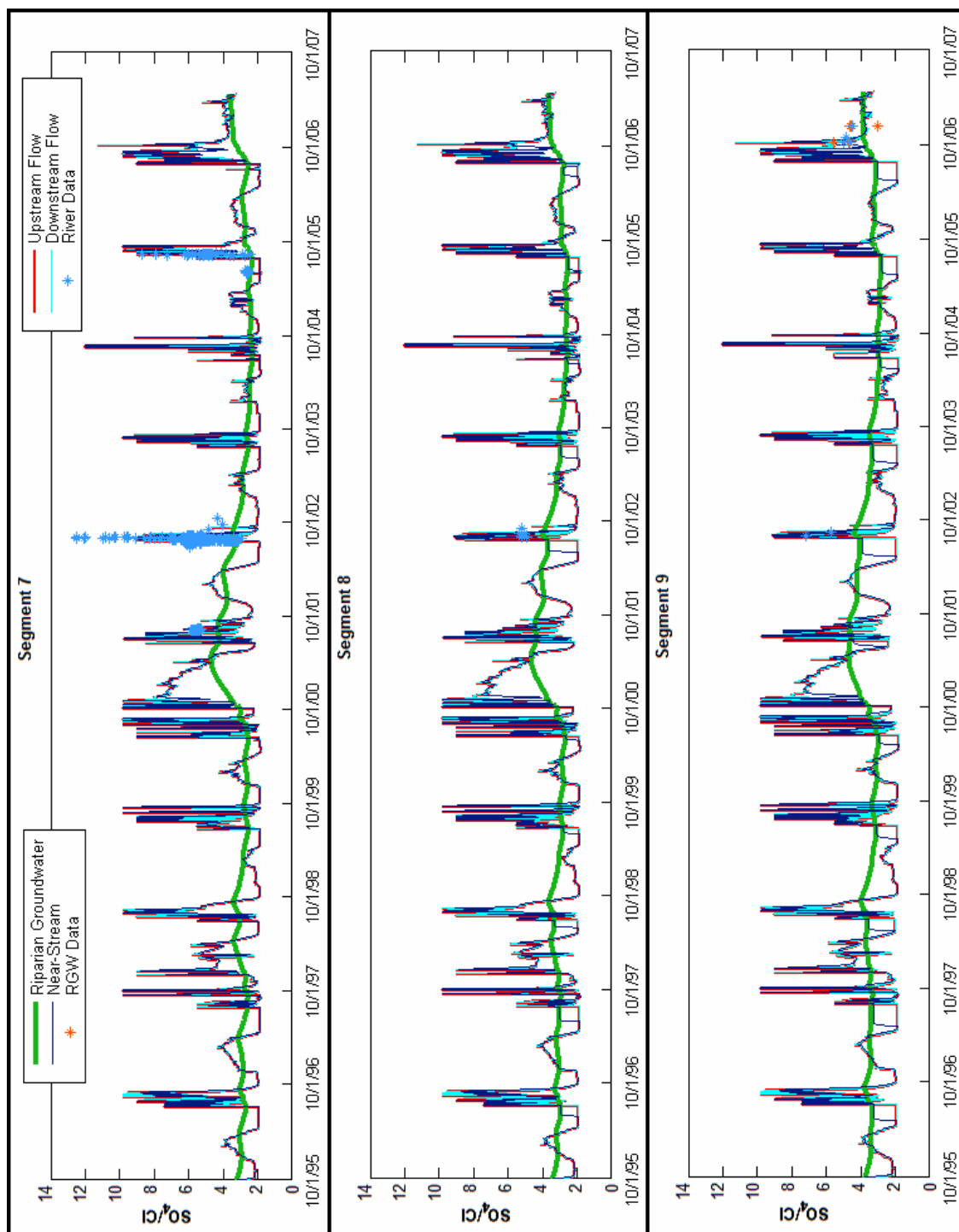


**Figure 38.** Post-optimization modeled riparian groundwater and near-stream zone  $SO_4/Cl$  values relative to basin groundwater and modeled river values entering and leaving segments 7, 8 and 9.

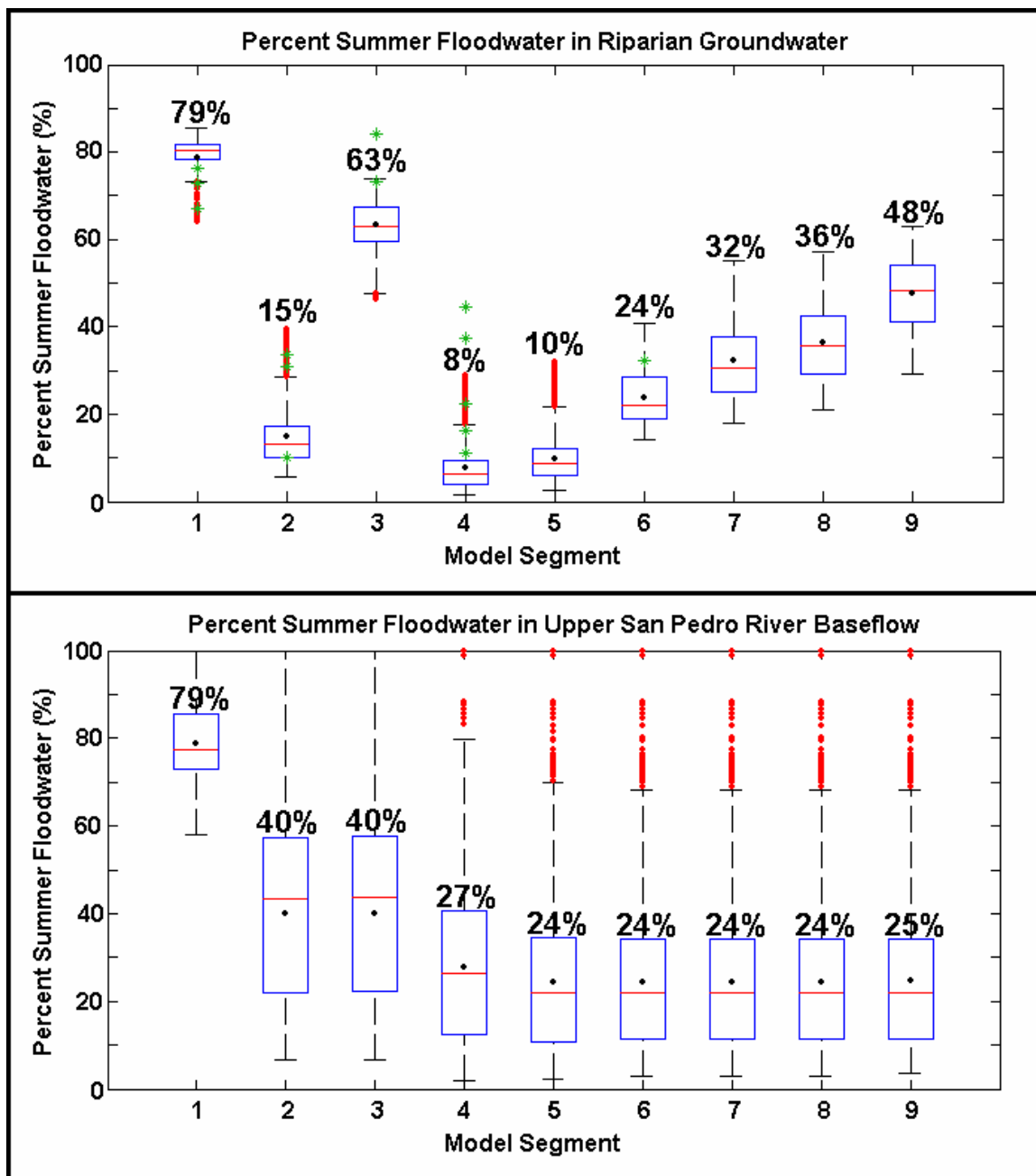


**Figure 39.** Percent monsoon floodwater in the riparian groundwater (top) and in river baseflow (bottom) for each model segment. Median values are indicated by horizontal red lines, quartile ranges by blue boxes and range of values by black brackets. Black dots and text are mean values and red points show statistical outliers. Green asterisks indicate mixing model results from Baillie et al. (2007).

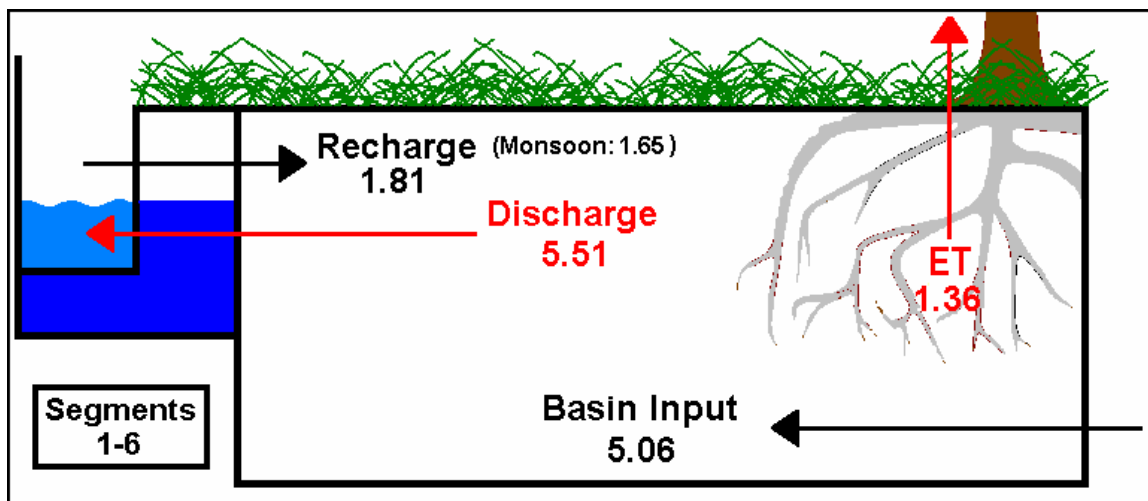


**Figure 40.** Cumulative flux during model time domain (10/1/95 to 4/23/07) for model segments 1-6. Units for each flux are  $10^7 \text{ m}^3$ .

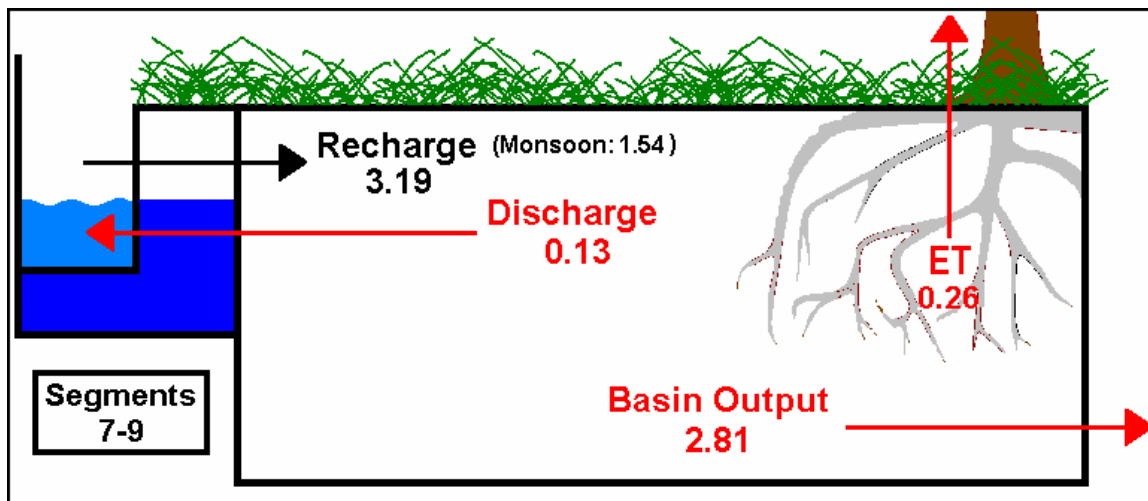


**Figure 41.** Cumulative flux during model time domain (10/1/95 to 4/23/07) for model segments 7-9. Units for each flux are  $10^7 \text{ m}^3$ .

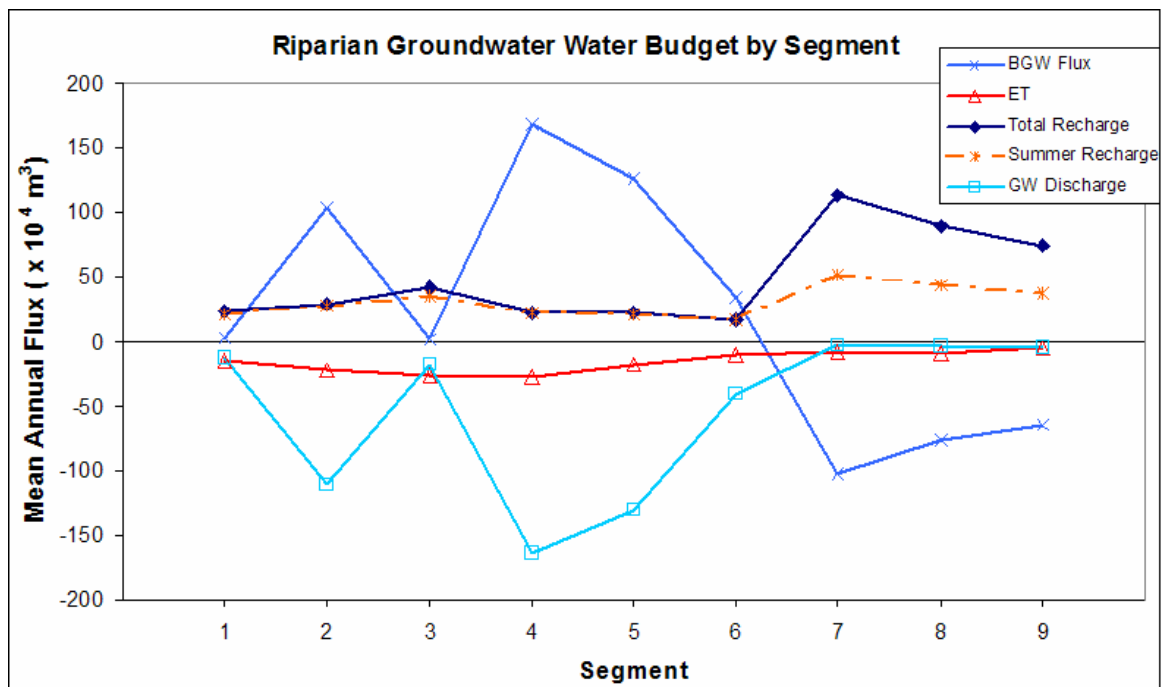


**Figure 42.** Mean annual basin groundwater (*BGW Flux*), evapotranspirative (*ET*), and river recharge/groundwater discharge fluxes for each model segment during the model time domain (10/1/95 to 4/23/07). Change in riparian groundwater storage is omitted due to the three-to-four order of magnitude difference relative to these fluxes.

## APPENDIX B: TABLES

## LIST OF TABLES

Table 1: Hydrologic characteristics of vegetation condition classes (information from Leenhouts, et al).....	111
Table 2: Summary of model parameters and state variables .....	112-113
Table 3: Vegetative cover data.....	114
Table 4: Basin groundwater flux requirements .....	114
Table 5: Data used to derive model river input chemistry .....	115
Table 6: Model base case parameter set .....	116
Table 7: Sensitivity Analysis: Parameter ranges, units and rank of importance.....	117
Table 8: Sensitivity Analysis: ‘Optimal’ parameter set.....	118
Table 9: Modeled riparian fluxes (cumulative).....	119

**Table 1.** Hydrologic characteristics of vegetation-based condition class model (information from Stromberg et al. in Leenhouts, et al. (2005))

Condition Class	Flow Permanence (%)		Mean floodplain groundwater depth (m)		Ground-water fluctuation (m)
	2002	2003	2002	2003	
<b>1</b>	48	17	2.5	3.5	1.8
<b>2</b>	78 ± 15	63 ± 21	2.5 ± 0.6	3.0 ± 0.9	0.9 ± 0.7
<b>3</b>	100 ± 0	98 ± 4	1.6 ± 0.5	1.7 ± 0.5	0.3 ± 0.0

Parameters			
	Name	Abbreviation	Description
Entire Domain	Diffusivity	$D$	Ratio of transmissivity to specific yield, used to determine aquifer transmissivity
	Specific Yield	$S_y$	Amount of water released from storage per area per drop in hydraulic head
	RGW Reservoir Depth	$RGWdepth$	Depth of the riparian groundwater reservoir used in calculating storage volume
	RGW Reservoir Width	$RGWwidth$	Width of the riparian groundwater reservoir used in calculating storage and exchange
	Near-stream zone volume	$V_{ns}$	Zone encompassing the river; continually-saturated
Segment - Specific	Basin Groundwater Flux	$Q_{bgw}$	Amount of water lost/added to RGW from the basin aquifer (per meter river length)
	Model Segment Length	$SegLength$	Length of river represented by each segment
	No-Flow River Stage	$ZeroFlowStage$	River stage at which river discharge entering a segment equals zero
	Surface Elevation	$Surf\_elev$	Average elevation of land surface at a well transect in each model segment
	River entrenchment	$Entrenchment$	Difference between surface elevation and low/no-flow groundwater levels

**Table 2a.** Summary of parameters important in determining the state, and thus the behavior, of the model.

State Variables			
	Name	Abbreviation	Description
Time - Constant	Basin Groundwater Chemistry	<i>Chem.bgw</i>	SO <sub>4</sub> , Cl, δ <sup>18</sup> O and δ <sup>2</sup> H values for basin groundwater inputs for gaining segments
	Initial Groundwater Chemistry	<i>Chem.rgw, (t=1)</i>	Initial SO <sub>4</sub> , Cl, δ <sup>18</sup> O and δ <sup>2</sup> H values for RGW reservoirs for each model segment
	Initial Groundwater Elevations	<i>InitGWElev</i>	Initial elevations of the water level in each RGW reservoir
Time - Variable	Riparian groundwater chemistry	<i>Chem.rgw</i>	SO <sub>4</sub> , Cl, δ <sup>18</sup> O and δ <sup>2</sup> H values for RGW reservoirs for each model segment
	Near-stream zone chemistry	<i>Chem.ns</i>	SO <sub>4</sub> , Cl, δ <sup>18</sup> O and δ <sup>2</sup> H values for NSZ reservoirs for each model segment
	River chemistry entering segment	<i>Chem.Rin</i>	SO <sub>4</sub> , Cl, δ <sup>18</sup> O and δ <sup>2</sup> H values for streamflow entering each segment
	River chemistry leaving segment	<i>Chem.Rout</i>	SO <sub>4</sub> , Cl, δ <sup>18</sup> O and δ <sup>2</sup> H values for streamflow leaving each segment
	River discharge entering segment	<i>Q<sub>in</sub></i>	River discharge entering each segment
	River discharge leaving segment	<i>Q<sub>out</sub></i>	River discharge leaving each segment
	Riparian groundwater volume	<i>V<sub>rgw</sub></i>	Volume of water stored within each RGW reservoir
	Groundwater Elevation	<i>GWElev</i>	Elevation of the water level in each RGW reservoir

**Table 2b.** Summary of state variables important in determining the state, and thus the behavior, of the model.

**Table 3.** Proportion of land surface within 100 meters of main river channel covered by the four phreatophyte groups. Determined from land cover data collected and distributed by EPA/USDA-ARS (2003).

Segment	Cottonwood	Mesquite	Sacaton	Tamarisk
1	0.4225	0.0306	0.0158	0
2	0.3255	0.0192	0.2484	0
3	0.3594	0.0865	0.3197	0
4	<b>0.3934</b>	<b>0.0687</b>	<b>0.2589</b>	<b>0</b>
5	0.3125	0.0668	0.1702	0
6	0.2432	0.1730	0.0545	0
7	0.1482	0.3962	0.0473	0
8	0.1593	0.4314	0.0258	0
9	0.0315	0.4155	0.0561	0.1517

**Table 4.** Requirements for the magnitude and direction of basin groundwater flux ( $Q_{bgw}$ ) with respect to riparian groundwater.

Parameter	Requirement
$Q_{bgw}(1)$	Must be positive and less than 0.183 m <sup>2</sup> /day
$Q_{bgw}(2)$	Must be greater than 0.220 m <sup>2</sup> /day
$Q_{bgw}(3)$	Must be greater than -0.619 m <sup>2</sup> /day and less than $Q_{bgw}(1)$
$Q_{bgw}(4)$	Must be greater than 0.252 m <sup>2</sup> /day
$Q_{bgw}(5)$	Must be greater than 0.188 m <sup>2</sup> /day
$Q_{bgw}(6)$	Must be greater than 0.120 m <sup>2</sup> /day
$Q_{bgw}(7)$	Must be negative and greater than -0.474 m <sup>2</sup> /day
$Q_{bgw}(8)$	Must be negative
$Q_{bgw}(9)$	Must be negative

	<i>n</i>	SO <sub>4</sub>	Cl	SO <sub>4</sub> /Cl	<i>n</i>	δ <sup>18</sup> O	δ <sup>2</sup> H
<b>Early Monsoon High Flow</b>	2	21.32	2.87	7.42	3	-9.08	-63.2
<b>Mid-Monsoon High Flow</b>	0	-	-	-	3	-6.57	-41.9
<b>Late-Monsoon High Flow</b>	4	26.75	3.20	8.09	7	-5.86	-39.4
<b>Monsoon Low Flows</b>	3	22.24	3.46	6.12	12	-7.30	-53.1
<b>Spring Floods</b>	1	3.37	0.95	3.57	1	-7.00	-36.5
<b>Spring Baseflow</b>	4	86.58	9.99	8.76	23	-6.30	-47.8
<b>Autumn/Winter Baseflow</b>	3	79.48	9.42	8.20	27	-6.74	-49.7

**Table 5.** Data used in deriving model input values for SO<sub>4</sub>/Cl, δ<sup>18</sup>O and δ<sup>2</sup>H grouped by time of year and hydrograph condition (*n*= number of samples available for each group). *n* values for groups differ because all samples were analyzed for δ<sup>18</sup>O and δ<sup>2</sup>H but not for anion concentrations. Data is from the Palominas USGS gauge and was either retrieved from the USGS-NWIS database or unpublished data collected during the Baillie et al. (2007) study.

**Table 6a.** Segment-specific parameters for model base case.

**Segment-Specific Parameters**

	$Q_{bgw}$ (m <sup>2</sup> /day)	Segment Length (m)	Surface Elevation (m)	Entrenchment (m)
Segment 1	0.005	4660	1288.44	1.68
Segment 2	0.300	5975	1261.57	2.08
Segment 3	-0.250	6000	1252.63	1.78
Segment 4	0.280	6080	1233.62	2.04
Segment 5	0.280	5200	1223.00	1.97
Segment 6	0.120	4900	1213.21	2.03
Segment 7	-0.300	4900	1200.00	2.29
Segment 8	-0.350	4380	1186.01	2.70
Segment 9	-0.400	4650	1150.46	1.54

**Table 6b.** Base case parameters for entire model domain.

<b>Diffusivity</b>	3090 m <sup>2</sup> /day
<b>Specific Yield</b>	0.32
<b>RGW Reservoir Width</b>	100 m
<b>RGW Reservoir Depth (BLS)</b>	10 m
<b>Near-stream zone volume</b>	10 m <sup>2</sup>

Parameter	Range Limits		Units	Importance and Importance Rank											
	Lower	Upper		Water Balance Outputs					Chem/isotopic Outputs						
				Q	ET	GW Elev	RGW	NSZ	River						
Diffusivity	210	5115	[m <sup>2</sup> /day]	0.89	13	0.84	13	0.89	13	0.91	20	0.93	20	0.94	20
Sy	0.05	0.42	[-]	0.11	1	0.22	3	0.20	2	0.15	3	0.18	3	0.19	3
RGW_width	40	160	[m]	0.71	10	0.50	7	0.78	12	0.77	18	0.80	19	0.75	16
ETMult	0	3	[-]	0.33	3	0.12	1	0.35	3	0.54	12	0.50	11	0.38	7
RGWDepth	1	20	[m]	1.00	14	1.00	14	1.00	14	0.46	10	0.71	16	0.81	19
Qbgw(1)	0.001	0.182	[m <sup>2</sup> /day]	0.25	2	0.46	5	0.20	1	0.42	9	0.32	7	0.25	5
Qbgw(2)	0.22	1	[m <sup>2</sup> /day]	0.36	4	0.59	8	0.43	6	0.40	8	0.31	6	0.27	6
Qbgw(3)	-0.618	0.181	[m <sup>2</sup> /day]	0.55	6	0.71	10	0.60	8	0.58	14	0.51	12	0.51	11
Qbgw(4)	0.252	1	[m <sup>2</sup> /day]	0.48	5	0.48	6	0.41	4	0.27	4	0.22	4	0.21	4
Qbgw(5)	0.188	1	[m <sup>2</sup> /day]	0.61	8	0.62	9	0.61	9	0.34	5	0.31	5	0.39	8
Qbgw(6)	0.12	1	[m <sup>2</sup> /day]	0.59	7	0.42	4	0.43	5	0.15	2	0.15	2	0.17	2
Qbgw(7)	-0.474	-0.001	[m <sup>2</sup> /day]	0.85	12	0.72	11	0.72	11	0.46	11	0.47	10	0.48	9
Qbgw(8)	-1	-0.001	[m <sup>2</sup> /day]	0.78	11	0.78	12	0.62	10	0.38	7	0.43	9	0.51	10
Qbgw(9)	-1	-0.001	[m <sup>2</sup> /day]	0.71	9	0.21	2	0.43	7	0.36	6	0.40	8	0.55	12
Vns	1	20	[m <sup>2</sup> ]	-	-	-	-	-	-	0.63	15	0.61	14	0.68	15
PALRivChem	0.5	1.5	[SO <sub>4</sub> ],[‰]	-	-	-	-	-	-	0.14	1	0.12	1	0.12	1
BGWChem1	-1σ	+1σ	[SO <sub>4</sub> ],[‰]	-	-	-	-	-	-	0.97	21	0.99	21	0.99	21
BGWChem2	-1σ	+1σ	[SO <sub>4</sub> ],[‰]	-	-	-	-	-	-	0.81	19	0.79	18	0.76	18
BGWChem4	-1σ	+1σ	[SO <sub>4</sub> ],[‰]	-	-	-	-	-	-	0.64	16	0.64	15	0.60	13
BGWChem5	-1σ	+1σ	[SO <sub>4</sub> ],[‰]	-	-	-	-	-	-	0.55	13	0.58	13	0.62	14
BGWChem6	-1σ	+1σ	[SO <sub>4</sub> ],[‰]	-	-	-	-	-	-	0.70	17	0.72	17	0.75	17

**Table 7.** Ranges, units and rank of importance (for hydrologic and chemical/isotopic system states and fluxes) for each of the 21 parameters altered during one-at-a-time sensitivity analysis. \*The absence of importance value and rank for a given parameter indicates no sensitivity of the output class to any perturbation of the parameter. \*\*'1σ' ranges used for basin groundwater chemistry perturbation were 0.4‰ (δ<sup>18</sup>O) and 0.4 (SO<sub>4</sub>/Cl) (after basin groundwater end-member (Baillie et al., 2007)).

**Table 8.** ‘Optimal’ parameter set based on manual calibration. Segment length, entrenchment and land surface elevations were unchanged from the base case parameter set.

<b>Segment-Specific Parameters</b>				
	<b>Q<sub>bgw</sub> (m<sup>2</sup>/day)</b>	<b>Segment Length (m)</b>	<b>Surface Elevation (m)</b>	<b>Entrenchment (m)</b>
Segment 1	0.020	4660	1288.44	1.68
Segment 2	0.500	5975	1261.57	2.08
Segment 3	0.010	6000	1252.63	1.78
Segment 4	0.800	6080	1233.62	2.04
Segment 5	0.700	5200	1223.00	1.97
Segment 6	0.200	4900	1213.21	2.03
Segment 7	-0.600	4900	1200.00	2.29
Segment 8	-0.500	4380	1186.01	2.70
Segment 9	-0.400	4650	1150.46	1.54

<b>Diffusivity</b>	1760 m <sup>2</sup> /day
<b>Specific Yield</b>	0.16
<b>RGW Reservoir Width</b>	100 m
<b>RGW Reservoir Depth (BLS)</b>	10 m
<b>Near-stream zone volume</b>	10 m <sup>2</sup>

Segment	Q <sub>bgw</sub>	ET	Groundwater Discharge (x 10 <sup>5</sup> m <sup>3</sup> )	Total Recharge	Summer Recharge	ΔStorage	Percent Total Recharge in Summer (%)
1	3.75	16.32	14.95	27.52	25.01	0.003	90.9
2	119.97	25.21	128.44	33.66	31.97	0.012	95.0
3	2.41	30.54	20.12	48.24	40.36	0.014	83.7
4	195.31	32.18	189.41	26.26	25.18	0.019	95.9
5	146.03	20.18	151.47	25.61	24.39	0.014	95.2
6	39.39	11.73	47.41	19.76	18.80	0.005	95.2
7	-118.16	9.11	3.10	130.37	59.78	0.001	45.9
8	-88.02	11.13	4.41	103.55	50.14	0.002	48.4
9	-74.75	5.48	5.28	85.51	43.78	0.001	51.2
<b>Total</b>	<b>225.92</b>	<b>161.86</b>	<b>564.61</b>	<b>500.47</b>	<b>319.41</b>	<b>0.07</b>	<b>-</b>

Relative Proportions			Average %
Upper (1-6)	0.84	0.36	92.6
Lower (7-9)	0.16	0.64	48.5

**Table 9.** Cumulative basin groundwater ( $Q_{bgw}$ ), evapotranspirative ( $ET$ ), and river recharge/groundwater discharge fluxes for each model segment during the model time domain (10/1/95 to 4/23/07). Relative proportions of each flux occurring in the upper ~70% of the model (segments 1-6) and lower ~30% (segments 7-9) are also shown for comparison.

## APPENDIX C: CONDITION SCORE BIOINDICATORS

Bioindicator Variables (from Stromberg et al., 2005)

- 1 - Number of 10-cm Fremont cottonwood + Goodding willow size classes in flood plain
- 2 - Fremont cottonwood + Goodding willow basal area (m<sup>2</sup>/ha)
- 3 - Fremont cottonwood + Goodding willow relative basal area (%)
- 4 - Maximum vegetation height (m) in flood plain
- 5 - Shrublands cover in flood plain (%)
- 6 - Absolute cover of streamside hydric perennial herbs (%)
- 7 - Relative cover of streamside hydric perennial herbs (%)
- 8 - Absolute cover of streamside hydric herbs (%)
- 9 - Relative cover of streamside hydric herbs (%)

## APPENDIX D: MODEL ENTRENCHMENT DEPTHS

Segment	Entrenchment (m)
1	1.68
2	2.08
3	1.78
4	2.04
5	1.97
6	2.03
7	2.29
8	2.70
9	1.54

## APPENDIX E: PALOMINAS RIVER WATER QUALITY DATA

River chemical/isotopic values at Palominas; basis for model input

Data Source	Date	$\delta^{18}\text{O}$ per mil	$\delta^2\text{H}$ per mil	Chloride mg/L	Sulfate mg/L
USGS-NWIS	8/31/94	-5.42	-38.3	6.3	89
USGS-NWIS	12/15/94	-11.11	-83.8	7.9	90
USGS-NWIS	3/15/95	-8.25	-63.2	8.7	75
USGS-NWIS	6/21/95	-7.95	-59.5		
USGS-NWIS	3/12/96	-7.42	-54.5	8.1	86
USGS-NWIS	7/15/96	-7.85	-53.9	3.1	23
USGS-NWIS	8/12/99	-6.03	-44.6		
USGS-NWIS	8/26/99	-6.92	-50.4		
USGS-NWIS	12/21/99	-7.10	-52.3		
USGS-NWIS	1/26/00	-7.08	-51.5		
USGS-NWIS	2/24/00	-6.88	-50.8		
USGS-NWIS	3/28/00	-6.70	-49.4		
USGS-NWIS	4/27/00	-5.34	-45.7		
USGS-NWIS	6/28/00	-11.92	-86.4		
USGS-NWIS	7/26/00	-6.88	-52.5		
USGS-NWIS	10/3/00	-6.55	-48.6		
USGS-NWIS	11/30/00	-7.39	-53.1		
USGS-NWIS	12/21/00	-7.18	-52.5		
USGS-NWIS	3/5/01	-6.94	-51.4		
USGS-NWIS	3/28/01	-6.98	-50.0		
USGS-NWIS	4/26/01	-6.91	-50.9		
USGS-NWIS	6/1/01	-7.07	-52.9		
USGS-NWIS	6/28/01	-7.00	-48.9		
USGS-NWIS	7/26/01	-5.93	-39.6		
USGS-NWIS	8/14/01	-5.96	-37.5	4	25.2
USGS-NWIS	8/15/01	-5.84	-38.6	2.91	14.1
USGS-NWIS	8/16/01	-6.47	-44.5	3.06	17.2
USGS-NWIS	8/24/01	-6.61	-46.2		
USGS-NWIS	8/30/01	-6.53	-48.4		
USGS-NWIS	9/27/01	-6.68	-48.9		
USGS-NWIS	10/19/01	-6.46	-47.5		
USGS-NWIS	11/29/01	-6.63	-49.0		
USGS-NWIS	12/27/01	-6.84	-51.9		
USGS-NWIS	1/30/02	-7.00	-50.8		
USGS-NWIS	2/28/02	-6.72	-50.3		
USGS-NWIS	3/28/02	-6.61	-48.8		

APPENDIX E – *continued*

<b>Data Source</b>	<b>Date</b>	<b><math>\delta^{18}\text{O}</math> per mil</b>	<b><math>\delta^2\text{H}</math> per mil</b>	<b>Chloride mg/L</b>	<b>Sulfate mg/L</b>
USGS-NWIS	5/1/02	-6.43	-47.7		
USGS-NWIS	5/23/02	-6.20	-48.1		
USGS-NWIS	6/27/02	-5.52	-45.0		
S. Lemon Thesis	6/29/02			9.7	76.4
S. Lemon Thesis	7/4/02			10.5	75.8
S. Lemon Thesis	7/22/02			8.2	70.9
S. Lemon Thesis	7/30/02			3.6	33.8
USGS-NWIS	8/1/02	-8.60	-62.0		
S. Lemon Thesis	8/12/02			4.1	35.7
S. Lemon Thesis	8/31/02			9.5	75.5
S. Lemon Thesis	9/20/02			10.5	57.3
S. Lemon Thesis	10/18/02			11.3	74.2
USGS-NWIS	12/23/02	-7.00	-52.2		
USGS-NWIS	1/30/03	-6.71	-51.1		
USGS-NWIS	2/10/03	-6.82	-50.3		
USGS-NWIS	2/27/03	-6.89	-49.7		
USGS-NWIS	3/27/03	-6.51	-49.0		
USGS-NWIS	5/1/03	-6.12	-47.1		
USGS-NWIS	11/25/03	-5.92	-44.4		
BAILLIE THESIS	12/13/03	-6.26	-45	13.3	124.9
USGS-NWIS	2/3/04	-6.45	-49.2		
USGS-NWIS	2/24/04	-6.53	-47.6		
BAILLIE THESIS	3/7/04	-6.53	-47	7.8	61.5
BAILLIE THESIS	3/28/04	-6.19	-45	10.6	87.6
USGS-NWIS	4/2/04	-6.05	-45.3		
BAILLIE THESIS	4/3/04	-7.00	-36	0.9	3.4
BAILLIE THESIS	4/24/04	-6.07	-46	13.5	111.2
USGS-NWIS	4/28/04	-6.08	-45.5		
USGS-NWIS	6/3/04	-4.50	-40.0		
USGS-NWIS	6/25/04	-8.40	-63.9		
BAILLIE THESIS	7/15/04	-8.07	-60.8	3.1	11.1
USGS-NWIS	7/29/04	-7.20	-44.1		
BAILLIE THESIS	8/5/04	-5.70	-45	1.7	10.5
BAILLIE THESIS	8/17/04	-5.53	-30.5	1.4	16.5
USGS-NWIS	8/31/04	-5.12	-40.8		
BAILLIE THESIS	9/6/04	-7.42	-52	4.2	38.4
USGS-NWIS	10/7/04	-6.37	-48.5		
USGS-NWIS	10/29/04	-6.64	-48.5		
BAILLIE THESIS	11/2/04	-6.10	-47		

APPENDIX E – *continued*

<b>Data Source</b>	<b>Date</b>	<b><math>\delta^{18}\text{O}</math> per mil</b>	<b><math>\delta^2\text{H}</math> per mil</b>	<b>Chloride mg/L</b>	<b>Sulfate mg/L</b>
USGS-NWIS	11/30/04	-6.46	-46.2		
USGS-NWIS	1/5/05	-7.20	-52.3		
USGS-NWIS	2/4/05	-6.88	-49.3		
USGS-NWIS	3/3/05	-6.95	-51.3		
USGS-NWIS	4/8/05	-6.31	-47.5		
USGS-NWIS	5/12/05	-6.09	-47.4		
USGS-NWIS	6/9/05	-5.34	-44.6		
USGS-NWIS	8/12/05	-9.11	-63.8		
USGS-NWIS	9/9/05	-6.10	-36.8		
<b>This study</b>	8/5/06	-7.46	-49.2	2.6	19.6
<b>This study</b>	10/7/06	-6.98	-46.7	6.7	74.2
<b>This study</b>	10/7/06	-6.78	-46.2	6.0	67.5
<b>This study</b>	10/27/06	-6.80	-49.5	7.8	58.2
<b>This study</b>	12/9/06	-6.96	-51.5	7.1	55.3

## APPENDIX F: HEREFORD RUNOFF SAMPLE DATA

<b>Date</b>	<b><math>\delta^{18}\text{O}</math> per mil</b>	<b><math>\delta^2\text{H}</math> per mil</b>	<b>Chloride mg/L</b>	<b>Sulfate mg/L</b>
7/15/04	-12.5	-92	1.7	25.7

## APPENDIX G: NEAR-RIPARIAN BASIN GROUNDWATER DATA

Data for basin groundwater inputs grouped by model segment

Segment	Well Depth (ft)	Data Source	Date	$\delta^{18}\text{O}$ per mil	$\delta^2\text{H}$ per mil	Chloride mg/L	Sulfate mg/L
1	unknown	USGS-NWIS	9/13/99	-7.96	-54.1	12.4	4.6
	unknown	USGS-NWIS	9/14/94			5.5	9.0
	205	USGS-NWIS	6/24/96	-8.12	-57.8	16.0	11.0
	unknown	USGS-NWIS	9/14/99	-7.95	-55.3	4.2	8.5
	117	USGS-NWIS	11/13/96	-6.75	-50.4	9.9	35.0
	203.5	USGS-NWIS	7/3/01	-7.27	-51.1		
		USGS-NWIS	8/24/01	-7.25	-50.8	3.7	7.6
		USGS-NWIS	10/18/01	-7.23	-50.9	3.5	8.9
	BAILLIE THESIS	8/18/04	-7.26	-51.5	3.4	9.7	
2	unknown	BAILLIE THESIS	6/23/04	-8.6	-58.7	7.9	17.9
	unknown	BAILLIE THESIS	6/23/04	-8.6	-58.8	7.8	17.9
	475	USGS-NWIS	2/24/55			20.0	50.0
		USGS-NWIS	8/4/89			4.4	9.0
3	unknown	BAILLIE THESIS	6/23/04	-9.6	-66.2	6.0	8.8
	unknown	USGS-NWIS	9/8/99	-8.42	-58.4	6.0	10.6
4	unknown	USGS-NWIS	3/12/03	-8.11	-56.8		
	180	USGS-NWIS	3/28/95	-9.59	-67.9	4.2	9.3
	300	USGS-NWIS	9/1/99	-8.39	-58.6	6.1	10.2
5	unknown	USGS-NWIS	3/12/03	-8.6	-59.3		
	unknown	USGS-NWIS	11/18/03	-7.92	-56.6		
	unknown	USGS-NWIS	8/27/99	-8.39	-58.0	6.9	14.6
6	29	USGS-NWIS	7/5/01	-7.68	-52.2	1.5	4.5
	90	USGS-NWIS	3/29/88			3.8	5.8

## APPENDIX H: MODEL CODE

## MODEL (MATLAB) CODE &amp; RELATED MODEL FUNCTIONS

## “Model”

```

%%%%%%%%%%%%%%%%%%%%%%%%%%%%%%%%%%%%%%%%%%%%%%%%%%%%%%%%%%%%%%%%%%%%%%%%
%%
%% Stream-Aquifer Exchange Model
%%
%%%%%%%%%%%%%%%%%%%%%%%%%%%%%%%%%%%%%%%%%%%%%%%%%%%%%%%%%%%%%%%%%%%%%%%%
clear all;close all;clc;
%-----%
% Loading data and determining if there is %
% inflow from side channels within the model domain %
%-----%
load PAL_Riv.m; % Columns: day #, Q(cfs),Gage ht(m)
PalQ=PAL_Riv(:,2)*86400/35.313378458; % Converts flow from cfs to m3/day
N_data=length(PAL_Riv); % No. of timesteps ('t')
load LSP_Riv.m;
load Char_Riv.m; % Columns: day# (i.e. 39156); Q(cfs); gage height (m)
CharQ=[Char_Riv(:,1) 86400*Char_Riv(:,2)/35.313378458];
load Tomb_Riv.m;
TombQ=[Tomb_Riv(:,1) 86400*Tomb_Riv(:,2)/35.313378458];
load PALRivChem.m; load VegFrac.m;
load Month.m; load DOY.m;
load SegLength.m; % Length of each segment (in meters)
N_seg=length(SegLength);
[SideInflow,Chem.side]=InflowDays(N_data,PAL_Riv,Rel_Monsoon_Basin);
% Calls fxn "InflowDays" (rows: days columns: segments)
SideInflow=86400*SideInflow/35.313378458;
%-----%
% Making blank matrices for later use %
%-----%
Gage_ht=zeros(N_data,N_seg); % Rows: time / columns: segments
Chem.bgw=zeros(1,4,N_seg);
% Chemistry of basin groundwater additions will be static in time
Chem.rgw=zeros(N_data,4,N_seg); % Columns: SO4,Cl,18O,2H (L to R)
Chem.ns=zeros(N_data,4,N_seg); % " " "
Chem.Rin=zeros(N_data,4,N_seg); % River chem ENTERING reach
Chem.Rout=zeros(N_data,4,N_seg); % River chem LEAVING reach
Chem.side=zeros(N_data,4,N_seg);
% Chem of floodwater entering from side channels (made up)
Q=zeros(N_data,4,N_seg); % Columns: 1. Qbgw(+0/-, time-constant)
% 2. Qrgw (+0/-)
% 3. Qsin(+0)

```

```

%      4. Qsout(+0)
Vrgw=zeros(N_data,N_seg); % Volume of RGW tank per meter of river (m2)
GWElev=zeros(N_data,N_seg);
DailyET=zeros(N_data,N_seg);
Grad=zeros(N_data,N_seg);
RiverCond=zeros(N_data,N_seg);

%-----%
%      Initializing the system      %
%-----%
load Daquifer.m;      % Diffusivity for each segment (units: m/day)
D=Daquifer;          % Changes name to 'D'
D(:)=1760;           % Post-SA diffusivity value
load Qbgw.m;         % Fluxes into each segment (UNITS: m2/day)
load Surf_elev.m;    % Land surface elevations (& top of RGW tank)
load Entrenchment.m; % Distance b/w river bottom and land surface(m)
load ZeroFlowStage.m; % Y-intercept in Q/Stage plots
load InitGWElev.m;
load ChemBgw.m;
if Rel_Monsoon_Basin==1;
    ChemBgw(:,1)=0;
    ChemBgw(:,2)=1;
end
for z=1:N_seg;
    % Makes BGW chem into a 'plate' with front row as segment 1 chem
    Chem.bgw(1,,:z)=ChemBgw(z,:);
    Q(:,1,z)=Qbgw(z);
    if ChemBgw(z,2)>0;
        ChemBgwSO4_Cl(z)=ChemBgw(z,1)/ChemBgw(z,2);
    else
        ChemBgwSO4_Cl(z)=0;
    end
end;
% Chem.rgw(1,,:)=Chem.bgw; % RGW at first time step is 100% BGW
Chem.rgw(1,,:1)=[77.3691 13.8470 -7.2055 -49.0051];
Chem.rgw(1,,:2)=[24.1093 6.9422 -8.5643 -58.5449]; % These values are
Chem.rgw(1,,:3)=[48.8458 9.6442 -7.6392 -51.6699]; % 10-1-06 values
Chem.rgw(1,,:4)=[30.8479 15.4903 -8.4951 -58.5021]; % (day #4019)
Chem.rgw(1,,:5)=[20.3332 7.0612 -8.0272 -54.9019]; % from a run with
Chem.rgw(1,,:6)=[23.3436 24.9219 -7.9695 -53.8624]; % RGW chemistry
Chem.rgw(1,,:7)=[34.9797 10.8888 -7.9002 -53.9805]; % same as BGW
Chem.rgw(1,,:8)=[37.4821 10.9147 -7.8011 -53.1713]; % (8-15-07)
Chem.rgw(1,,:9)=[37.8834 10.0809 -7.7536 -52.7299];
if Rel_Monsoon_Basin==1;
    Chem.rgw(1,1:2,1)=[82.1854 1.0000]; % 5th iteration results:
    Chem.rgw(1,1:2,2)=[29.3488 1.0000]; % All segments have converged
    Chem.rgw(1,1:2,3)=[69.4978 1.0000]; % to 3 decimal places
    Chem.rgw(1,1:2,4)=[19.7063 1.0000];
    Chem.rgw(1,1:2,5)=[22.1006 1.0000];
    Chem.rgw(1,1:2,6)=[37.8016 1.0000];
end;

```

```

Chem.rgw(1,1:2,7)=[41.7695 1.0000];
Chem.rgw(1,1:2,8)=[45.8203 1.0000];
Chem.rgw(1,1:2,9)=[54.4789 1.0000];
end
Chem.ns(1,:)=Chem.rgw(1,:); % NSZ at first time step is same as RGW
Q(:,3,1)=PalQ;
load PALRivChemData4.m;
PALRivChemData=PALRivChemData4;
if Rel_Monsoon_Basin==1;
    for t=1:length(PAL_Riv);
        if Month(t)>5 & Month(t)<11;
            PALRivChemData(t,1)=100;
            % Flow at PAL from June 1-Oct 31 is considered 100% floodwater
            PALRivChemData(t,2)=1;
        else
            PALRivChemData(t,1)=0;
            % Flow at PAL from June 1-Oct 31 is considered 0% floodwater
            PALRivChemData(t,2)=1;
        end
    end
end
end
Chem.Rin(:,1,1)=PALRivChemData(:,1); % SO4
Chem.Rin(:,2,1)=PALRivChemData(:,2); % Cl
Chem.Rin(:,3,1)=PALRivChemData(:,3); % d18O
Chem.Rin(:,4,1)=PALRivChemData(:,4); % d2H
for seg=1:N_seg;
    if Qbgw(seg)>0;
        ReachChar(seg)=1; % + BGW discharge makes these GW-gaining reaches
    else
        ReachChar(seg)=2; % - BGW discharge makes these GW-losing reaches
    end;
end;
%-----%
%           Parameters           %
%-----%
Sy=0.16; % Specific yield (assumed constant throughout entire domain)
        % **It is also assumed that there is no vadose zone storage
Pars.Vns=10*Sy; % Volume of near-stream zone (channel + subsurface)
RGW_width=100; % width of RGW tank is 100 m at all segments
PorousTankWidth=RGW_width*Sy;
        % ---> multiply by specific yield so that water level changes are
        % for a porous medium and not for an "underground void"-type tank
RGWDepth=10; % RGW tank depth
Riv_bottom=Surf_elev-Entrenchment-ZeroFlowStage;
RGW_bottom=Riv_bottom-RGWDepth+ZeroFlowStage;
Vrgw_max=(Surf_elev-RGW_bottom)*RGW_width*Sy;
for seg=1:9;
    GWElev(1,seg)=InitGWElev(seg); % initial GWElev & Vrgw x 9 segments
    Vrgw(1,seg)=(GWElev(1,seg)-RGW_bottom(seg))*PorousTankWidth;
end;

```

```

%%%%%%%%%%%%%%%%%%%%%%%%%%%%%%%%%%%%%%%%%%%%%%%%%%%%%%%%%%%%%%%%%%%%%%%%
%%%%%%%%%%%%%%%%%%%%%%%%%%%%%%%%%%%%%%%%%%%%%%%%%%%%%%%%%%%%%%%%%%%%%%%% MODEL CALCULATIONS %%%%%%%%%%%%%%%%%%%%%%%%%%%%%%%%%%%%%%%%%%%%%%%%%%%%%%%%%%%%%%%%%%%%%%%%%
%%%%%%%%%%%%%%%%%%%%%%%%%%%%%%%%%%%%%%%%%%%%%%%%%%%%%%%%%%%%%%%%%%%%%%%%
for t=1:N_data; % all times
  for seg=1:9; % all segments
    V_rgwPreET(t,seg)=Vrgw(t,seg)+Q(t,1,seg);
    % new RGW volume = initial volume + flux w.r.t. BGW (units: m2)
    % --> sign of Qgbw reflects gaining/losing
    if V_rgwPreET(t,seg)>Vrgw_max(seg);
      % ensuring bucket doesn't overflow after BGW addition
      V_rgwPreET(t,seg)=Vrgw_max(seg);
      GWElev(t,seg)=Surf_elev(seg);
      Q(t,1,seg)=V_rgwPreET(t,seg)-Vrgw(t,seg);
    end
    if Q(t,1,seg)<0 & Vrgw(t,seg)<abs(Q(t,1,seg));
      V_rgwPreET(t,seg)=0;
      Q(t,1,seg)=-Vrgw(t,seg);
    end
    if ReachChar(seg)==1; % Calc chemical changes for GW-gaining reach
      New_SO4(t,seg)=ConcRecalc(Chem.bgw(1,1,seg),Chem.rgw(t,1,seg),...
        Qbgw(seg),Vrgw(t,seg)); % gives chem/iso values post BGW add'n
      New_Cl(t,seg)=ConcRecalc(Chem.bgw(1,2,seg),Chem.rgw(t,2,seg),...
        Qbgw(seg),Vrgw(t,seg)); % Vrgw(t,seg) is initial volume
      New_18O(t,seg)=ConcRecalc(Chem.bgw(1,3,seg),Chem.rgw(t,3,seg),...
        Qbgw(seg),Vrgw(t,seg));
      New_2H(t,seg)=ConcRecalc(Chem.bgw(1,4,seg),Chem.rgw(t,4,seg),...
        Qbgw(seg),Vrgw(t,seg));
    end;
    if ReachChar(seg)==2; % Calc chemical changes for GW-losing reach
      % no change in chemistry in RGW when losing w.r.t. BGW
      New_SO4(t,seg)=Chem.rgw(t,1,seg);
      New_Cl(t,seg)=Chem.rgw(t,2,seg);
      New_18O(t,seg)=Chem.rgw(t,3,seg);
      New_2H(t,seg)=Chem.rgw(t,4,seg);
    end;
    %----- ET removals (after BGW has been either added or subtracted) -----%
    DepthToGW(t,seg)=Surf_elev(seg)-GWElev(t,seg);
    DailyET(t,seg)=New_ETCalc(Month(t),GWElev(t,seg),Surf_elev(seg),...
      VegFrac(seg,1),VegFrac(seg,2),VegFrac(seg,3),VegFrac(seg,4),...
      DOY(t,seg);
    TotalET(t,seg)=DailyET(t,seg)*RGW_width;
    V_rgwPostET(t,seg)=V_rgwPreET(t,seg)-TotalET(t,seg);
    % Volume in RGW after ET removal = Vol before ET - ET volume
    GWElev_postET(t,seg)=RGW_bottom(seg)+V_rgwPostET(t,seg)/PorousTankWidth;
    % Elev. of water table = elev of bottom + water depth in RGW
    if Rel_Monsoon_Basin==1;
      PostET_SO4(t,seg)=New_SO4(t,seg);
      PostET_Cl(t,seg)=New_Cl(t,seg);
      % gives chemical signatures after ET (only SO4 and Cl change)
    else

```

```

PostET_SO4(t,seg)=ET_Recalc(V_rgwPreET(t,seg),V_rgwPostET(t,seg),...
    New_SO4(t,seg)); % chem. conc. after ET (only SO4 and Cl change)
PostET_Cl(t,seg)=ET_Recalc(V_rgwPreET(t,seg),V_rgwPostET(t,seg),...
    New_Cl(t,seg));
end
PostET_18O(t,seg)=New_18O(t,seg);

PostET_2H(t,seg)=New_2H(t,seg);
    % ET does not fractionate, thus per mil values will not change
Chem.rgw(t,1,seg)=PostET_SO4(t,seg);
Chem.rgw(t,2,seg)=PostET_Cl(t,seg);
Chem.rgw(t,3,seg)=PostET_18O(t,seg);
Chem.rgw(t,4,seg)=PostET_2H(t,seg);
%----- end of ET calculations -----%
%-----%
%-Adding surface flow to the river (if it enters within the model domain)-%
%-----%
if SidelInflow(t,seg)>0;
    % Adding flow if it enters the river from side channels below PAL
    for s=1:4;
        % Recalculates stream chemistry for the 4 species (SO4,Cl,18O,2H)
        Chem.Rin(t,s,seg)=ConcRecalc(Chem.side(t,s,seg),Chem.Rin(t,s,seg),...
            SidelInflow(t,seg),Q(t,3,seg));
    end;
    Q(t,3,seg)=SidelInflow(t,seg)+Q(t,3,seg); % Adds side channel flow
end;
%-----%
% Determining if the river is gaining/neutral/losing and exchanging water %
%-----%
Gage_ht(t,seg)=StageFromQ(Q(t,3,seg),seg);
    % Calc. river stage from discharge entering model segment
Riv_Elev(t,seg)=Riv_bottom(seg)+Gage_ht(t,seg);
    % Elev. of river surface = elev of river bottom + gage ht
if GW_Elev_postET(t,seg)==Riv_Elev(t,seg); % NO EXCHANGE if NO GRADIENT
    RiverCond(t,seg)=0;
        % River and aquifer do not interact w/o gradient
    Q(t,4,seg)=Q(t,3,seg);
        % ... meaning that Q out = Q into the reach
    Chem.Rout(t,:,seg)=Chem.Rin(t,:,seg);
        % ... and river chemistry doesn't change
    GW_Elev_final=GW_Elev_postET(t,seg);
else
    % Calculating volume of water exchanged b/w river, NSZ and aquifer
    [RiverCond(t,seg),Q(t,4,seg),Chem.Rout(t,:,seg),Chem.ns(t,:,seg),...
        Chem.rgw(t,:,seg),GW_Elev_final,FinalVrgw(t,seg),Grad(t,seg)]=...
        RivAqNSZ(t,seg,Chem,D(seg),GW_Elev_postET(t,seg),Riv_Elev(t,seg),...
            RGW_width,Pars.Vns,SegLength(seg),V_rgwPostET(t,seg),Q(t,3,seg),...
            Riv_bottom(seg),RGW_bottom(seg),Gage_ht(t,seg),PorousTankWidth,...
            Sy,Vrgw_max(seg));
    % The above function ("RivAqNSZ") calculates

```



**“ConcRecalc”**

```
function [C_new]=ConcRecalc(Cin,Cprev,Vin,Vprev);  
    % recalculates the concentration of a reservoir based on previous volume  
    % and amount added from a second reservoir (& respective concentrations)  
Vtot=Vin+Vprev;  
C_new=(Cin*Vin+Cprev*Vprev)/Vtot;
```

## “New\_ETCalc”

```

function [ETforToday]=New_ETCalc(Month,GWElev,Surf_elev,FracCot,...
    FracMesq,FracSac,FracTam,DOY,seg);
% Function calculating the amount of ET lost for a given depth to GW,
% season and combination of species as plant cover
DepthToGW=Surf_elev-GWElev; % (m)
ETforToday=0; % ET=0 unless specified differently below
%%%%%%%%%%%%%%%%%%%%%%%%%%%%%%%%%%%%%%%%%%%%%%%%%%%%%%%%%%%%%%%%%%%%%%%%
%%%%%%%%%%%%%%%%%%%%%%%%%%%%%%%%%%%%%%%%%%%%%%%%%%%%%%%%%%%%%%%%%%%%%%%% ET for spring (April-May) %%%%%%%%%
%%%%%%%%%%%%%%%%%%%%%%%%%%%%%%%%%%%%%%%%%%%%%%%%%%%%%%%%%%%%%%%%%%%%%%%%
if Month<6 & Month>3;
    if DepthToGW<=0.75 & DepthToGW>=0; % WT is 0 to 0.75 m BLS
        MesqET=0; % mm/day
        CotET=FracCot*(1.904*DepthToGW); % mm/day
        TamET=0; % mm/day
        SacET=FracSac*(1.4653*DepthToGW); % mm/day
        Evap=-4.5749*DepthToGW+4.5749; % mm/day
    end
    if DepthToGW>0.75 & DepthToGW<=1; % WT is 0.75 to 1 m BLS
        MesqET=0;
        CotET=FracCot*(4.488*DepthToGW-1.938);
        TamET=0;
        SacET=FracSac*(4.3959*DepthToGW-2.1979);
        Evap=-4.5749*DepthToGW+4.5749;
    end
    if DepthToGW>1 & DepthToGW<=1.5; % WT is 1 to 1.5 m BLS
        MesqET=0;
        CotET=FracCot*(0.612*DepthToGW+1.938);
        TamET=0;
        SacET=FracSac*(0.1465*DepthToGW+2.0514);
        Evap=0;
    end
    if DepthToGW>1.5 & DepthToGW<=2; % WT is 1.5 to 2 m BLS
        MesqET=0;
        CotET=FracCot*2.856;
        TamET=0;
        SacET=FracSac*2.2712;
        Evap=0;
    end
    if DepthToGW>2 & DepthToGW<=3; % WT is 2 to 3 m BLS
        MesqET=FracMesq*(1.36*DepthToGW-2.72);
        CotET=FracCot*2.856;
        TamET=FracTam*(1.36*DepthToGW-2.72);
        SacET=FracSac*(-0.0733*DepthToGW+2.4177);
        Evap=0;
    end
    if DepthToGW>3 & DepthToGW<=4; % WT is 3 to 4 m BLS

```

```

MesqET=FracMesq*(1.53*DepthToGW-3.23);
CotET=FracCot*(-1.428*DepthToGW+7.14);
TamET=FracTam*(1.768*DepthToGW+3.944);
SacET=FracSac*(-1.099*DepthToGW+5.4948);
Evap=0;
end
if DepthToGW>4 & DepthToGW<=5;           % WT is 4 to 5 m BLS
    MesqET=FracMesq*2.89;
    CotET=FracCot*(-1.088*DepthToGW+5.78);
    TamET=FracTam*(0.136*DepthToGW+2.584);
    SacET=FracSac*(-1.099*DepthToGW+5.4948);
    Evap=0;
end
if DepthToGW>5 & DepthToGW<=6;           % WT is 5 to 6 m BLS
    MesqET=FracMesq*2.89;
    CotET=FracCot*(-0.34*DepthToGW+2.04);
    TamET=FracTam*3.264;
    SacET=0;
    Evap=0;
end
if DepthToGW>6 & DepthToGW<=7;           % WT is 6 to 7 m BLS
    MesqET=FracMesq*2.89;
    CotET=0;
    TamET=FracTam*3.264;
    SacET=0;
    Evap=0;
end
if DepthToGW>7 & DepthToGW<=8;           % WT is 7 to 8 m BLS
    MesqET=FracMesq*2.89;
    CotET=0;
    TamET=FracTam*(-0.204*DepthToGW+4.692);
    SacET=0;
    Evap=0;
end
if DepthToGW>8 & DepthToGW<=9;           % WT is 8 to 9 m BLS
    MesqET=FracMesq*(0.0272*DepthToGW+2.6724);
    CotET=0;
    TamET=FracTam*(-1.7*DepthToGW+16.66);
    SacET=0;
    Evap=0;
end
if DepthToGW>9 & DepthToGW<=10;          % WT is 9 to 10 m BLS
    MesqET=FracMesq*2.9172;
    CotET=0;
    TamET=FracTam*(-1.36*DepthToGW+13.6);
    SacET=0;
    Evap=0;
end
if DepthToGW>10 & DepthToGW<=11;         % WT is 10 to 11 m BLS
    MesqET=2.9172;

```

```

CotET=0;
TamET=0;
SacET=0;
Evap=0;
end
if DepthToGW>11 & DepthToGW<=12;           % WT is 11 to 12 m BLS
    MesqET=FracMesq*(-0.5372*DepthToGW+8.8264);
    CotET=0;
    TamET=0;
    SacET=0;
    Evap=0;
end
if DepthToGW>12 & DepthToGW<=13;           % WT is 12 to 13 m BLS
    MesqET=FracMesq*(-0.68*DepthToGW+10.54);
    CotET=0;
    TamET=0;
    SacET=0;
    Evap=0;
end
if DepthToGW>13 & DepthToGW<=14;           % WT is 13 to 14 m BLS
    MesqET=FracMesq*(-1.7*DepthToGW+23.8);
    CotET=0;
    TamET=0;
    SacET=0;
    Evap=0;
end
if DepthToGW>14;                             % WT is more than 14 m BLS
    MesqET=0;
    CotET=0;
    TamET=0;
    SacET=0;
    Evap=0;
end
if seg==1; % segment-specific ET-smoothing parameters
    SFD=66.15;Shift=92;Warp=3.6;
end
if seg==2;
    SFD=66.15;Shift=92;Warp=3.6;
end
if seg==3;
    SFD=64;Shift=92;Warp=3.6;
end
if seg==4;
    SFD=66.15;Shift=92;Warp=3.701;
end
if seg==5;
    SFD=66.15;Shift=92;Warp=3.701;
end
if seg==6;
    SFD=66.15;Shift=92;Warp=3.701;
end

```

```

end
if seg==7;
    SFD=62;Shift=92;Warp=3.5;
end
if seg==8;
    SFD=64.2;Shift=92;Warp=3.6;
end
if seg==9;
    SFD=66;Shift=92;Warp=3.69;
end
ETforToday=(CotET+MesqET+SacET+TamET+Evap)/1000; % converts to m/day
ETforToday=ETforToday*Warp*sin((DOY-Shift)/SFD)*(365-DOY)/365;
end
%%%%%%%%%%%%%%%%%%%%%%%%%%%%%%%%%%%%%%%%%%%%%%%%%%%%%%%%%%%%%%%%%%%%%%%%%%
%
%%%%%%%%%%%%%%%%%%%%%%%%%%%%%%%%%%%%%%%%%%%%%%%%%%%%%%%%%%%%%%%%%%%%%%%%%% ET for summer (June-Sept)
%%%%%%%%%%%%%%%%%%%%%%%%%%%%%%%%%%%%%%%%%%%%%%%%%%%%%%%%%%%%%%%%%%%%%%%%%%
%%%%%%%%%%%%%%%%%%%%%%%%%%%%%%%%%%%%%%%%%%%%%%%%%%%%%%%%%%%%%%%%%%%%%%%%%%
%
if Month<10 & Month>5;
    if DepthToGW<=0.75 & DepthToGW>=0; % WT is 0 to 0.75 m BLS
        MesqET=0; % mm/day
        CotET=FracCot*(2.8*DepthToGW); % mm/day
        TamET=0; % mm/day
        SacET=FracSac*(2.1548*DepthToGW); % mm/day
        Evap=-6.7278*DepthToGW+6.7278; % mm/day
    end
    if DepthToGW>0.75 & DepthToGW<=1; % WT is 0.75 to 1 m BLS
        MesqET=0;
        CotET=FracCot*(6.6*DepthToGW-2.85);
        TamET=0;
        SacET=FracSac*(6.4645*DepthToGW-3.2323);
        Evap=-6.73*DepthToGW+6.73;
    end
    if DepthToGW>1 & DepthToGW<=1.5; % WT is 1 to 1.5 m BLS
        MesqET=0;
        CotET=FracCot*(0.9*DepthToGW+2.85);
        TamET=0;
        SacET=FracSac*(0.2155*DepthToGW+3.0168);
        Evap=0;
    end
    if DepthToGW>1.5 & DepthToGW<=2; % WT is 1.5 to 2 m BLS
        MesqET=0;
        CotET=FracCot*4.2;
        TamET=0;
        SacET=FracSac*3.34;
        Evap=0;
    end
    if DepthToGW>2 & DepthToGW<=3; % WT is 2 to 3 m BLS
        MesqET=FracMesq*(2*DepthToGW-4);

```

```

CotET=FracCot*4.2;
TamET=FracTam*(2*DepthToGW-4);
SacET=FracSac*(-0.1077*DepthToGW+3.5555);
Evap=0;
end
if DepthToGW>3 & DepthToGW<=4;           % WT is 3 to 4 m BLS
    MesqET=FracMesq*(2.25*DepthToGW-4.75);
    CotET=FracCot*(-2.1*DepthToGW+10.5);
    TamET=FracTam*(2.6*DepthToGW+5.8);
    SacET=FracSac*(-1.6161*DepthToGW+8.0806);
    Evap=0;
end
if DepthToGW>4 & DepthToGW<=5;           % WT is 4 to 5 m BLS
    MesqET=FracMesq*4.25;
    CotET=FracCot*(-1.6*DepthToGW+8.5);
    TamET=FracTam*(0.2*DepthToGW+3.8);
    SacET=FracSac*(-1.6161*DepthToGW+8.0806);
    Evap=0;
end
if DepthToGW>5 & DepthToGW<=6;           % WT is 5 to 6 m BLS
    MesqET=FracMesq*4.25;
    CotET=FracCot*(-0.5*DepthToGW+3);
    TamET=FracTam*4.8;
    SacET=0;
    Evap=0;
end
if DepthToGW>6 & DepthToGW<=7;           % WT is 6 to 7 m BLS
    MesqET=FracMesq*4.25;
    CotET=0;
    SacET=0;
    TamET=FracTam*4.8;
    Evap=0;
end
if DepthToGW>7 & DepthToGW<=8;           % WT is 7 to 8 m BLS
    MesqET=FracMesq*4.25;
    CotET=0;
    SacET=0;
    TamET=FracTam*(-0.3*DepthToGW+6.9);
    Evap=0;
end
if DepthToGW>8 & DepthToGW<=9;           % WT is 8 to 9 m BLS
    MesqET=FracMesq*(0.04*DepthToGW+3.93);
    CotET=0;
    SacET=0;
    TamET=FracTam*(-2.5*DepthToGW+24.5);
    Evap=0;
end
if DepthToGW>9 & DepthToGW<=10;          % WT is 9 to 10 m BLS
    MesqET=FracMesq*4.29;
    CotET=0;

```

```

SacET=0;
TamET=FracTam*(-2*DepthToGW+20);
Evap=0;
end
if DepthToGW>10 & DepthToGW<=11;           % WT is 10 to 11 m BLS
    MesqET=4.29;
    CotET=0;
    TamET=0;
    SacET=0;
    Evap=0;
end
if DepthToGW>11 & DepthToGW<=12;           % WT is 11 to 12 m BLS
    MesqET=FracMesq*(-0.79*DepthToGW+12.98);
    CotET=0;
    TamET=0;
    SacET=0;
    Evap=0;
end
if DepthToGW>12 & DepthToGW<=13;           % WT is 12 to 13 m BLS
    MesqET=FracMesq*(-1*DepthToGW+15.5);
    CotET=0;
    TamET=0;
    SacET=0;
    Evap=0;
end
if DepthToGW>13 & DepthToGW<=14;           % WT is 13 to 14 m BLS
    MesqET=FracMesq*(-2.5*DepthToGW+35);
    CotET=0;
    TamET=0;
    SacET=0;
    Evap=0;
end
if DepthToGW>14;                             % WT is more than 14 m BLS
    MesqET=0;
    CotET=0;
    TamET=0;
    SacET=0;
    Evap=0;
end
if seg==1;
    SFD=76;Shift=92;Warp=2.679;
end
if seg==2;
    SFD=76;Shift=92;Warp=2.679;
end
if seg==3;
    SFD=76;Shift=92;Warp=2.78;
end
if seg==4;
    SFD=84;Shift=88.5;Warp=2.9;
end

```

```

end
if seg==5;
    SFD=73.7;Shift=91;Warp=2.68;
end
if seg==6;
    SFD=74;Shift=93;Warp=2.8;
end
if seg==7;
    SFD=75;Shift=91;Warp=2.68;
end
if seg==8;
    SFD=76;Shift=89;Warp=2.68;
end
if seg==9;
    SFD=76;Shift=105;Warp=2.679;
end
ETforToday=(CotET+MesqET+SacET+TamET+Evap)/1000; % converts to m/day
ETforToday=ETforToday*Warp*sin((DOY-Shift)/SFD)*(365-DOY)/365;
end
%%%%%%%%%%%%%%%%%%%%%%%%%%%%%%%%%%%%%%%%%%%%%%%%%%%%%%%%%%%%%%%%%%%%%%%%%%
%%%%%%%%%%%%%%%%%%%%%%%%%%%%%%%%%%%%%%%%%%%%%%%%%%%%%%%%%%%%%%%%%%%%%%%%%% ET for autumn (Oct-Nov) %%%%%%%%%%%
%%%%%%%%%%%%%%%%%%%%%%%%%%%%%%%%%%%%%%%%%%%%%%%%%%%%%%%%%%%%%%%%%%%%%%%%%%
if Month<12 & Month>9;
    if DepthToGW<=0.75 & DepthToGW>=0;           % WT is 0 to 0.75 m BLS
        MesqET=0;
        CotET=FracCot*(0.4467*DepthToGW);
        TamET=0;
        SacET=FracSac*(0.9355*DepthToGW);
        Evap=-4.29*DepthToGW+4.29;
    end
    if DepthToGW>0.75 & DepthToGW<=1;           % WT is 0.75 to 1 m BLS
        MesqET=0;
        CotET=FracCot*(1.0529*DepthToGW-0.4546);
        TamET=0;
        SacET=FracSac*(2.8065*DepthToGW-1.4032);
        Evap=-4.29*DepthToGW+4.29;
    end
    if DepthToGW>1 & DepthToGW<=1.5;           % WT is 1 to 1.5 m BLS
        MesqET=0;
        CotET=FracCot*(0.1636*DepthToGW+0.4346);
        TamET=0;
        SacET=FracSac*(0.0935*DepthToGW+1.3097);
        Evap=0;
    end
    if DepthToGW>1.5 & DepthToGW<=2;           % WT is 1.5 to 2 m BLS
        MesqET=0;
        CotET=FracCot*0.68;
        TamET=0;
        SacET=FracSac*1.45;
        Evap=0;
    end
end

```

```

end
if DepthToGW>2 & DepthToGW<=3;           % WT is 2 to 3 m BLS
    MesqET=FracMesq*(0.6867*DepthToGW-1.3734);
    CotET=FracCot*0.68;
    TamET=FracTam*(0.8333*DepthToGW+1.6667);
    SacET=FracSac*(-0.0468*DepthToGW+1.5435);
    Evap=0;
end
if DepthToGW>3 & DepthToGW<=4;           % WT is 3 to 4 m BLS
    MesqET=FracMesq*(0.7726*DepthToGW-1.631);
    CotET=FracCot*(-0.345*DepthToGW+1.715);
    TamET=FracTam*(1.0833*DepthToGW-2.4167);
    SacET=FracSac*(-0.7016*DepthToGW+3.5081);
    Evap=0;
end
if DepthToGW>4 & DepthToGW<=5;           % WT is 4 to 5 m BLS
    MesqET=FracMesq*1.4593;
    CotET=FracCot*(-0.2552*DepthToGW+1.356);
    TamET=FracTam*(0.0833*DepthToGW+1.5833);
    SacET=FracSac*(-0.7016*DepthToGW+3.5081);
    Evap=0;
end
if DepthToGW>5 & DepthToGW<=6;           % WT is 5 to 6 m BLS
    MesqET=FracMesq*1.4593;
    CotET=FracCot*(-0.0798*DepthToGW+0.4786);
    TamET=FracTam*2;
    SacET=0;
    Evap=0;
end
if DepthToGW>6 & DepthToGW<=7;           % WT is 6 to 7 m BLS
    MesqET=FracMesq*1.4593;
    CotET=0;
    SacET=0;
    TamET=FracTam*2;
    Evap=0;
end
if DepthToGW>7 & DepthToGW<=8;           % WT is 7 to 8 m BLS
    MesqET=FracMesq*1.4593;
    CotET=0;
    SacET=0;
    TamET=FracTam*(-0.125*DepthToGW+2.875);
    Evap=0;
end
if DepthToGW>8 & DepthToGW<=9;           % WT is 8 to 9 m BLS
    MesqET=FracMesq*(0.0207*DepthToGW+1.2935);
    CotET=0;
    SacET=0;
    TamET=FracTam*(-1.0417*DepthToGW+10.208);
    Evap=0;
end

```

```

if DepthToGW>9 & DepthToGW<=10;           % WT is 9 to 10 m BLS
    MesqET=FracMesq*1.48;
    CotET=0;
    SacET=0;
    TamET=FracTam*(-0.8333*DepthToGW+8.3333);
    Evap=0;
end
if DepthToGW>10 & DepthToGW<=11;         % WT is 10 to 11 m BLS
    MesqET=FracMesq*1.48;
    CotET=0;
    TamET=0;
    SacET=0;
    Evap=0;
end
if DepthToGW>11 & DepthToGW<=12;         % WT is 11 to 12 m BLS
    MesqET=FracMesq*(-0.2782*DepthToGW+4.5406);
    CotET=0;
    TamET=0;
    SacET=0;
    Evap=0;
end
if DepthToGW>12 & DepthToGW<=13;         % WT is 12 to 13 m BLS
    MesqET=FracMesq*(-0.3434*DepthToGW+5.3221);
    CotET=0;
    TamET=0;
    SacET=0;
    Evap=0;
end
if DepthToGW>13 & DepthToGW<=14;         % WT is 13 to 14 m BLS
    MesqET=FracMesq*(-0.8584*DepthToGW+12.018);
    CotET=0;
    TamET=0;
    SacET=0;
    Evap=0;
end
if DepthToGW>14;                           % WT is more than 14 m BLS
    MesqET=0;
    CotET=0;
    TamET=0;
    SacET=0;
    Evap=0;
end
if seg==1;
    SFD=76;Shift=92;Warp=15.73;
end
if seg==2;
    SFD=77;Shift=91;Warp=10;
end
if seg==3;
    SFD=76;Shift=92;Warp=10;
end

```



**“ET\_Recalc”**

```
function [NewConc]=ET_Recalc(V_rgwPreET,V_rgwPostET,Old_Conc);  
    NewConc=Old_Conc*V_rgwPreET/V_rgwPostET;  
% recalculates SO4 and Cl concentrations in RGW after removal of  
% water via ET (which is assumed not to fractionate isotopically)
```

## “StageFromQ”

```

function [Stage]=StageFromQ(Q,seg);
% 'StageFromQ' is a function that determines the average river stage (m)
% from the discharge (m3/day) coming into any segment of the river
%%%%%%%%%%%%%%%%%%%%%%%%%%%%%%%%%%%%%%%%%%%%%%%%%%%%%%%%%%%%%%%%%%%%%%%% CURVE PARAMETERS
%%%%%%%%%%%%%%%%%%%%%%%%%%%%%%%%%%%%%%%%%%%%%%%%%%%%%%%%%%%%%%%%%%%%%%%%
if seg==1;    % Q/Stage relationship based on PAL data
% Coeff=1728000; x_int=.9;  exp=2.05;% PAL transect data (J. Leenhouts)
  Coeff=2100000; x_int=.7;  exp=1.8; % based on entire PAL gage record
end;
if seg==2;    % Q/Stage relationship based on KOL data
  Coeff=518400; x_int=1.5;  exp=2.8;
end;
if seg==3;    % Q/Stage relationship based on HUN data
  Coeff=604800; x_int=.9;  exp=3.4;
end;
if seg==4;    % Q/Stage relationship based on COT data
  Coeff=518400; x_int=1.8;  exp=2.9;
end;
if seg==5;    % Q/Stage relationship based on LSP data
  Coeff=181440; x_int=.2;  exp=3.3;
end;
if seg==6;    % Q/Stage relationship based on CHAR gage data
  Coeff=950400; x_int=.5;  exp=2.54;
end;
if seg==7;    % Q/Stage relationship based on CHM data
  Coeff=2592000; x_int=.7;  exp=2.4;
end;
if seg==8;    % Q/Stage relationship based on FBK data
  Coeff=1728000; x_int=.5;  exp=2.4;
end;
if seg==9;    % Q/Stage relationship based on CON data
  Coeff=1123200; x_int=.6;  exp=3;
end;
%----- ACTUAL CALCULATION -----
  Stage=x_int+(Q/Coeff)^(1/exp);
%----- END OF FUNCTION 'StageFromQ' -----

```

## “RivAqNSZ”

```

function [RiverCond,Q_out,ChemRout,Chemns,Chemrgw,GW_Elev_final,...
    V_rgwFinal,Grad]=RivAqNSZ(t,seg,Chem,D,GW_Elev,Riv_Elev,RGW_width,...
    Vnsz,SegLength,V_rgw_i,Q_in,Riv_bottom,RGW_bottom,Gage_ht_i,...
    PorousTankWidth,Sy,Vrgw_max);
% 'RivAqNSZ' is a function determining the amount and direction of water
% exchanged b/w the river, NSZ and RGW... AFTER IT HAS BEEN DETERMINED
% THAT EXCHANGE HAPPENS (i.e. gradient is non-zero)
% -->All volumes and river flux (q) is for one meter of stream length
% INPUTS:
% t = time step number (i.e. 4002)
% seg = stream segment #
% Chem = structure with ch0.emistry of ALL SEGMENTS AT ALL TIMES
% D = diffusivity value of THIS segment
% GW_Elev = GW elevation at start
% Riv_Elev = river elevation at start
% RGW_width = width of bucket (constant)
% PorousTankWidth=Width of empty tank needed to simulate mixing volume
%   of a porous tank of RGW width (i.e. porosity x RGW width)
% Vnsz = volume at this time step
% SegLength = length of segment (in meters)
% V_rgw_i = initial volume of RGW tank--before Riv/NSZ/Aq interaction
% Q_in = river discharge coming into the segment
% Riv_bottom = elevation of river bottom
% RGW_bottom = elevation of RGW bottom
% Gage_ht_i = river stage pre-exchange w/ RGW
% OUTPUTS:
% RiverCond = whether it's gaining (1) or losing (-1)
% Q_out = discharge out of segment 'seg' at time 't'
% ChemRout = 1x4 array of concentrations leaving river segment
% Chemns = 1x4 array of NSZ chem AFTER exchange
% Chemrgw = 1x4 array of RGW chem AFTER exchange
% GW_Elev = elevation of water table in RGW AFTER exchange
% Riv_Elev = elevation of river surface AFTER exchange
% V_rgwFinal = volume of RGW AFTER exchange
%%%%%%%%%%%%%%%%%%%%%%%%%%%%%%%%%%%%%%%%%%%%%%%%%%%%%%%%%%%%%%%%%%%%%%%%% INITIALIZING %%%%%%%%%%%%%%
ChemRin=Chem.Rin(t,.,seg);
ChemNSZi=Chem.ns(t,.,seg);
Chemrgw=Chem.rgw(t,.,seg);
ChemNSZf=zeros(1,4);
%%%%%%%%%%%%%%%%%%%%%%%%%%%%%%%%%%%%%%%%%%%%%%%%%%%%%%%%%%%%%%%%%%%%%%%%% WATER BALANCE %%%%%%%%%%
Grad=(GW_Elev-Riv_Elev)/(0.5*RGW_width);
% Hydraulic gradient: dh/dl--> NEGATIVE when river is LOSING
T=D*Sy;
% Diffusivity [m2/day] x Specific Yield [-] = T [m2/day]
q=T*Grad;
% Calc. flux per meter of river (+: gaining RIVER, -: losing)--(m2/day)
V_rgwFinal=V_rgw_i-q; % Length-specific volume of RGW tank (m2)
Q=q*SegLength;

```

```

% Volume of water added/lost along ENTIRE REACH ('SegLength' in meters)
Q_out=Q_in+Q; % Volume of streamflow leaving the model section
%----- Making sure water doesn't flow uphill -----
GW_Elev_postEx=RGW_bottom+(V_rgwFinal/PorousTankWidth);
if q<0 & GW_Elev_postEx>Riv_Elev;
    % in losing conditions, water won't flow 'uphill' into RGW res.
    GW_Elev_postEx=Riv_Elev;
    V_rgwFinal=(GW_Elev_postEx-RGW_bottom)*PorousTankWidth;
    q=V_rgw_i-V_rgwFinal;
    Q=q*SegLength;
    Q_out=Q_in+Q;
    V_rgwFinal=V_rgw_i-q; % Length-specific volume of RGW tank (m2)
end
if q>0 & GW_Elev_postEx<Riv_Elev;
    % in gaining conditions, water won't flow 'uphill' into river
    GW_Elev_postEx=Riv_Elev;
    V_rgwFinal=(GW_Elev_postEx-RGW_bottom)*PorousTankWidth;
    q=V_rgw_i-V_rgwFinal;
    Q=q*SegLength; % Volume added/lost along the entire reach
    Q_out=Q_in+Q; % Streamflow volume leaving model section
    V_rgwFinal=V_rgw_i-q; % Length-specific volume of RGW tank (m2)
end
%-----
if V_rgwFinal>Vrgw_max;
    % disallows RGW bucket from holding more than it's maximum volume
    V_rgwFinal=Vrgw_max;
    q=V_rgw_i-Vrgw_max;
    % must be NEGATIVE since river HAS to be losing to fill up RGW tank
    Q=q*SegLength;
    Q_out=Q_in+Q;
    V_rgwFinal=V_rgw_i-q;
end
if Q_out<0;
    % Making sure streamflow is either 0 or + (when river dries up)
    Q_out=0;
    Q=-Q_in; % Vol of water lost = volume in (when dries up)
    q=Q/SegLength;
    V_rgwFinal=V_rgw_i-q;
end;
if q<0;
    Q=-q*SegLength;
    % Makes 'Q' a positive quantity regardless of flux direction,
    % BUT...sign of 'q' still indicates direction
end
%-----%
%% Chemistry of the river & RGW does not change when the river is neutral %
%-----%
if q==0;
    RiverCond=0;
    ChemRout=ChemRin;

```

```

ChemNSZf=ChemNSZi;
GW_Elev_final=GW_Elev;
V_rgwFinal=V_rgw_i;
end;
%%%%%%%%%%%%%%%%%%%%%%%%%%%%%%%%%%%%%%%%%%%%%%%%%%%%%%%%%%%%%%%%%%%%%%%%
%%%%%%%%%%%%%%%%%%%%%%%%%%%%%%%%%%%%%%%%%%%%%%%%%%%%%%%%%%%%%%%%%%%%%%%% Determining chemistry of the river & RGW %%%%%%%%%
%%%%%%%%%%%%%%%%%%%%%%%%%%%%%%%%%%%%%%%%%%%%%%%%%%%%%%%%%%%%%%%%%%%%%%%%
if q>0; % RIVER IS GAINING
RiverCond=1;
if q<Vnsz; % when flux to river is LESS than NSZ volume,
% all additions to streamflow come from NSZ
for comp=1:4; % Calc. for 4 diff. chemical species (per meter of river)
ChemNSZf(comp)=((Vnsz-q)*ChemNSZi(comp)+q*Chemrgw(comp))/Vnsz;
% final NSZ chemistry
if Q_out>0; % When river is flowing
ChemRout(comp)=(Q_in*ChemRin(comp)+Q*ChemNSZi(comp))/Q_out;
% final river chemistry
else % When river has no flow
ChemRout(comp)=ChemNSZf(comp);
% Need to define river chem. when there is no flow???
end
end;
else % when flux to river is greater or equal to volume of NSZ,
% some add'ns to streamflow come from NSZ and some from RGW
Q_fromNSZ=Vnsz*SegLength;
Q_fromRGW=Q-Q_fromNSZ; % Vol. from RGW = flux to river - NSZ vol.
for comp=1:4; % Calc. for 4 diff. species
if Q_out>0;
ChemRout(comp)=(Q_in*ChemRin(comp)+Q_fromNSZ*ChemNSZi(comp)+...
Q_fromRGW*Chemrgw(comp))/Q_out;
% Adds NSZ and RGW water to the river
else % Useless loop
ChemRout(comp)=0;
end
ChemNSZf(comp)=Chemrgw(comp);
% When NSZ empties, replaced entirely w. water from RGW
end;
end;
end;
%----- RIVER IS LOSING -----%
if q<0;
RiverCond=-1;
ChemRout=ChemRin; % When river is losing, river chem doesn't change
q_ab=-q; % Makes flux a positive number
if q_ab<Vnsz;
% when recharge < NSZ volume, all streamflow goes into NSZ
for comp=1:4; % Calc. for 4 diff. species
ChemNSZf(comp)=((Vnsz-q_ab)*ChemNSZi(comp)+q_ab*ChemRin(comp))/Vnsz;
% river losses go into NSZ...
Chemrgw(comp)=(q_ab*ChemNSZi(comp)+V_rgw_i*Chemrgw(comp))/V_rgwFinal;

```

```

                                % ... & NSZ losses go into RGW
end;
else      % when recharge is >= volume of NSZ, some streamflow goes
          %          into NSZ (+ some NSZ water goes into RGW)
for comp=1:4;      % Calc. for 4 diff. species
q_fromRiver=q_ab-Vnsz;
Chemrgw(comp)=(V_rgw_i*Chemrgw(comp)+q_fromRiver*ChemRin(comp)+...
              Vnsz*ChemNSZi(comp))/V_rgwFinal;
ChemNSZf(comp)=ChemRin(comp);
end;
end;
end;
%-----FINALIZING VARIABLES-----%
GW_Elev_final=RGW_bottom+(V_rgwFinal/PorousTankWidth);
Chemns=ChemNSZf;
ChemNSZf=[];
%----- END OF FUNCTION 'RivAqNSZ' -----

```

## REFERENCES

- Baillie MN, Hogan JF, Ekwurzel B, Wahi AK, Eastoe CJ. 2007. Quantifying water sources to a semiarid riparian ecosystem, San Pedro River, Arizona. *J. Geophys. Res.*, 112, G03S02.
- Baird KJ, Stromberg JC, Maddock T. 2005. Linking riparian dynamics and groundwater: An ecohydrologic approach to modeling groundwater and riparian vegetation. *Environ Manage* 36(4):551-64.
- Brooks PD, and Lemon MM. 2007. Spatial variability in dissolved organic matter and inorganic nitrogen concentrations in a semiarid stream, San Pedro River, Arizona, *J. Geophys. Res.*, 112, G03S05.
- Chanat JG and Hornberger GM. 2003. Modeling catchment-scale mixing in the near-stream zone-implications for chemical and isotopic hydrograph separation. *Geophys Res Lett* 30(2).
- Coplen TB. 1995. Reporting of stable carbon, hydrogen and oxygen abundances, Vienna, International Atomic Energy Agency, IAEA Tecdoc, 825, 31-34.
- Cox WB and Stephens DB. 1988. Field study of ephemeral stream-aquifer interaction. Proceedings of the FOCUS Conference on Southwestern Ground Water Issues. National Water Well Association, Dublin OH. 1988.p 337-358, 11 Fig.
- Craig H. 1957. Isotopic standards for carbon and oxygen and correction factors for mass spectrometric analysis of carbon dioxide, *Geochim. Cosmochim. Acta.*, 12, 133-149.
- Freeze RA and Cherry JA. 1979. *Groundwater*, Prentice-Hall, Englewood Cliffs, NJ. 604 p.
- Gehre M, Hoefling R, Kowski P, Strauch G. 1996. Sample preparation device for quantitative hydrogen isotope analysis using chromium metal, *Analytical Chemistry*, 68, 4414-4417.
- Gillespie JB and Perry CA. 1988. Channel infiltration along the Pawnee River and its tributaries, West Central Kansas. Available from Books and Open File Report Section, USGS Box 25425. USGS Water Resources Investigations Report 88-4055:5 ref.

- Gonfiantini R. 1978. Standards for stable isotope measurements in natural compounds, *Nature*, 271, 534-536.
- Goodrich DC, Lane LJ, Shillito RM, Miller SN, Syed KH, Woolhiser DA. 1997. Linearity of basin response as a function of scale in a semiarid watershed. *Water Resour Res* 33(12):2951-65.
- Goodrich DC, Williams DG, Unkrich CL, Hogan JF, Scott RL, Hultine KR, Pool D, Coes AL, Miller S. 2004. Comparison of methods to estimate ephemeral channel recharge, Walnut Gulch, San Pedro River Basin, Arizona, in *Groundwater Recharge in a Desert Environment: the Southwestern United States*, edited by J.F. Hogan, F.M. Phillips, and B.R. Scanlon, American Geophysical Union, Washington D.C., 77-99.
- Harrington GA, Cook PG, Herczeg AL. 2002. Spatial and temporal variability of ground water recharge in central Australia: A tracer approach. *Ground Water* 40(5):518-28.
- Leenhouts JM, Stromberg JC, Scott RL, Lite SJ, Dixon M, Rychener T, Makings E, Geological Survey, Tucson, AZ. 2005. Hydrologic requirements of and consumptive ground-water use by riparian vegetation along the San Pedro River, Arizona. United States Geological Survey. 174 p.
- Kepner WG, Semmens DJ, Heggem DT, Evanson EJ, Edmonds CM, Scott SN, and Ebert DW. 2003. The San Pedro River Geo-data Browser and Assessment Tools. EPA/600/C-03/008; ARS/152432. U.S. Environmental Protection Agency, Office of Research and Development, Las Vegas, NV.
- Marie JR and Hollett KJ. Determination of hydraulic characteristics and yield of aquifers underlying Vekol Valley, Arizona, using several classical and current methods. USGS. 63 p. .
- McDonnell JJ, Stewart MK, Owens IF. 1991. Effect of catchment-scale subsurface mixing on stream isotopic response. *Water Resources Research*. p 3065-3073:22.
- Osterkamp WR, Lane LJ, Savard CS. 1994. Recharge estimates using a geomorphic/distributed-parameter simulation approach, Amargosa River basin. *Water Resour Bull* 30(3):493-507.

- Pearce AJ, Stewart MK, Sklash MG. 1986. Storm runoff generation in humid headwater catchments: 1. where does the water come from. *Water Resources Research*, Vol.22:76.
- Peters NE and Ratcliffe EB. 1998. Tracing hydrologic pathways using chloride at the Panola Mountain Research Watershed, Georgia, USA. *Water, Air, Soil Pollut* 105(1-2):263-75.
- Pinder GF, Bredehoeft JD, Cooper HH. 1969. Determination of aquifer diffusivity from aquifer response to fluctuations in river stage. *Water Resources Res* p850-855:9.
- Plummer LN, Bexfield LM, Anderholm SK, Sanford WE, Busenberg E. 2004. Hydrochemical tracers in the Middle Rio Grande Basin, USA: 1. Conceptualization of groundwater flow. *Hydrogeol J* 12(4):359-88.
- Ponce VM, Pandey RP, Kumar S. 1999. Groundwater recharge by channel infiltration in El Barbon Basin, Baja California, Mexico. *J Hydrol (Amst)* 214(1-4):1-7.
- Pool DR, and Coes AL. 1999. Hydrogeologic investigations of the Sierra Vista subwatershed of the Upper San Pedro Basin, Cochise County, Southeast Arizona. USGS Water-Resources Investigation Report 99-4197, 41p.
- Reynolds RJ. 1987. Diffusivity of a glacial-outwash aquifer by the floodwave-response technique. *Ground Water*. Vol.25:12.
- Rushton K. 2007. Representation in regional models of saturated river-aquifer interaction for gaining/losing rivers. *J Hydrol (Amst)* 334(1-2):262-81.
- Sanford WE, Plummer LN, McAda DP, Bexfield LM, Anderholm SK. 2004. Hydrochemical tracers in the Middle Rio Grande Basin, USA: 2. Calibration of a groundwater-flow model. *Hydrogeol J* 12(4):389-407.
- Sorman AU, Abdulrazzak MJ, Morel-Seytoux HJ. 1997. Groundwater recharge estimation from ephemeral streams. Case study: Wadi Tabalah, Saudi Arabia. *Hydrol. Process* 11(12):1607-19.
- Squillace PJ. 1996. Observed and simulated movement of bank-storage water. *Ground Water* 34(1):121-34.

- Stephens DB. 1988. Field study of ephemeral stream infiltration and recharge. Available from National Technical Information Service, Springfield VA 22161 as PB89-115554/AS, Price Codes: A09 in Paper Copy Technical Completion Report No. 228:6 append. USGS contract 14,08-0001-G1241. USGS state project 1423658. USGS project G1241-06.
- Stromberg JC, Lite SJ, Dixon M, Rychener T, Makings E. 2005. Relations between Streamflow Regime and Riparian Vegetation Composition, Structure, and Diversity within the San Pedro Riparian National Conservation Area, Arizona. *in*: Hydrologic requirements of and consumptive ground-water use by riparian vegetation along the San Pedro River, Arizona. United States Geological Survey. 174 p.
- van Griensven A and Meixner T. 2006. Methods to quantify and identify the sources of uncertainty for river basin water quality models. Alliance House 12 Caxton Street London SW1H 0QS UK: IWA Publishing.
- Wahi AK, Ekwurzel B, Hogan JF, Baillie MN, Eastoe CJ (accepted). Geochemical quantification of recharge from a semiarid mountain range, Ground Water.
- Waichler SR and Wigmosta MS. 2004. Application of hydrograph shape and channel infiltration models to an arid watershed. J Hydrol Eng 9(5):433-9.
- Whitaker MPL. 2000. Estimating bank storage and evapotranspiration using soil physical and hydrological techniques in a gaining reach of the San Pedro River, Arizona. University of Arizona, Ph.D. Dissertation.